

**PHOTOINDUCED ELECTRON TRANSFER PROCESSES  
IN FULLERENE-ANILINE AND FULLERENE-  
HETEROAROMATIC DYADS**

THESIS SUBMITTED TO  
THE UNIVERSITY OF KERALA  
IN PARTIAL FULFILMENT OF THE REQUIREMENTS  
FOR THE DEGREE OF  
DOCTOR OF PHILOSOPHY  
IN CHEMISTRY  
UNDER THE FACULTY OF SCIENCE

BY  
**V. BIJU**


PHOTOCHEMISTRY RESEARCH UNIT  
REGIONAL RESEARCH LABORATORY (CSIR)  
TRIVANDRUM-695 019, KERALA, INDIA

FEBRUARY, 1999

## STATEMENT

I hereby declare that the matter embodied in this thesis is the result of investigations carried out by me at the Photochemistry Research Unit of the Regional Research Laboratory (CSIR), Trivandrum, under the guidance of Dr. K. George Thomas and the same has not been submitted elsewhere for a degree.

In keeping with the general practice of reporting scientific observations, due acknowledgement has been made wherever the work described is based on the findings of other investigators.



V. Biju



**Dr. K. George Thomas**  
SCIENTIST

PHOTOCHEMISTRY RESEARCH UNIT  
REGIONAL RESEARCH LABORATORY (CSIR)  
TRIVANDRUM-695 019, INDIA

---

Telephone: 91-471-490392 Fax: 91-471-490186  
E. Mail: kgt@csrtrtd.rcn.nic.in

February 17, 1999

### CERTIFICATE

Certified that the work embodied in this thesis entitled: **“Photoinduced Electron Transfer Processes in Fullerene-Aniline and Fullerene-Heteroaromatic Dyads”** has been carried out by Mr. V. Biju under my supervision and the same has not been submitted elsewhere for a degree.

K. George Thomas

(Thesis Supervisor)

## ACKNOWLEDGEMENTS

It is with great pleasure that I place on record my deep sense of gratitude to Dr. K. George Thomas, my research supervisor, for suggesting the research problem and for his guidance and encouragement, leading to a successful completion of this work.

I would like to express my sincere thanks to Professor M. V. George for his encouragement and help throughout the tenure of this work. Also, I wish to thank Dr. G. Vijay Nair, Director, Regional Research Laboratory, Trivandrum and Dr. A. D. Damodaran, former Director, Regional Research Laboratory, Trivandrum for providing me the necessary facilities for carrying out this work and their constant support.

I wish to acknowledge the help rendered by Dr. Prashant V. Kamat and Dr. D. M. Guldi of Notre Dame Radiation Laboratory, USA for the laser flash photolysis experiments reported in this thesis. I express my gratitude to Professor J. Chandrasekhar, Department of Organic Chemistry, Indian Institute of Science, Bangalore, for helping me to do molecular mechanics calculations presented in this work.

Also, I would like to thank all members of the Organic Chemistry Division, Regional Research Laboratory, Trivandrum and Professor C. P. Joshua and Professor K. N. Rajasekharan of the University of Kerala for their help and cooperation.

I express my thanks to Dr. Suresh Das, Dr. A. Ajayaghosh, Dr. D. Ramaiah, Dr. K. R. Gopidas and other members of the Photochemistry Research Unit for

their suggestions and support. I acknowledge the help rendered to me by Mrs. Sarada Nair during various stages of my work. I also express my thanks to Dr. M. Muneer and all former members of the Photochemistry Research Unit for their help and encouragement. Thanks are also due to all my friends and well wishers in the various sections of the Regional Research Laboratory.

Finally, I am deeply indebted to all the members of my family for their invaluable support and encouragement.

Trivandrum

February, 1999

V. Biju

## CONTENTS

	Page
<b>Statement</b>	ii
<b>Certificate</b>	iii
<b>Acknowledgements</b>	iv
<b>Preface</b>	vi
<b>Chapter 1. Photoinduced Electron Transfer Processes in Donor-Bridge-Acceptor Systems: A Brief Review and Objectives of the Present Investigation</b>	1
1.1. Photoinduced electron transfer process	1
1.1.1. D-B-A systems with flexible spacer groups	5
1.1.2. D-B-A systems with rigid spacer groups	6
1.2. Fullerene based donor-acceptor systems	8
1.2.1. Photophysical and electron accepting properties of fullerenes	8
1.2.2. Functionalized fullerene derivatives	9
1.2.3. Fullerene based donor acceptor systems	10
1.3. Objectives of the present investigation	13
1.4. References	14

<b>Chapter 2. Photophysical and Orientation Dependent Electron Transfer Processes in Fullerene-Aniline Dyads</b>	
2.1. Abstract	18
2.2. Introduction	19
2.3. Results and Discussion	22
2.4. Conclusions	49
2.5. Experimental Section	50
2.6. References	59
<b>Chapter 3. Photoinduced Intramolecular Electron Transfer Processes in Clusters of Fullerene-Aniline and Bis(fullerene)-Aniline Dyads</b>	
3.1. Abstract	62
3.2. Introduction	63
3.3. Results and Discussion	66
3.4. Conclusions	89
3.5. Experimental Section	89
3.6. References	95
<b>Chapter 4. Effect of Varying the Donor Strength on Photoinduced Electron Transfer Processes in C<sub>60</sub>-based Dyads</b>	
4.1. Abstract	98
4.2. Introduction	99
4.3. Results and Discussion	101
4.4. Conclusions	118
4.5. Experimental Section	118
4.6. References	132

## PREFACE

Fullerenes are found to be excellent acceptors of electrons and  $C_{60}$ , for example has the ability to accommodate up to six electrons. Since the intermolecular charge-transfer complexes of  $C_{60}$  with electron donors have shown to possess interesting optoelectronic and photovoltaic properties, the covalent linkages of  $C_{60}$  with electron donors can lead to the generation of interesting materials with potential application in this area. In the present investigation, we have undertaken the design and the photoinduced electron transfer studies of a few fullerene based donor-bridge-acceptor [D-B-A] systems containing anilines and heteroaromatic groups as donors. The main objectives of the present investigations were (i) to study the rate and efficiency of photoinduced electron transfer processes in these fullerene based D-B-A systems, as a function of distance and orientation of the donor-acceptor pair and by varying the redox properties of donor group and (ii) to compare the dynamics of photoinduced electron transfer processes in fullerene-aniline dyads in solutions and clusters.

In the Chapter 1 of the thesis, a brief overview of the photoinduced electron transfer processes in donor-acceptor systems, with particular reference to  $C_{60}$  based systems, is presented.

In the Second Chapter, examples of remarkably large orientation effects, which can control the photoinduced electron transfer in a series of fullerene-aniline dyads (Chart 2.3), are reported. The difference in orientation is achieved by attaching an anilinic donor to the *ortho*- as well as the *para*-



positions of the phenyl groups of fullero(1-methyl-2-phenyl)pyrrolidine, linked by methylene chains. Minimum energy conformation, based on molecular mechanics calculations indicated the folded conformations for the *ortho*-substituted dyads and extended ones for the *para*-substituted dyads. On the basis of steady-state fluorescence and time resolved flash photolysis studies, the rate constants for charge separation ( $k_{CS}$ ) and their efficiencies ( $\phi_{CS}$ ) were investigated. The marked increase in the  $k_{CS}$  and  $\phi_{CS}$  values, observed in the case of the *ortho*-substituted dyads are attributed to a topographically controlled electron transfer process.

The Third Chapter of the thesis deals with the photophysical and electron transfer studies in clusters of fullerene-aniline dyads. In this Chapter the synthesis of two new bisbuckminsterfullerene derivatives has been reported (Chart 3.1). Fullerene-aniline dyads and model compounds listed in Chart 3.1, form stable and optically transparent clusters at room temperature. Clusters of these dyads can be visualized as a self assembled antenna system containing hydrophobic fullerene units as the central core, with appended anilinic groups. Ground and excited state properties of the clusters of the dyads and the model compounds were compared with their corresponding monomeric forms in homogeneous solutions. Charge transfer interaction between the photoexcited fullerene and aniline moieties led to the production of radical anions of  $C_{60}$  and found to be more efficient in clusters. This was independently confirmed through the presence of an absorption band of the fullerene radical anion in the NIR region (1010 nm). The intermolecular electron transfer processes between the

clusters of fulleropyrrolidine and various electron donors (Chart 3.2) were also investigated.

The last Chapter of the thesis describes a detailed investigation of the rate of light induced electron transfer processes in two series of fullerene based D-B-A systems by varying the energetics of the donor groups. The first series consist of fullerene-based systems possessing heteroaromatic groups such as phenothiazine and phenoxazine as donor groups (Chart 4.1) and the second one consists of substituted anilines such as *p*-anisidine and *p*-toluidine as donor groups (Chart 4.2). The photoinduced electron transfer processes in these systems were compared with an unsubstituted fullerene-aniline dyad and a model compound (Chart 4.2). In contrast to the behavior of the unsubstituted fullerene-aniline dyad, an efficient intramolecular electron transfer is observed in the case of fullerene-based dyads containing heteroaromatics and *p*-substituted anilines as donor groups, even in a nonpolar solvent such as toluene.

---

# The Chart numbers listed in this preface refer to those given in the different Chapters of this thesis.

## Chapter 1

### Photoinduced Electron Transfer Processes in Donor-Bridge-Acceptor Systems: A Brief Review and Objectives of the Present Investigation

#### 1.1. Photoinduced Electron Transfer Process

Photoinduced electron transfer processes play a dominant role in several chemical and biological processes. In natural photosynthesis, for example, the early events involve the absorption of sunlight by antenna chromophores, followed by a series of electron transfer reactions.<sup>1-3</sup> The transferred electron, in principle can be reverted back to the donor molecule and the process is referred to as back electron transfer (b.e.t.). In the natural photosynthetic system, the electron transfer occurs along cascades of donor and acceptor systems, in order to prevent the back electron transfer.<sup>1-3</sup> Photosynthetic systems are complex in nature and attempts have been made by several groups of workers to design model systems, which can mimic the various processes in natural photosynthesis. Studies on photoinduced electron transfer processes form an active area of current interest and several up-to-date books and reviews are currently available.<sup>4-10</sup> We shall be limiting the present coverage, however, to some general aspects related to inter- and intramolecular photoinduced electron transfer processes. Equation (1.1)



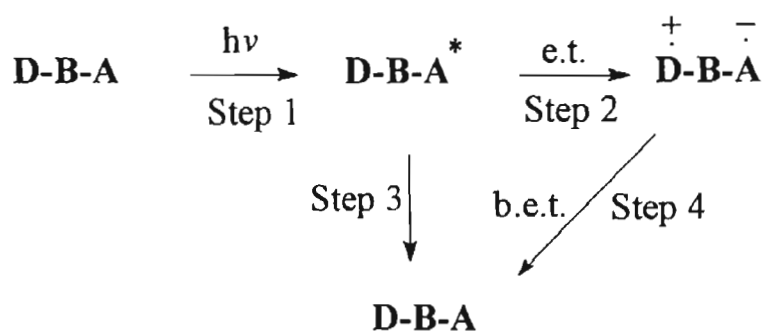
represents the intermolecular PET reaction between the donor (D) and the acceptor (A) groups in a reaction system. The electron transfer can proceed either through a reductive quenching of the excited state of A by the donor D or through an oxidative quenching of the excited state of D by the acceptor A.

The simplest covalently linked model system is a dyad (Chart 1.1) in which a donor group is covalently linked to an acceptor through a bridging unit. Various physical



Chart 1.1

processes that can occur in a dyad on photoexcitation are illustrated in Scheme 1.1. The photoexcitation of the acceptor group (Step 1 in Scheme 1.1), can in principle, lead to the transfer of an electron to its singlet or triplet state to form a charge-separated state (Step 2). The stabilization of the charge-separated state is very crucial for avoiding the energy wasting back electron transfer process (Step 4).



Scheme 1.1

Most of the earlier research efforts in this area were focused on the design of photosynthetic model systems which can mimic the primary events of electron transfer. Design of novel donor-acceptor systems has now become a promising field of study, primarily due to the potential applications of such systems in the design of optoelectronic devices.<sup>9,11-15</sup> Various applications of donor-acceptor systems are indicated in Chart 1.2 (adapted from reference 15). A molecular rectifier

based on donor-acceptor system 1 (Chart 1.3) has been reported by Aviram and Ratner.<sup>16</sup> Recently, Mehring has proposed the use of a donor-bridge-acceptor system as a molecular information storage unit having bistability.<sup>17</sup>

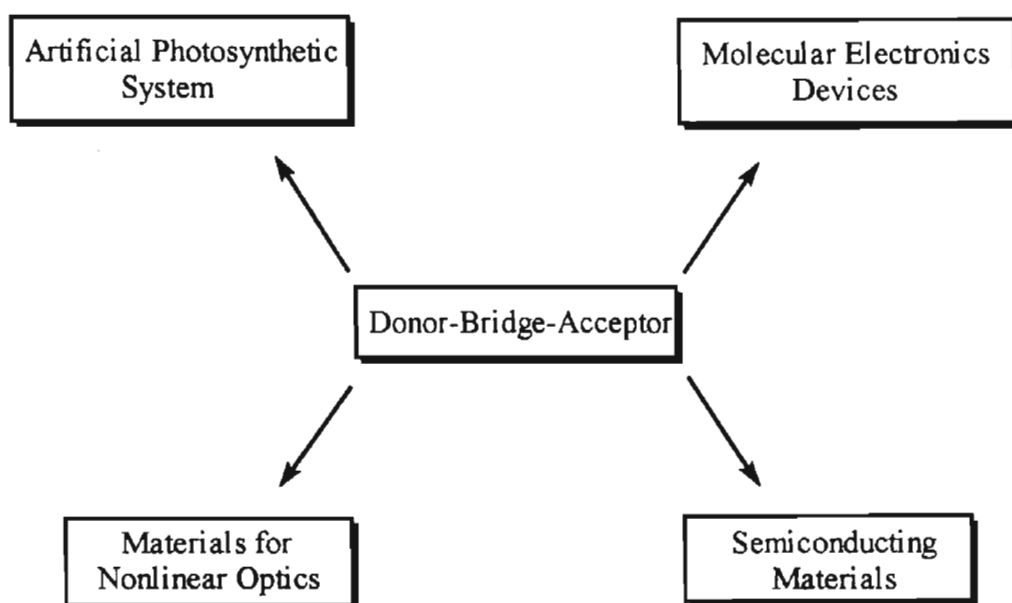


Chart 1.2

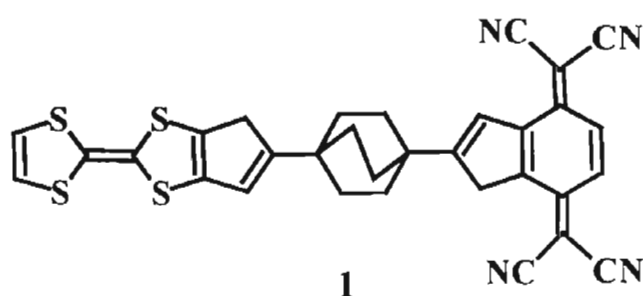


Chart 1.3

The feasibility of photoinduced electron transfer process between a donor and an acceptor is decided by the overall change in free energy, which can be estimated using the Rehm-Weller equation (Equation 1.2).<sup>18-19</sup> The free energy change ( $\Delta G$ ) can be predicted from the oxidation potential of the donor ( $E_{D^+/D}$ ), reduction potential of the acceptor ( $E_{A/A^-}$ ) and the excited state energy of the reactant ( $E^*$ ).

$$\Delta G(\text{eV}) = [E_{(D^+/D)} - E_{(A/A^-)} - e^2/\epsilon d] - E^* \quad (\text{Eq. 1.2})$$

The term  $e^2/\epsilon d$  is the free energy gained in bringing the two radical ion pairs to an encounter distance 'd' in a solvent of dielectric constant ' $\epsilon$ ', where, 'e' is the electronic charge. When  $\epsilon$  is high, this term can be neglected.

The most successful and widely used theory of electron transfer is that of Marcus which correlates the rate of electron transfer ( $k_{et}$ ) with the free energy change ( $\Delta G$ ).<sup>20-22</sup> The rate of electron transfer increases with increase of  $\Delta G$  value, reaches a maximum and then decreases with increase in driving force and the later part is known as the Marcus inverted region. The inverted region has been experimentally proven by different groups using intramolecular electron transfer studies in organic<sup>23-28</sup> as well as inorganic donor-acceptor systems.<sup>29</sup>

The electron transfer process can take place either by a through space or a through bond mechanism.<sup>4,5</sup> For through space electron transfer, the required condition is that the orbitals of the donor and the acceptor should overlap. This orbital overlap, in turn, depends on the distance of separation and orbital orientation. If the spacer group can act as a conductor of electronic charge, the electron transfer will take place by a through bond mechanism. In this case, the molecular bridge provides a pathway by which the donor and acceptor orbitals can overlap and electron transfer takes place by a super exchange mechanism. A through bond mechanism is favoured in systems containing rigid spacers and through space mechanism may be valid when the donor-acceptor distance is less and effective spacial interaction is possible. There are also systems in which through space and through bond mechanisms coexist.

Varying the spacer group can effectively control the degrees of freedom of donor and acceptor moieties. When the spacer group is rigid, the photoinduced electron transfer processes take place at a fixed distance, whereas in flexible systems several orientations are possible and hence distance is variable.

### 1.1.1. D-B-A systems with flexible spacer groups

The dynamic competition between the direct electron transfer and exciplex formation in donor-acceptor systems with flexible spacer groups has been investigated by several groups of workers. This competition mainly depends on solvent characteristics such as polarity and viscosity and on temperature and length of the spacer. Two idealized ground-state geometries, extended and folded, are illustrated in Chart 1.4. The ion pairs resulting from both the conformations were observed in polar solvents while the exciplex formation prevails, through a folded conformation, in nonpolar solvents.

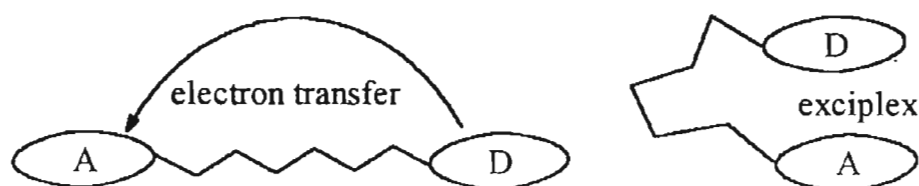


**Chart 1.4**

Eisenthal and co-workers have studied the competition between exciplex formation and electron transfer in anthracene-bridge-aniline dyads.<sup>30,31</sup> Davidson and co-workers have studied these effects in systems such as  $\omega$ -(1-naphthyl),N-alkylpyrrole.<sup>32</sup> Mattaga has carried out similar studies in pyrene-bridge-aniline systems.<sup>33</sup> In general, exciplex formation is favoured in nonpolar solvents, whereas electron transfer is more favoured in polar solvents for all these systems.

### 1.1.2. D-B-A Systems with rigid spacer groups

When a donor-acceptor system is connected by a rigid spacer group, their distance of separation as well as orientation become more or less frozen. In such a frozen geometry, it is easy to study the effect of distance and orientation on the rate of electron transfer processes. Among the two processes, i.e. photoinduced electron transfer and exciplex formation, the latter does not take place in rigid systems as the possibility of donor and acceptor to approach each other is less. In such cases, electron transfer takes place by either a through bond or through space mechanism. Covalently linked donor-acceptor systems, with various donor acceptor combinations have been reported by different groups of workers. Studies of the various factors which control the photoinduced charge separation processes such as the energetics of the donor and the acceptor, distance and orientation between the donor and the acceptor, nature of the spacer, solvent and temperature have been investigated and several reviews, with extensive compilation of the results, are available.<sup>4,8</sup> Majority of the studies on D-B-A systems have concentrated on the design of covalently linked porphyrin-quinone dyads.<sup>4,8</sup> One of the major limitations of these systems is the short lifetimes (ps) of the charge separated species. Attempts have been made to enhance the charge separation by involving heterogeneous and microheterogeneous systems.<sup>6,8</sup> Some of these include the use of colloids, micelles, vesicles, interfaces, polyelectrolytes and other host systems such as cyclodextrins and zeolites.<sup>6,8</sup>

Another strategy employed to slow down the charge recombination process is by the use of triad systems,<sup>34,35</sup> which involves a multistep electron transfer pathway for efficient charge separation. In order to achieve this, Gust and co-workers



have undertaken a detailed investigation of intramolecular photoinduced electron transfer processes in carotenoid-porphyrin-quinone systems **2-5** (Chart 1.5).<sup>34,35</sup> In these systems, they observed the formation of long lived charge-separated states at large distances, following two successive one electron transfer processes, first from photoexcited porphyrin to quinone and then from carotenoid to the oxidized porphyrin. These studies were further extended to tetrads and pentads where it was found that the charge-separated states are long-lived for the pentads (55  $\mu$ s). Such supramolecular donor-acceptor systems, which generate long lived charge separated states, can resemble the charge separation step in the photosynthetic reaction center and are promising elements in future solar energy harvesting devices.

Even though several types of donors have been used in the design of model systems, most of the studies regarding acceptors have been limited to either quinones or viologens. The physical properties of  $C_{60}$  are in contrast to such commonly used small size planar acceptors and the photophysical and electron

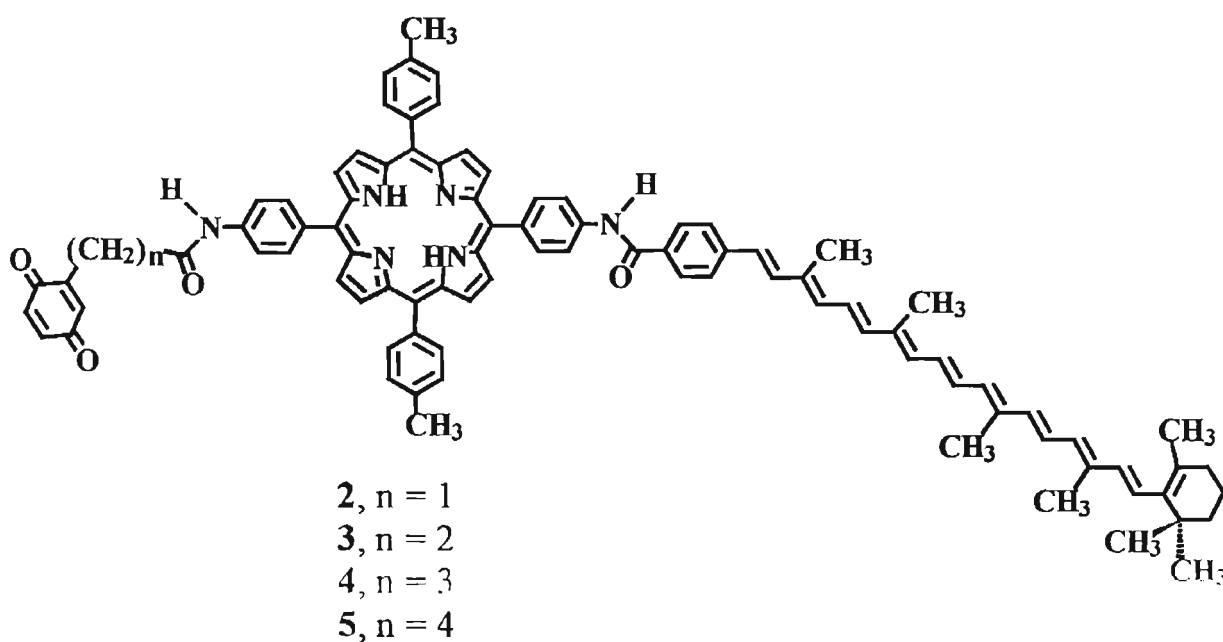


**Chart 1.5**

accepting properties as well as the stability of  $C_{60}$  make it an ideal candidate for the design of donor-acceptor systems.

## 1.2. Fullerene Based Donor-Acceptor Systems

### 1.2.1. Photophysical and electron accepting properties of fullerenes

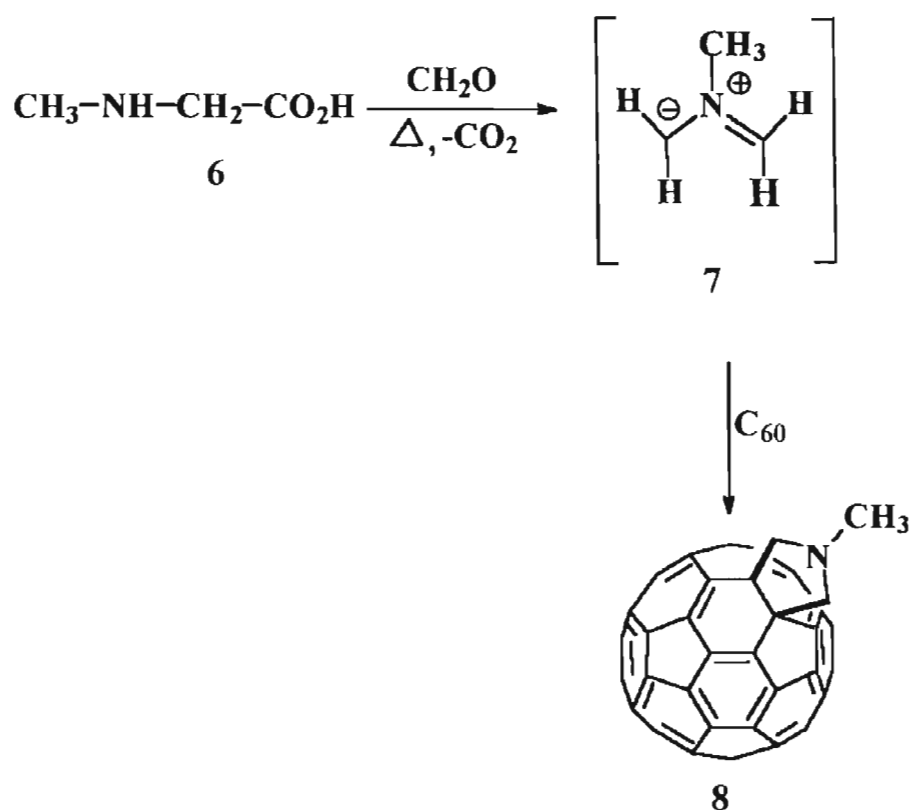
Fullerene and some of its functionalized derivatives are excellent electron acceptors and have been extensively used for the design of fullerene based dyads. The photophysical and electron accepting properties of  $C_{60}$  and its derivatives have been extensively investigated by several groups of workers in recent years and some of these results have been summarized in a recent review.<sup>36</sup>  $C_{60}$  absorbs light throughout the visible region.<sup>37</sup> The relatively low energy gap between the excited singlet and triplet states of  $C_{60}$  (5.5 kcal/mol) facilitates efficient intersystem crossing and hence the triplet state is formed in high yield (95%).<sup>38</sup> Fullerenes, particularly  $C_{60}$ , are excellent photosensitizers for the generation of singlet oxygen.  $C_{60}$  is found to be a good acceptor of electrons with the ability to accommodate up to six electrons reversibly and forms intermolecular charge-transfer complexes with electron donors.<sup>39,40</sup>

Intermolecular charge-transfer complexes of  $C_{60}$  with electron donors have been shown to possess interesting photovoltaic properties.<sup>41</sup> Covalent linkages of  $C_{60}$  with selected electron donors can lead to the generation of interesting new materials with potential applications in artificial solar energy harvesting systems. Recently, it has been reported that  $C_{60}$  and some of its derivatives show photoconducting, photovoltaic<sup>41-45</sup> and optical limiting<sup>46</sup> behaviour. The donor-acceptor systems based on  $C_{60}$  are expected to have potential application in optoelectronic devices.<sup>47</sup>

$C_{60}$  can generate singlet oxygen in almost quantitative yields. However,  $C_{60}$  is highly hydrophobic and its solubility is very low in polar solvents such as water. This limits its use in biological systems. There have been several successful attempts to design water-soluble fullerene derivatives containing hydroxyl or carboxyl functional groups without losing their ability to generate singlet oxygen. There are several reports in the literature in which fullerene derivatives have been used in biological fields for the singlet oxygen sensitized DNA cleavage<sup>48</sup> and HIV-1 protease inhibition.<sup>49</sup>

### 1.2.2. Functionalized fullerene derivatives

Cycloaddition is a convenient method for the functionalization of  $C_{60}$ , in which the double bond between two six membered rings acts as an ene component. The difficulty with this is again the formation of multiple adducts, as  $C_{60}$  is an electron deficient polyolefin (superalkene), which can give addition reactions with nucleophiles and radicals.<sup>50</sup> The possibility of multiple addition can be avoided by using 1,3-dipoles and dienes under controlled conditions. The general methods for the functionalization of  $C_{60}$  are (1+2), (2+2), (3+2) and (4+2) cycloaddition reactions. Among these, the most widely accepted method is the (3+2) addition of a 1,3-dipolar species such as azomethine ylide, generated *in situ* either by the ring opening of aziridines or as an intermediate formed in the reaction of an  $\alpha$ -amino acid with an aldehyde, to  $C_{60}$ . All these reactions have been extensively reviewed recently.<sup>50</sup> A representative example of a (3+2) cycloaddition reaction is indicated in Scheme 1.2.<sup>50</sup> In the present investigation, we have adopted a similar methodology for the synthesis of  $C_{60}$ -based donor-acceptors.



Scheme 1.2

### 1.2.3. Fullerene based donor acceptor systems

Photoinduced electron transfer processes in several classes of donor-linked fullerene systems and their potential applications have been reviewed by Imahori and Sakata.<sup>47</sup> In a more recent review, Martin *et al.* have summarized the photochemical and electrochemical properties of covalently linked  $\text{C}_{60}$  derivatives, bearing electron donor or electron acceptor units.<sup>51</sup>

The intramolecular photochemical studies in a fullerene based donor-bridge-acceptor system was first reported by Gust and co-workers in which they have covalently linked the photosynthetic pigment porphyrin to  $\text{C}_{60}$  through a bicyclic bridge (9 in Chart 1.6).<sup>52</sup> They have observed that the excited state of  $\text{C}_{60}$  accepts an electron from porphyrin, resulting in the formation of a  $\text{C}_{60}$  radical anion and

porphyrin radical cation. Recently, Gust and co-workers have carried out a detailed investigation on the photoinduced charge separation and charge recombination processes in a carotene-porphyrin-C<sub>60</sub> triad system.<sup>53</sup> In this system, a long-lived charge separated state with reasonable quantum yield was generated through a two step electron transfer processes. Interestingly, the charge-separated state was observed, even at 77 K in a solvent glass. Sequential photoinduced electron transfer in a porphyrin-pyromellitimide-C<sub>60</sub> triad system was studied by Imahori *et al.*, wherein, they observed a fairly long-lived charge-separated state with moderate quantum yield.<sup>54</sup> The intramolecular photoinduced electron transfer (PET) processes in C<sub>60</sub>-aniline dyads possessing rigid spacers have been studied by Williams *et al.*<sup>55</sup> The rate of charge recombination was found to be considerably lower in the case of C<sub>60</sub>-aniline dyads, where the donor and acceptor are spaced across 11 bonds (dyad 10 in Chart 1.6).

The photoinduced electron transfer processes in a series of fullerene-ferrocene dyads have been reported by Guldi *et al.* (for representative examples, see dyads 11 and 12 in Chart 1.6).<sup>56</sup> Depending upon the nature of the spacer groups, two types of quenching mechanisms were observed. These include the through-bond electron transfer and the formation of a transient intramolecular exciplex.

In a more recent report,<sup>57</sup> Maggini *et al.* have studied the light-induced electron transfer processes in a [Ru(bp)<sub>3</sub>]<sup>2+</sup>-C<sub>60</sub> dyad (13 in Chart 1.6) with a rigid androstane spacer group. They have found that charge separation is efficient in polar solvents and the rate of back electron transfer reaction depends on the nature of the solvent used.

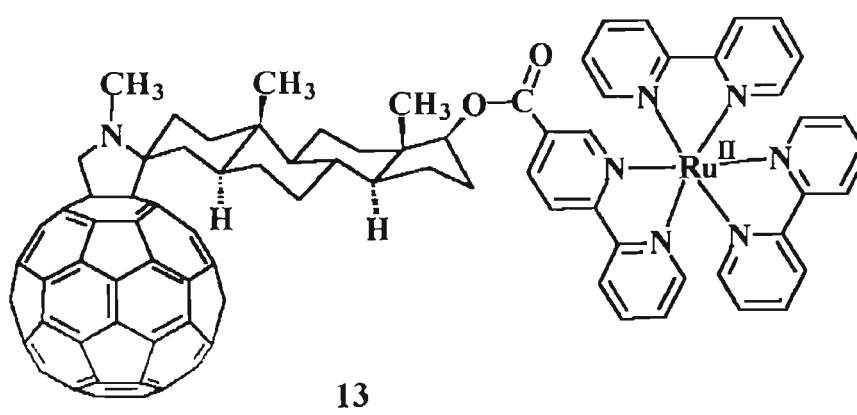
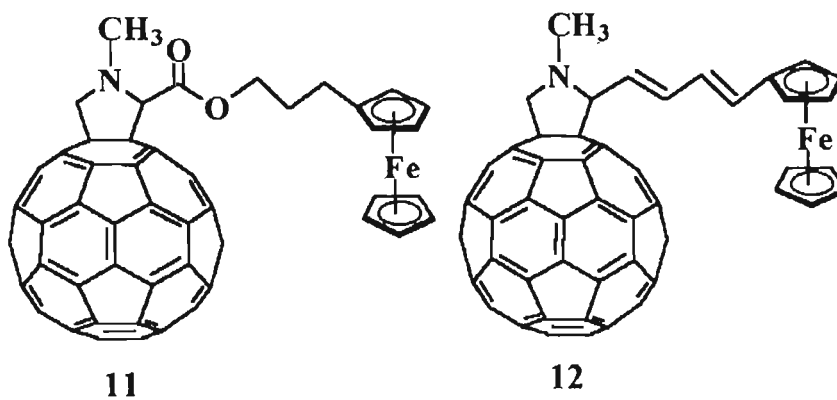
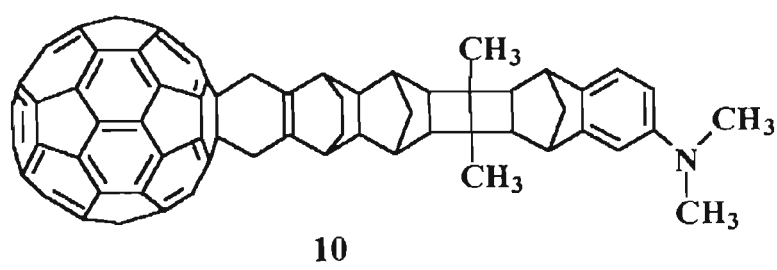
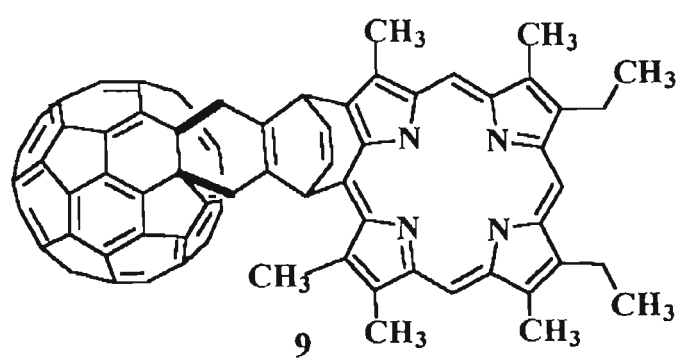


Chart 1.6

### 1.3. Objectives of the Present Investigation

Though, there have been several reports on the photophysical properties and electron transfer processes in fullerene based systems, many aspects of the dynamics of photoinduced electron transfer processes in these systems have not been addressed adequately. The design of several fullerene-based systems which can generate long-lived charge-separated states, on photoexcitation, is one of the main objectives of the present investigation. In order to achieve this goal, several classes of fullerene based dyads, in which the distance and orientation between the donor-acceptor pairs and the redox potentials of the donor group are varied, have been synthesized. The detailed photophysical and photoinduced electron transfer processes in these systems have been investigated.

Fullerene based donor acceptor systems can serve as building blocks for photovoltaic and optoelectronic devices. For device applications, it is desirable to have a detailed mechanistic understanding of their photophysical and electron transfer properties in the solid state. It is difficult to investigate the electron transfer processes in solids and the studies in optically transparent clusters can provide information bridging between their solution and solid state properties. Detailed investigations of the dynamics of photoinduced electron transfer processes in clusters of fullerene-aniline dyads have been undertaken and these results are compared with those of their monomeric forms in solutions.

#### 1.4. References

1. Deisenhofer, J.; Michel, H. *Angew. Chem. Int. Ed. Engl.*, **1989**, *28*, 829.
2. Huber, R. *Angew. Chem. Int. Ed. Engl.*, **1989**, *28*, 848.
3. Bixon, M.; Fajer, J.; Feher, G.; Freed, J. H.; Gamliel, D.; Hoff, A. J.; Levanon, H.; Mobius, K.; Nechushtai, R.; Norris, J. R.; Scherz, A.; Sessler, J. L.; Stehlik, D. *Special Issue on 'Primary events in photosynthesis: Problems, speculations controversies and future trends' Isr. J. Chem.*, **1992**, *32*, 369.
4. Fox, M. A.; Channon, M. (Eds.), *Photoinduced Electron Transfer Parts A-D*; Elsevier, Amsterdam, **1988**.
5. Kavarnos, G. J. *Fundamentals of Photoinduced Electron Transfer*, VCH, New York, **1993**.
6. Grätzel, M. (Ed.), *Heterogenous Photoinduced Electron Transfer*, CRC Publishers, Boca Raton, FL, **1988**.
7. Balton, J. R.; Mataga, N.; McLondon, G. (Eds.), *Electron Transfer in Inorganic, Organic and Biological Systems*, American Chemical Society; Washington, D.C., **1990**.
8. Mattay, J. (Ed.), *Photoinduced Electron Transfer, Parts I-IV*, Springer Verlag, Heidelberg, **1990**.
9. Balsani, V.; Juris, A.; Scandola, F. In *Homogeneous and Heterogeneous Photocatalysis*, Pelizzetti, E.; Serpone, N. (Eds.), D. Reidel Publishing Company, Dordercht, Holland, **1985**.
10. Marcus, R. A. *Angew. Chem. Int. Ed. Engl.*, **1993**, *32*, 1111.
11. Carter, F. L. *Molecular Electronic Devices*, Marcel Dekker, New York, **1982**.
12. Parthenopoulos, D. M.; Rentzepis, P. M. *Science*, **1989**, *245*, 843.
13. Willner, I.; Willner, B. In *Bioorganic Photochemistry Vol. 2: Biological Applications of Photochemical Switches*, H. Morrison (Ed.), Wiley, New York, 1993, pp 2-110.
14. Willner, I.; Rubin, S. *Angew. Chem. Int. Ed. Engl.*, **1996**, *35*, 367.



15. Martin, N.; Seoane, C. In *Handbook of Organic Conductive Molecules and Polymers, Vol. 1 Charge Transfer Salts, Fullerenes and Photoconductors*, John Wiley, New York, 1997.
16. Aviram, A.; Ratner, M. *Chem. Phys. Lett.*, 1974, 29, 277.
17. Mehring, M. *Springer Ser. Solid State Sci.*, 1989, 91, 242.
18. Rehm, D.; Weller, A. *Ber. Bunsenges Phys. Chem.*, 1969, 73, 834.
19. Rehm, D.; Weller, A. *Isr. J. Chem.*, 1970, 8, 259.
20. Marcus, R. A. *J. Chem. Phys.*, 1956, 24, 966.
21. Marcus, R. A. *J. Phys. Chem.*, 1963, 67, 853.
22. Marcus, R. A. *J. Chem. Phys.*, 1965, 43, 67.
23. Millar, J. R.; Calcaterra, L. T.; Closs, G. L. *J. Am. Chem. Soc.*, 1984, 106, 3047.
24. Closs, G. L.; Calcaterra, L. T.; Green, N. J.; Penfield, K. W.; Millar, J. R. *J. Phys. Chem.*, 1986, 90, 3673.
25. Gunner, M. R.; Robertson, D. E.; Dutton, P. L. *J. Phys. Chem.*, 1986, 90, 3783.
26. Nakabayashi, S.; Fijishima, A.; Honda, K. *J. Phys. Chem.*, 1983, 87, 3487.
27. Wasielewski, M. R.; Niemczyk, M. P. *J. Am. Chem. Soc.*, 1984, 106, 5043.
28. Wasielewski, M. R.; Niemczyk, M. P.; Svec, W. A.; Pewitt, E. B. *J. Am. Chem. Soc.*, 1985, 107, 1080.
29. Cohen, H.; Efrima, S.; Meyerstein, D.; Nutkovich, M.; Weighart, K. *Inorg. Chem.*, 1983, 22, 688.
30. Crawford, M. K.; Wang, Y.; Eisenthal, K. E. *Chem. Phys. Lett.*, 1981, 79, 529.
31. Wang, Y.; Crawford, M. C.; Eisenthal, K. E. *J. Am. Chem. Soc.*, 1982, 104, 5874.
32. Luo, X. -J.; Beddard, G. S.; Porter, G.; Davidson, R. S.; Whelan, T. D. *J. Chem. Soc. Faraday Trans. I*, 1982, 78, 3467.
33. Mataga, N. *Pure Appl. Chem.*, 1984, 56, 1255.
34. Gust, D.; Moore, T. A.; Moore, A. L. *Acc. Chem. Res.*, 1993, 26, 198.
35. Kurreck, H.; Huber, M. *Angew. Chem. Int. Ed. Engl.*, 1995, 34, 849.
36. Sun, Y. -P. In *Molecular and Supramolecular Photochemistry, Vol. 1*, Ramamurthy, V.; Schanze, K. S. (Eds.), 1997, pp 325-390.

37. Arbogast, J. W.; Foote, C. S. *J. Am. Chem. Soc.*, **1991**, *113*, 8886.
38. Arbogast, J. W.; Darmanyan, A. P.; Foote, C. S.; Rubin, Y.; Diederich, F. N.; Alvarez, M. M.; Whetten, R. B. *J. Phys. Chem.*, **1991**, *95*, 11.
39. Wang, Y. *J. Phys. Chem.*, **1992**, *96*, 764.
40. Sension, R. J.; Szarka, A. Z.; Smith, G. R.; Hochstrasser, R. M. *Chem. Phys. Lett.*, **1991**, *185*, 179.
41. Yu, G.; Gao, J.; Hummelen, J. C.; Heeger, A. J. *Science*, **1995**, *270*, 1789.
42. Wang, Y. *Nature (London)*, **1992**, *356*, 585.
43. Sariciftic, N. S.; Smilowitz, L.; Heeger, A. J.; Wudl, F. *Science*, **1993**, *258*, 1474.
44. Sauve, G.; Dimitrijevic, N. M.; Kamat, P. V. *J. Am. Chem. Soc.*, **1995**, *99*, 1199.
45. Watanabe, A.; Ito, O. *J. Chem. Soc. Chem. Commun.*, **1994**, 1285.
46. Linde, J. R.; Pong, R. G. S.; Bartoli, F. J.; Kafafi, Z. H. *Phys. Rev. B-Condensed Matter*, **1993**, *48*, 9447.
47. Imahori, H.; Sakata, Y. *Adv. Mater.*, **1997**, *9*, 537.
48. Tokuyama, H.; Yamago, S.; Nakamura, E.; Shiraki, T.; Sugiura, Y. *J. Am. Chem. Soc.*, **1993**, *115*, 7918.
49. Friedman, S. H.; Decamp, D. L.; Sigbesma, R. P.; Srdanov, G.; Wudl, F.; Kenyon, G. L. *J. Am. Chem. Soc.*, **1993**, *115*, 6506.
50. Hirsch, A. *The Chemistry of the Fullerenes*, Thieme, Stuttgart, **1994**, Chapter 4.
51. Martin, M.; Sanchez, L.; Illescas, B.; Perez, I. *Chem. Rev.*, **1998**, *98*, 2527.
52. Liddell, P. A.; Sumida, J. P.; MacPherson, A. N.; Noss, L.; Seely, G. R.; Clark, K. N.; Moore, A. L.; Moore, T. A.; Gust, D. *Photochem. Photobiol.*, **1994**, *60*, 537.
53. Liddell, P. A.; Kuciauskas, D.; Sumida, J. P.; Nash, B.; Nguyen, D.; Moore, A. L.; Moore, T. A.; Gust, D. *J. Am. Chem. Soc.*, **1997**, *119*, 1400.
54. Imahori, H.; Hagiwara, K.; Aoki, M.; Akiyama, T.; Taniguchi, S.; Okada, T.; Shirakawa, M.; Sakata, Y. *J. Am. Chem. Soc.*, **1996**, *118*, 11771.
55. Williams, R. M.; Koeberg, M.; Lawson, J. M.; An, Y. -Z.; Rubin, Y.; Paddon-Row, M. N.; Verhoeven, J. W. *J. Org. Chem.*, **1996**, *61*, 5055.

56. Guldi, D. M.; Maggini, M.; Scorrano, G.; Prato, M. *J. Am. Chem. Soc.*, **1997**, *119*, 974.
57. Maggini, M.; Guldi, D. M.; Mondini, S.; Scorrano, G.; Paolucci, F.; Ceroni, P.; Roffia, S. *Chem. Eur. J.*, **1998**, *4*, 1992.

## Chapter 2

### Photophysical and Orientation Dependent Electron Transfer Processes in Fullerene-Aniline Dyads

#### 2.1. Abstract

Synthesis and photoinduced electron transfer processes in a series of *ortho*- and *para*-substituted fullerene-aniline dyads are reported. Molecular mechanics calculations suggested folded conformations for *ortho*-substituted dyads and extended ones for *para*-substituted dyads. A weak charge-transfer band, resulting from the ground state interaction between the lone pair electrons of the anilinic nitrogen and C<sub>60</sub>, is observed around 700 nm for all the dyads under investigation. The fluorescence quantum yield of the dyads and the model compounds were found to be nearly identical in nonpolar solvents such as toluene, indicating the absence of any electron transfer process. A decrease in the quantum yield of fluorescence, however, was observed for the dyads in polar solvents, such as benzonitrile, which is attributed to an electron transfer process from the anilinic nitrogen to C<sub>60</sub>. The rate constants for charge separation ( $k_{CS}$ ), its efficiencies ( $\phi_{CS}$ ) and details of excited state properties of the dyads have been investigated using steady-state fluorescence and time resolved flash photolysis. The marked increase in the rate constants and quantum yields of charge separation, observed in the case of the *ortho*-substituted dyads are attributed to a topographically controlled electron transfer process. The intramolecular electron transfer processes in these systems were confirmed on the basis of time resolved flash photolysis studies.

## 2.2. Introduction

Light-induced electron transfer processes play a key role in photosynthetic systems<sup>1,2</sup> and in the design of artificial molecular devices based on donor-acceptor pairs.<sup>3</sup> In the case of natural photosynthetic systems, one of the prime factors responsible for the high efficiency of electron transfer is the well-defined orientation of various chromophoric units in the protein matrices.<sup>1,2</sup> As mentioned in Chapter 1, a model 'dyad' system consists of a donor group covalently linked to an acceptor group, through a spacer group. Several strategies have been adopted for the design of such donor-bridge-acceptor (D-B-A) systems, which can generate long lived, charge separated states with high efficiency and slow charge recombination rates.<sup>4-10</sup> Linked porphyrin-quinone systems have been extensively investigated as models to test the effect of distance, orientation and redox properties of the donor-acceptor pairs on charge separation and recombination processes.<sup>11-14</sup> These studies indicate that the nature of the bridging groups used in the D-B-A systems, plays a significant role in controlling the orientation and distance of separation of the donor-acceptor pair. Effect of distance and orientations on electron transfer processes in porphyrin-quinone systems 1 and 2 (Chart 2.1) have been reported by Osuka et al..<sup>13</sup> The fluorescence emission from the porphyrin is more efficiently quenched in the case of the *ortho*-substituted derivatives than for with *para*-substituted ones.

In this Chapter, we have discussed the results of our detailed investigation on the photophysical and orientation-dependent electron transfer studies of fullerene-aniline based D-B-A systems (5-8 in Chart 2.3). Photoinduced electron transfer processes in fullerene-based systems containing donors such as anilines, ferrocenes,

processes in fullerene-based systems containing donors such as anilines, ferrocenes, porphyrins and ruthenium complexes have been reviewed in Chapter 1. Fullerene-aniline based D-B-A systems under investigation have close resemblance to the polycyclic aromatic hydrocarbon-aniline pairs 3 and 4 (Chart 2.2). A brief overview of such systems is presented in Section 2.2.1.

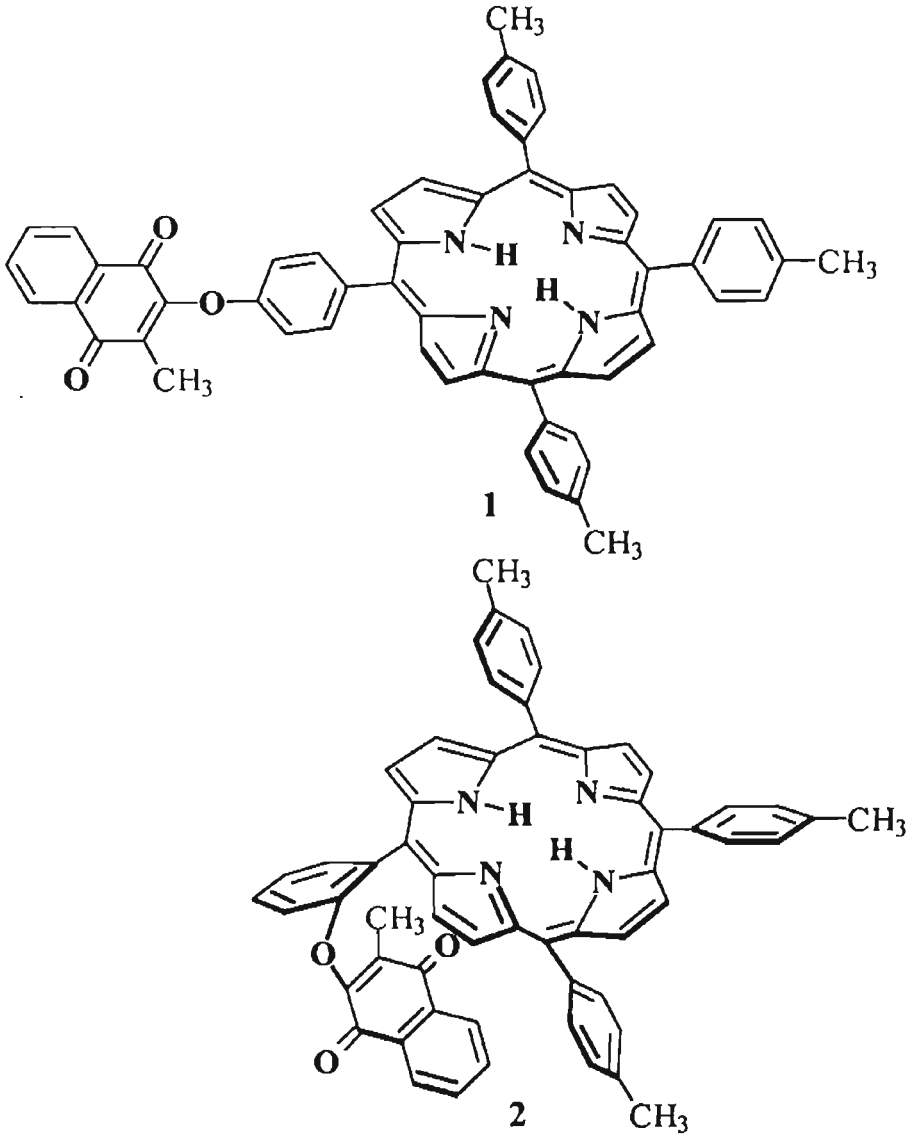


Chart 2.1

### 2.2.1. Aromatic hydrocarbon-aniline based D-B-A systems

Photoinduced intramolecular exciplex formation and competitive electron transfer in polycyclic aromatic hydrocarbon-aniline based dyads containing various hydrocarbon acceptor groups and polymethylene linker groups have been reported.<sup>14-16</sup> These competitive processes have been systematically examined in the case of 9-anthranyl-(CH<sub>2</sub>)<sub>3</sub>-N,N-dimethylaniline system **3** (Chart 2.2) by Eisenthal and co-workers<sup>14</sup> and 1-pyrenyl-(CH<sub>2</sub>)<sub>3</sub>-N,N-dimethylaniline system **4** (Chart 2.2) by Mataga and co-workers.<sup>15</sup>

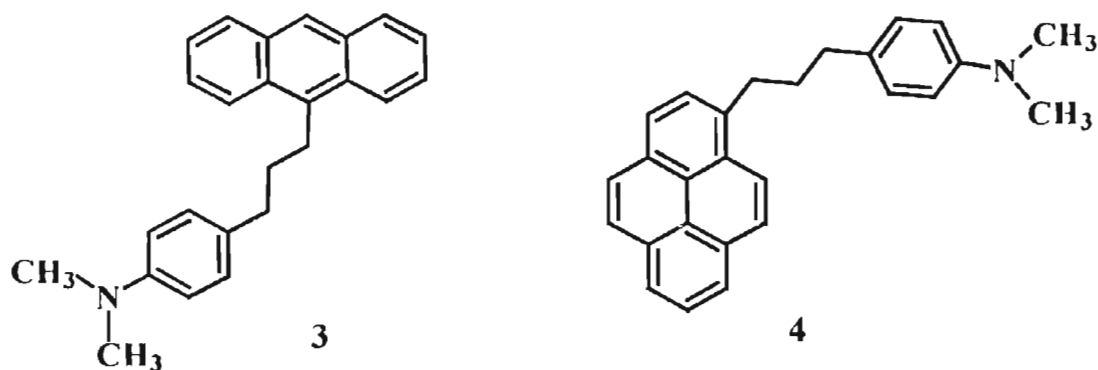


Chart 2.2

The effect of variation of chain length on electron transfer versus exciplex formation in 9-anthranyl-(CH<sub>2</sub>)<sub>n</sub>-N,N-dimethylaniline systems has been demonstrated by Yang and co-workers.<sup>16</sup> Depending on the polarity and chain length, two idealized extreme ground state conformations, folded and extended, have been reported. It has also been concluded that exciplex formation is more favorable in nonpolar solvents and in systems with shorter methylene chains.

In the present study, we have synthesized a series of D-B-A systems, by attaching an anilinic donor to the *ortho*- as well as *para*- positions of the phenyl

groups of fullerene(1-methyl-2-phenyl)pyrrolidine, linked by methylene chains (5-8 in Chart 2.3). Various light-induced processes in these systems were investigated employing both steady state and time resolved spectroscopy. These results are compared with photoprocesses in the model compounds 9 and 10 (Chart 2.3), which do not possess the appended anilinic donor group.

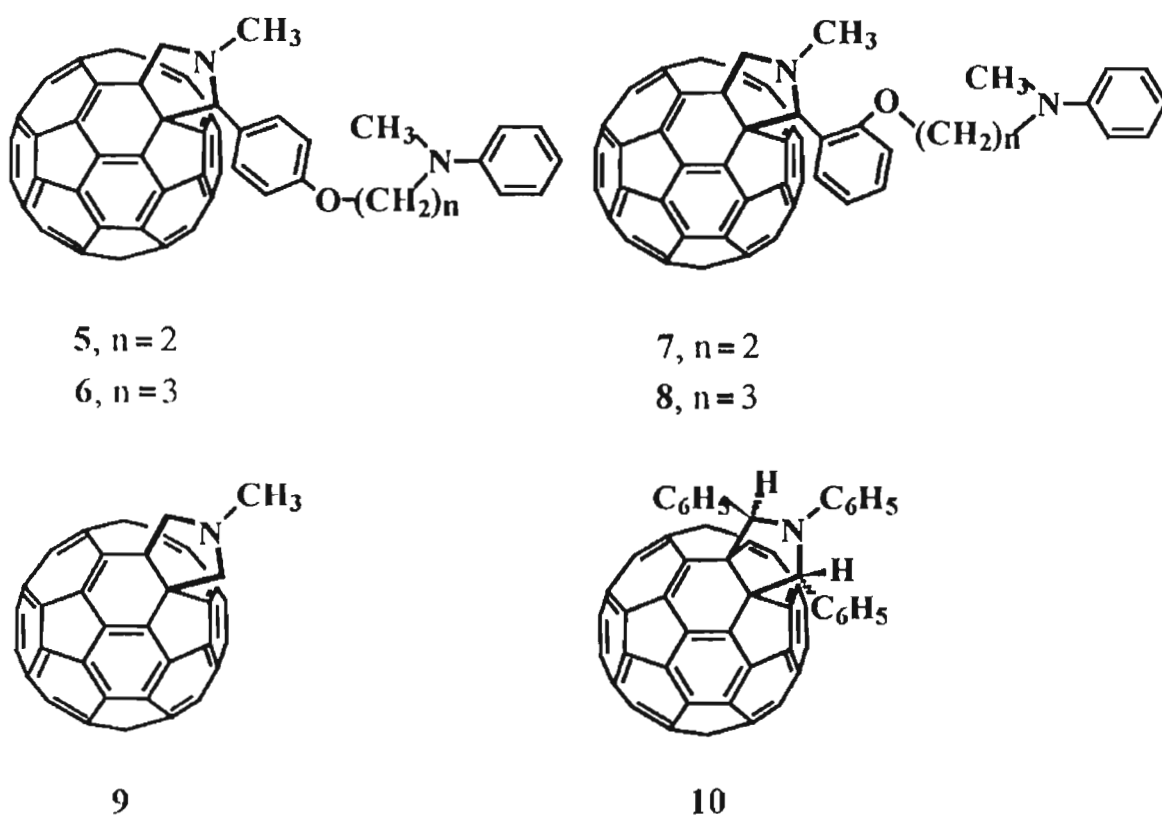


Chart 2.3

## 2.3. Results and Discussion

### 2.3.1. Synthesis and characterization

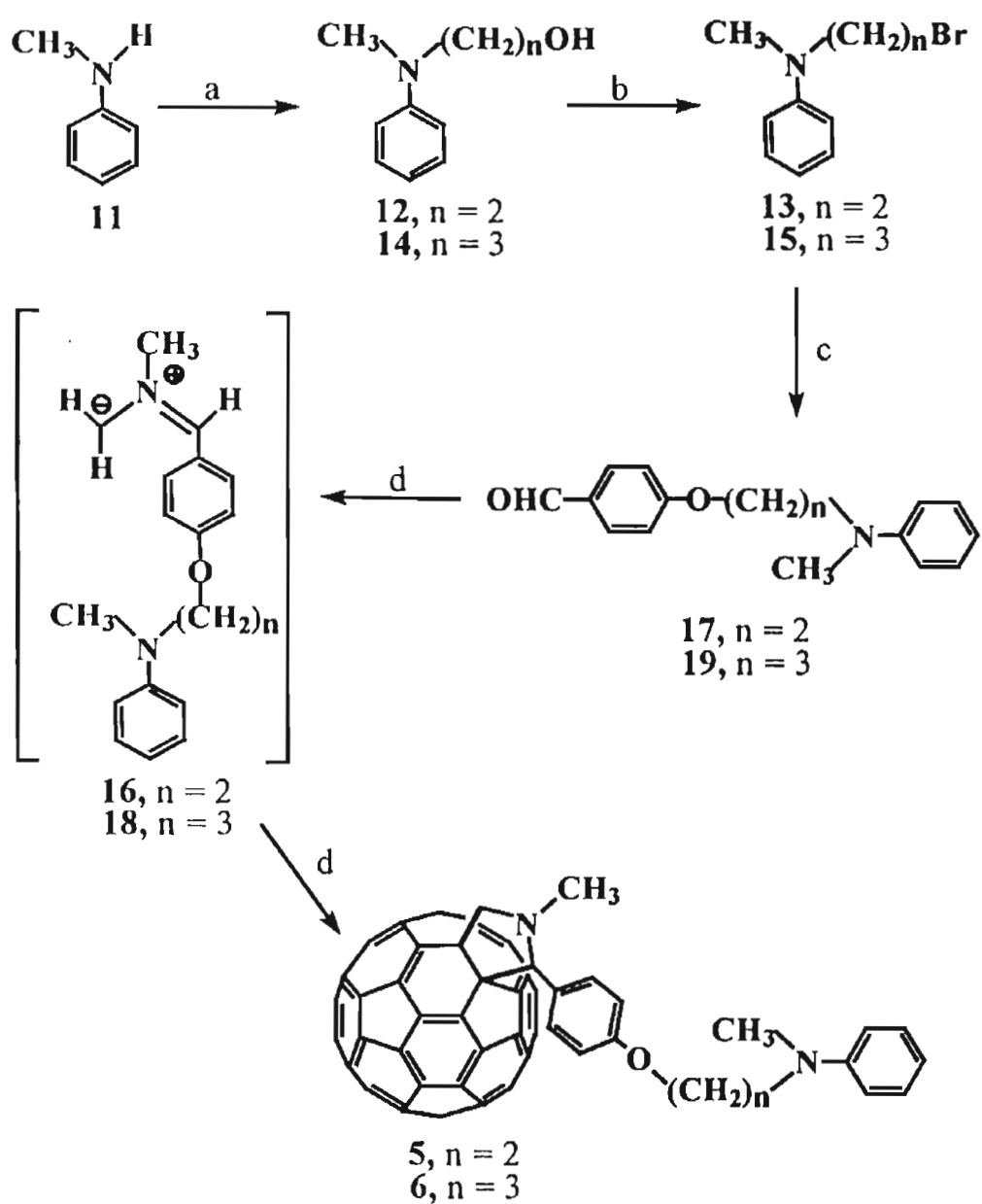
Cycloaddition reactions have been extensively used as a general method for functionalizing  $C_{60}$ <sup>17-27</sup> and are found to be useful for the synthesis of several novel  $C_{60}$  derivatives in which the fullerene properties are combined with those of other



classes of compounds. One of the most widely used methods for functionalizing  $C_{60}$  is the 1,3-dipolar cycloaddition reaction of an azomethine ylide to  $C_{60}$ . Several methods have been reported for the generation of azomethine ylides and one of the most successful approaches involves the decarboxylation of immonium salts, derived through the condensation of  $\alpha$ -amino acids with aldehydes.<sup>22</sup> In the present study, the decarboxylation route was adopted for the synthesis of the fullerene-aniline dyads 5-8.

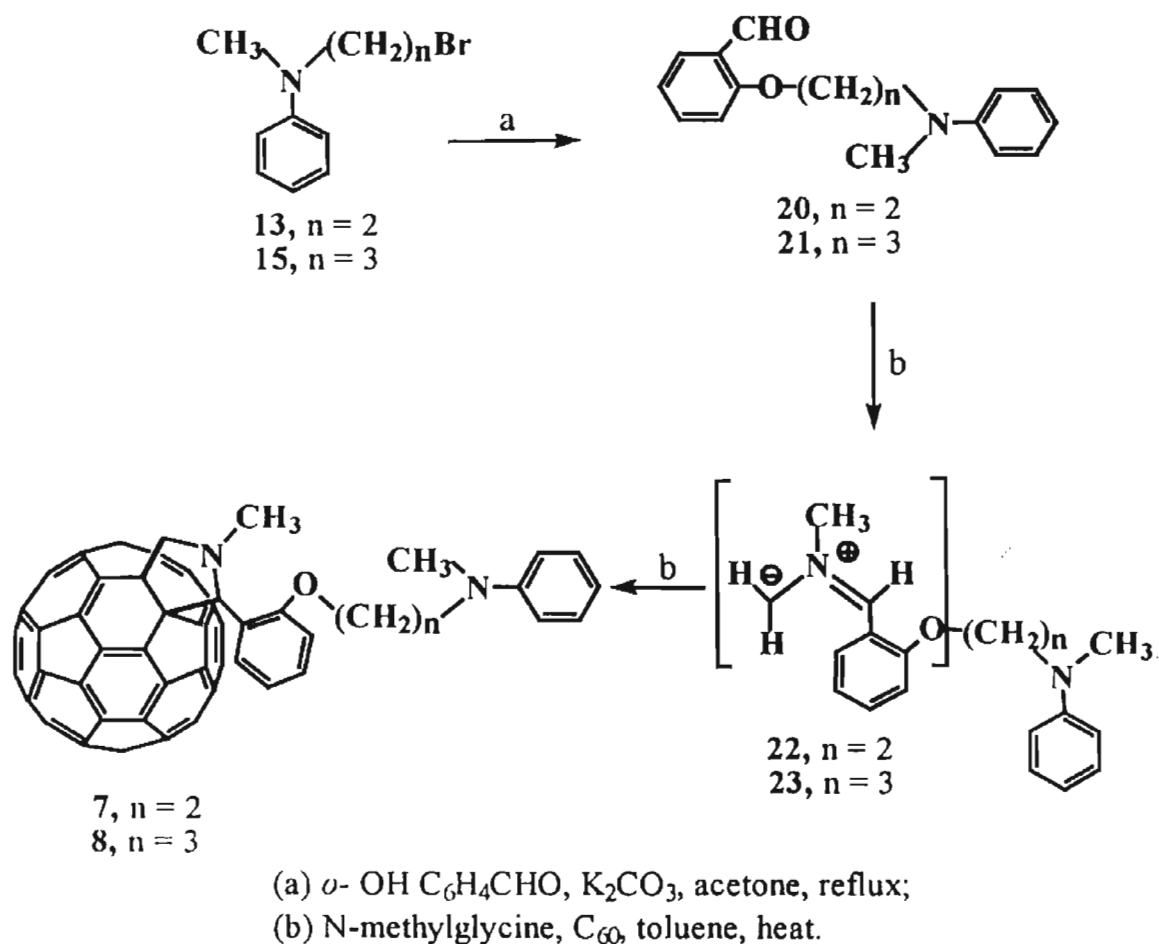
Synthesis of the *para*- and the *ortho*- substituted fullerene-aniline dyads 5-8 were achieved through the sequence of reactions shown in Schemes 2.1 and 2.2, respectively. N-methyl,N- $\{(\omega$ -hydroxy)-1-alkyl}anilines (12, 14) were prepared through reported procedures<sup>29a</sup> and they were converted to the corresponding N-methyl,N- $\{(\omega$ -bromo)-1-alkyl}anilines (13, 15) by treatment with phosphorous tribromide. The bromo- derivatives were further treated with the corresponding hydroxybenzaldehydes to yield the required aldehydes, N-methyl,N- $\{(\text{formylphenoxy})$ -alkyl}anilines (17,19,21 and 23). Synthesis of the fullerene-aniline dyads 5-8 was achieved by a 1,3-dipolar cycloaddition reaction of the azomethine ylides, generated through a thermal reaction of the corresponding aldehydes and N-methylglycine, with  $C_{60}$ . The crude reaction product, in each case, was purified by chromatography over silica gel (100-200 mesh) to give the appropriate dyads in a 45-50 % yield.

Thermal ring opening of aziridines is known to give rise to the corresponding azomethine ylides. The synthesis of the model fullerene system 10 was achieved by adopting this route (Scheme 2.3). Heating a mixture of  $C_{60}$  and 1,2,3-triphenylaziridine<sup>29b</sup> in refluxing toluene gave a mixture of two products, identified as fullero-1,2,5-triphenylpyrrolidine (10) and fullero-bis(1,2,5-triphenylpyrrolidine) (26).



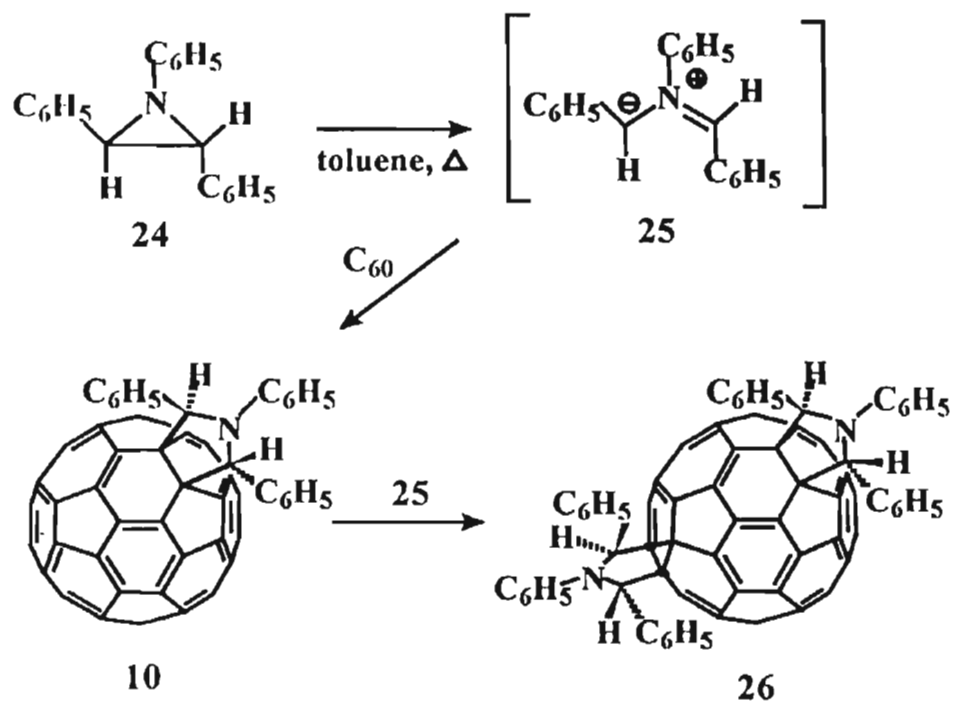
(a)  $\text{X(CH}_2\text{)}_2\text{OH}$  ( $\text{X} = \text{Cl/Br}$ ),  $\text{K}_2\text{CO}_3$ ,  $\text{I}_2$ ,  $n$ -butanol, reflux; (b)  $\text{PBr}_3$ ,  $\text{CH}_2\text{Cl}_2$ , room temperature; (c)  $p$ -OH  $\text{C}_6\text{H}_4\text{CHO}$ ,  $\text{K}_2\text{CO}_3$ , acetone, reflux; (d)  $N$ -methylglycine,  $\text{C}_{60}$ , toluene, heat.

Scheme 2.1

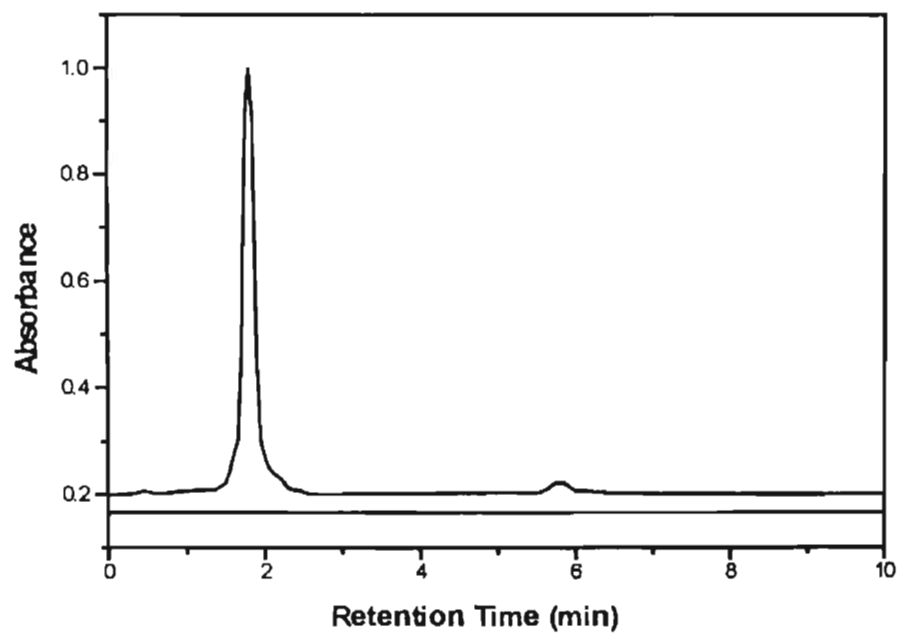


Scheme 2.2

It is known that the thermal ring opening of aziridines proceeds in a conrotatory mode, whereas the photochemical opening proceeds in a disrotatory manner.<sup>30</sup> The starting 1,2,3-triphenylaziridine would be expected to undergo thermal conrotatory ring opening to give the *trans*-azomethine ylide **25**, which on cycloaddition with C<sub>60</sub> would give the fullerene-1,2,5-triphenylpyrrolidine **10**, as shown in Scheme 2.3. It is inferred that the phenyl groups at 2 and 5 positions of the pyrrolidine moiety are *trans* with respect to each other on the assumption that the azomethine ylide **25** does not undergo isomerization to the *cis* form, prior to cycloaddition, although this possibility cannot be fully ruled out.<sup>31</sup>



Scheme 2.3

Figure 2.1. Chromatogram (HPLC)<sup>32</sup> of the dyad 5.

The bis-adduct **26** is formed through the further reaction of the mono-adduct **10** with the azomethine ylide **25**. HPLC analysis<sup>32</sup> of **26** using a Bucky Prep column, showed three peaks corresponding to three regio isomers in the ratio 1: 3: 5. Hirsh et al.<sup>28</sup> have carried out detailed studies on the regioselectivity of various bis-adducts of C<sub>60</sub>, formed from the corresponding mono-adducts. They have shown that out of the possible eight isomeric bis-adducts, the *e*-isomer and the *trans*-3 isomer predominate. Of these two, the *e*-isomer is formed more readily and in larger amounts. The photophysical studies of the bis-adduct have not been carried out at present due to the presence of different regio isomers.

All new compounds were fully characterized on the basis of analytical results and spectral data. Detailed experimental procedures for the synthesis, purification and characterization of the dyads, the model compounds and the precursors are given in Section 2.5. Purity of all the fullerene-aniline dyads and model compounds was confirmed by HPLC analysis.<sup>32</sup> As a representative example, the chromatogram of the fullerene-aniline dyad **5** is shown in Figure 2.1.

### 2.3.2. Computational studies

The different conformations of the fullerene-bridge-aniline dyads were obtained using the Sybyl force field method.<sup>29,33</sup> Computational studies suggest that the most stable conformations in the case of the *para*-substituted dyads **5** and **6** are the extended ones, while both the *ortho*-substituted dyads, **7** and **8** possess a folded conformation. Representative examples of the extended form of the dyad **6** and the folded form of the dyad **8** are displayed in Figures 2.2 and 2.3, respectively.

Based on calculations, the edge to edge distances between the anilinic nitrogen and C<sub>60</sub> were found to be much larger for the *para*-substituted compounds

(9.48 Å for 5 and 10.01 Å for 6), when compared to the *ortho*-substituted compounds (3.28 Å for 7 and 4.01 Å for 8). Computational studies also indicate that there is an additional advantage in using  $C_{60}$  as an acceptor, particularly in the case of the *ortho*-substituted dyads. This is mainly due to the spherical shape of  $C_{60}$ . Over the entire spherical structure,  $\pi$ - electron cloud is available and the folding of the anilinic group in proximity to anywhere on the surface of  $C_{60}$  may allow the transfer of an electron, with an enhanced rate.

In the folded conformation (Figure 2.3), a specific orientation may not be required between the donor and acceptor. In order to investigate this possibility in the *ortho*-substituted dyads, we have undertaken detailed studies of the ground and excited state properties of the fullerene-aniline systems, 5-8.

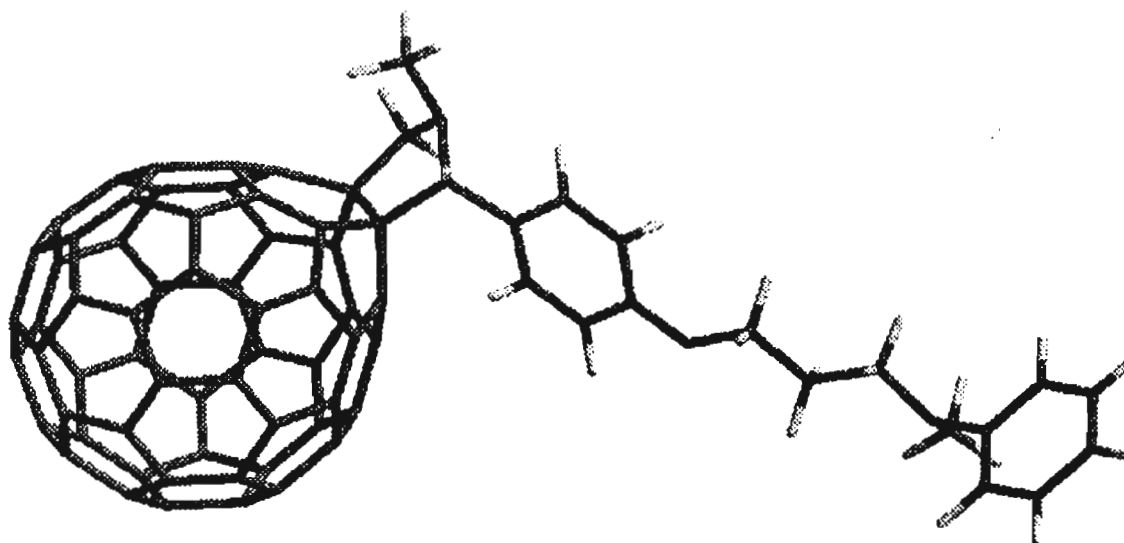


Figure 2.2. The minimum energy configuration of the dyad 6 obtained using molecular mechanics calculation.

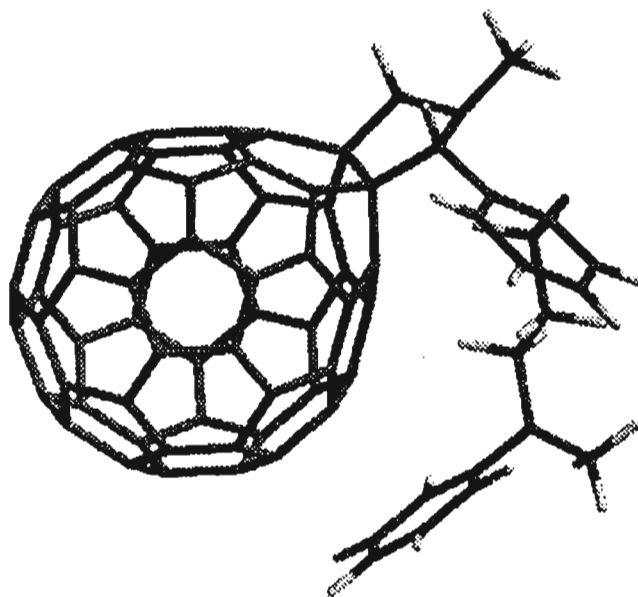


Figure 2.3. The minimum energy configuration of the dyad **8** obtained using molecular mechanics calculation.

### 2.3.3. NMR studies

Further information regarding the folding of the anilinic group on to the surface of  $C_{60}$  was obtained by comparing the  $^1H$  NMR spectra of the *para*- and the *ortho*- substituted dyads. Figure 2.4 illustrates the  $^1H$  NMR spectra, in the region 3.2-6.0 ppm, for the *para*- substituted dyad **6** and the *ortho*- substituted dyad **8**. The triplets observed at 3.54 and 4.01 ppm for the *para*- substituted dyad **6** (spectrum 'a' in Figure 2.4) can be assigned to the  $NCH_2$  (anilinic) and  $OCH_2$  protons, respectively. The doublets at  $\delta$  4.25 and  $\delta$  4.98 ppm correspond to the *exo*- and *endo*- protons of the pyrrolidine ring and their positions remain more or less the same for the *ortho*-substituted dyad **8** (spectrum 'b' in Figure 2.4). The singlet observed at  $\delta$  4.88 ppm for the *para*- substituted dyad **6** is due to the methyne proton of the pyrrolidine ring. Interestingly a large downfield shift is observed for this proton, in the case

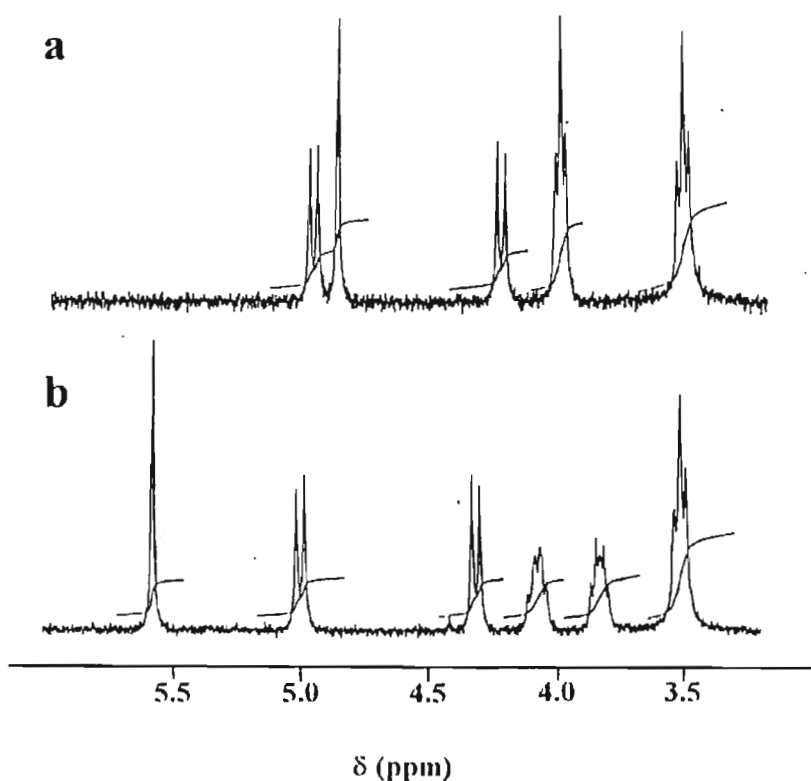


Figure 2.4. Comparison of the  $^1\text{H}$  NMR spectra ( $\delta$  3.2-6.0 ppm) of the *para*-substituted dyad and the *ortho*-substituted dyad: (a) **6**, (b) **8**.

of the *ortho*-substituted dyad **8**. Similarly, the  $\text{OCH}_2$  protons are observed as two separate multiplets in the case of the *ortho*-substituted dyad **8**, while for the *para*-substituted dyad **6**, it is a triplet. For the *ortho*-substituted dyad **8**, having three methylene groups, the  $\text{NCH}_2$  protons are observed as a triplet whereas for the *ortho*-substituted dyad **7**, having two methylene groups, the  $\text{NCH}_2$  protons are observed as two separate multiplets. These effects observed for the *ortho*-substituted dyads may be, originating from the spatial interactions of the  $\pi$ -electrons of  $\text{C}_{60}$  (as well as phenyl group) and the methylene groups, indicative of the proximity of  $\text{C}_{60}$  and anilinic donor group.



#### 2.3.4. Steady state absorption properties

Absorption spectra of the fullerene-aniline dyads **5-8** and the model compounds **9** and **10** in the visible region are significantly red-shifted and are distinctly different from that of the parent  $C_{60}$ . Figure 2.5 shows the absorption spectra of the dyad **5** and the model compound **10**, recorded in dichloromethane at room temperature.<sup>29</sup> In general, all the compounds under investigation possess a long wavelength band around 700 nm similar to those observed in substituted fulleropyrrolidines and methanofullerenes.<sup>34,35</sup> Recently, Bensasson et al. have reported the spectral properties of a few methanofullerenes and have suggested that the 700 nm band observed in these cases may be originating, either from one of the orbitally forbidden transition of  $C_{60}$  or from a spin-forbidden transition to the lowest triplet state.<sup>35</sup> In the case of the fullerene-aniline dyads **5-8** (Chart 2.3), there is an additional possibility of a long wavelength charge transfer band, due to the ground state electronic interaction between the donor and the acceptor moieties.

The existence of the charge transfer band in the dyads was established by investigating the influence of trifluoroacetic acid (TFA) on the absorption spectra of the dyads and model compounds. Addition of TFA (25 mM) to dichloromethane solutions of the dyads **5-8** resulted in a partial disappearance of the band around 700 nm. As a representative example, this spectral change in the case of the dyad **5** is shown in Figure 2.5. Protonation of the anilinic nitrogen inhibits the charge transfer interaction between the appended anilinic group and the fullerene. For all the dyads under investigation, these changes are completely reversed by adding pyridine (30 mM). By contrast, the absorption spectra of the model compounds **9** and **10** were found to be unaffected by the addition of TFA (up to 250 mM), ruling out the possibility of a

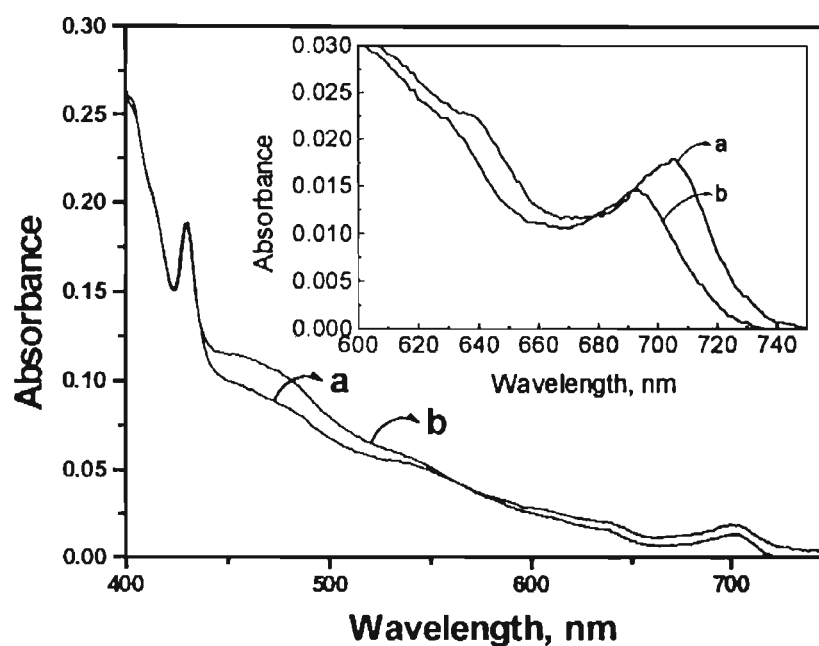


Figure 2.5. Absorption spectra of the fullerene-aniline dyad **5** (a) and the model compound **10** (b) in dichloromethane. Inset shows the effect of trifluoroacetic acid on long wavelength band of **5**: (a) 0 mM TFA, (b) 25 mM TFA.

ground state charge transfer interaction of the pyrrolidine ring nitrogen with  $C_{60}$ .

These results indicate that the 700 nm band observed in the case of the model fulleropyrrolidines **9** and **10** may be originating from a forbidden transition as indicated by Bensasson et al.. Merged together with this, a weak charge transfer band is also observed in the case of the dyads **5-8** in the same spectral region, resulting from the ground state electronic interaction between the lone pair of the anilinic nitrogen and the fullerene  $\pi$ -electron systems. In addition to the long wavelength band, the dyads **5-8** as well as the model fulleropyrrolidines (**9** and **10**) possess a sharp absorption band around 430 nm (Figure 2.5). This band is characteristic of mono functionalized  $C_{60}$ , which arises due to the deficiency of  $60-\pi$  electrons.<sup>35</sup>

### 2.3.5. Steady state emission properties<sup>29</sup>

$C_{60}$  exhibits weak fluorescence at room temperature with a quantum yield ( $\phi_f$ ) of  $2.2 \times 10^{-4}$  in toluene and both the fluorescence spectrum and  $\phi_f$  are found to be independent of the excitation wavelength.<sup>36</sup> The fluorescence spectral profile and properties of monofunctionalized fullerene derivatives are quite different from that of  $C_{60}$ . Results of systematic studies of the fluorescence properties of various classes of monofunctionalized fullerene derivatives, including fulleropyrrolidines, are reported in the literature. One of the noticeable features of these types of systems is the presence of a band around 700 nm, which is the mirror image of the 0-0 absorption band. Studies from our group and other groups indicate that the spectral profile and the quantum yields of model fulleropyrrolidines are independent of the nature of the solvent. Also, the emission properties are unaffected by the addition of TFA (0.2 M), indicating that the lone pair of nitrogen on the pyrrolidine ring, does not affect its emission behaviour. In a recent publication,<sup>34</sup> Prato and Maggini have addressed the interesting question, on how the fullerene spheroid influences the acid-base properties of the pyrrolidine nitrogen, by studying  $pK_{BH^+}$  of a substituted fulleropyrrolidine and its corresponding pyrrolidine. They have found that the fulleropyrrolidine derivatives are almost six orders of magnitude less basic than the corresponding pyrrolidine and these results can be attributed to some kind of through-space interaction of the nitrogen lone pair with the fullerene  $\pi$ -electron system. This was further confirmed by studying the reaction rates of fulleropyrrolidines with methyl iodide which was found to be much slower, indicating a diminished availability of the nitrogen lone pair in fulleropyrrolidine. From these results it is evident that the pyrrolidine nitrogen is not involved in the

quenching process. However, the linked aniline group can act as a good quencher for the singlet excited fullerene and details of the intermolecular fluorescence quenching studies, between the model compound **10** and N,N-dimethylaniline (DMA), are indicated below.

### 2.3.5.1. Fluorescence quenching of **10** by N,N-dimethylaniline (DMA)

In the present study, we have observed that the addition of N,N-dimethylaniline (DMA) to a solution of the model compound **10** in 1:1 toluene and acetonitrile led to the quenching of fluorescence of **10** (Figure 2.6). The bimolecular rate constant for quenching,  $k_q$  was estimated using the Stern-Volmer equation (Eq. 2.1), by plotting the ratio of the fluorescence intensity without DMA ( $I_0$ ) to the fluorescence intensity with DMA ( $I$ ), against the concentration of DMA,

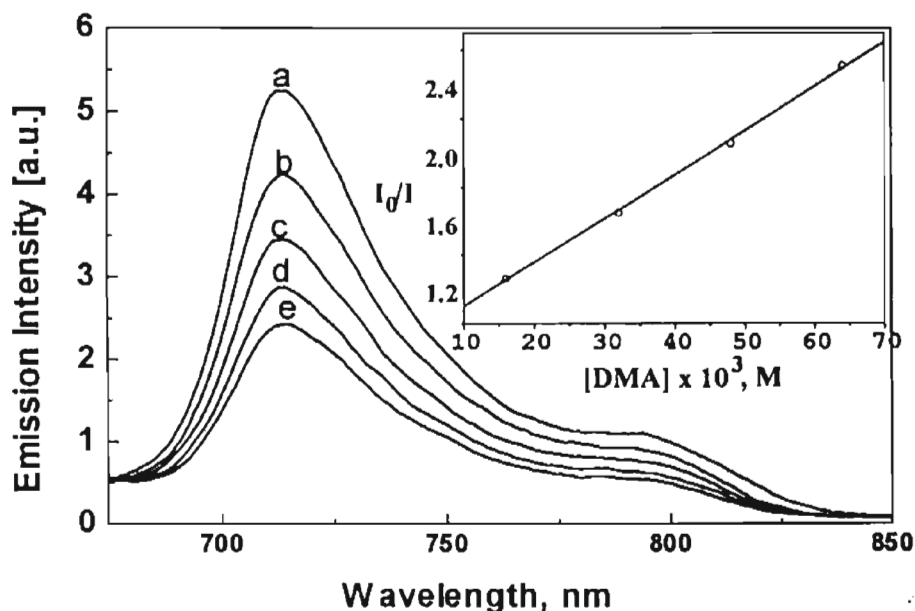


Figure 2.6. Influence of N,N-dimethylaniline [DMA] concentrations on the emission spectrum of **10** in toluene-acetonitrile (1:1) mixture. [DMA] (a) 16 mM, (b) 32 mM, (c) 48 mM, (d) 64 mM. Inset shows the plot of the ratio of fluorescence intensities ( $I_0/I$ ) against DMA concentration.

$$I/I_0 = 1 + K_{sv} [\text{DMA}] \quad (\text{Eq. 2.1})$$

$$= 1 + k_q \tau [\text{DMA}] \quad (\text{Eq. 2.2})$$

where,  $K_{sv}$  is the Stern-Volmer constant and  $\tau$ , is the fluorescence lifetime of **10** in the absence of DMA. A linear plot was obtained (inset of Figure 2.6) and the bimolecular rate constant  $k_q$  was estimated as  $3.8 \times 10^{10} \text{ M}^{-1}\text{s}^{-1}$ . The fluorescence spectral profiles of the dyads **5-8** were found to be nearly identical to that of the model compound and we have investigated in detail the emission properties of these dyads.

### 2.3.5.2. Fluorescence emission properties of dyads 5-8

The fluorescence properties<sup>37-42</sup> of the dyads were investigated in solvents of varying polarity and are summarized in Table 2.1. The fluorescence spectral profiles and the quantum yields of the dyads **5-8** and the model compound **9**<sup>43,44</sup> were found to be nearly identical in a nonpolar solvent such as toluene, indicating the absence of any electron transfer process (Figure 2.7). A comparison of the emission spectra of the *ortho*- and the *para*- substituted dyads in a polar solvent such as benzonitrile is shown in Figure 2.8. In the present case, a marked decrease in the quantum yield of fluorescence was observed particularly for the *ortho*-substituted dyads (Table 2.1).

In general, a decrease in the quantum yield of fluorescence was observed for the dyads **5-8** with increase in solvent polarity and representative examples are displayed in Figures 2.9 and 2.10. Similar results were reported for other fullerene-aniline dyads connected through rigid spacers and fullerene-ferrocene dyads.<sup>43,45,46</sup> The decrease in the fluorescence yield in polar solvents is due to the reductive quenching of the singlet excited states of fullerene by the aniline moiety in the dyads. This was confirmed by studying the effect of addition of TFA on the emission properties of the dyads.

Table 2.1. Fluorescence quantum yield ( $\phi_f$ ), rate constant of charge separation ( $k_{cs}$ ) and quantum yield of charge separation ( $\phi_{cs}$ ) for the dyads 5-8

Solvent	5		6		7		8	
	$\Phi_f \times 10^4$	$k_{cs} \times 10^{-9} \text{ s}^{-1}$ ( $\phi_{cs}$ )	$\Phi_f \times 10^4$	$k_{cs} \times 10^{-9} \text{ s}^{-1}$ ( $\phi_{cs}$ )	$\Phi_f \times 10^4$	$k_{cs} \times 10^{-9} \text{ s}^{-1}$ ( $\phi_{cs}$ )	$\Phi_f \times 10^4$	$k_{cs} \times 10^{-9} \text{ s}^{-1}$ ( $\phi_{cs}$ )
Toluene	6.9		6.8		6.7		6.6	
Dichloro- methane	4.4	0.28 (26%)	3.3	0.64 (45%)	1.7	2.0 (72%)	1.0	4.7 (86%)
Benzonitrile	3.1	0.73 (48%)	3.08	0.74 (49%)	0.2	21.5 (97%)	0.25	18.8 (96%)

$k_{cs}$  values were estimated as  $[(\phi_{ref}/\phi)-1]/\tau_{ref}$  where  $\phi_{ref}$  and  $\tau_{ref}$  are the fluorescence quantum yield and lifetime of the model compound 9 [ $\phi_{ref}^{4.7a} = 6.0 \times 10^{-4}$ ,  $\tau_{ref} = 1280 \text{ ps}$ ].  $\phi_{cs}$  values are estimated as  $k_{cs}/[(1/\tau_{ref}) - k_{cs}]$ .

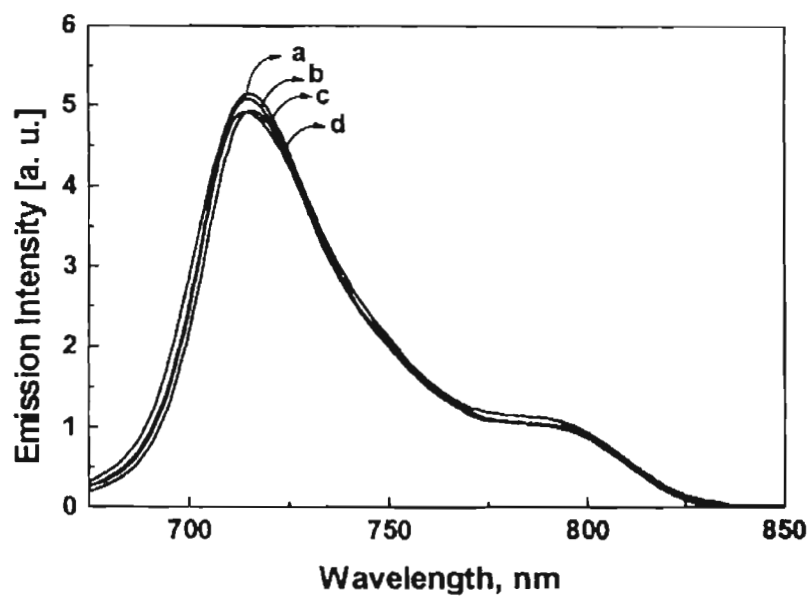


Figure 2.7. Emission spectra of the fullerene-aniline dyads 5-8 in toluene: (a) 5, (b) 6, (c) 8, (d) 7 (Absorbance of the solutions were adjusted to 0.1 at the excitation wavelength, 470 nm).

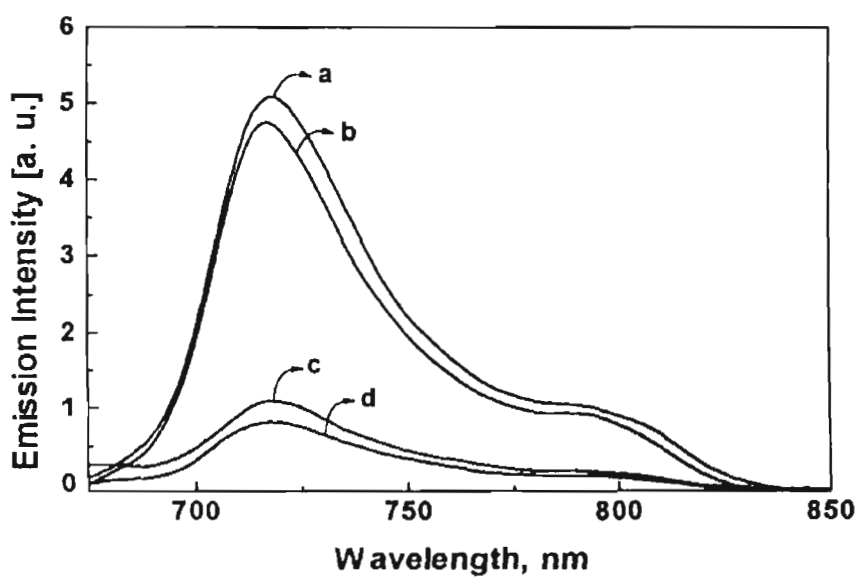


Figure 2.8. Emission spectra of the fullerene-aniline dyads 5-8 in benzonitrile: (a) 5, (b) 6, (c) 8, (d) 7 (Absorbance of the solutions were adjusted to 0.1 at the excitation wavelength, 470 nm).

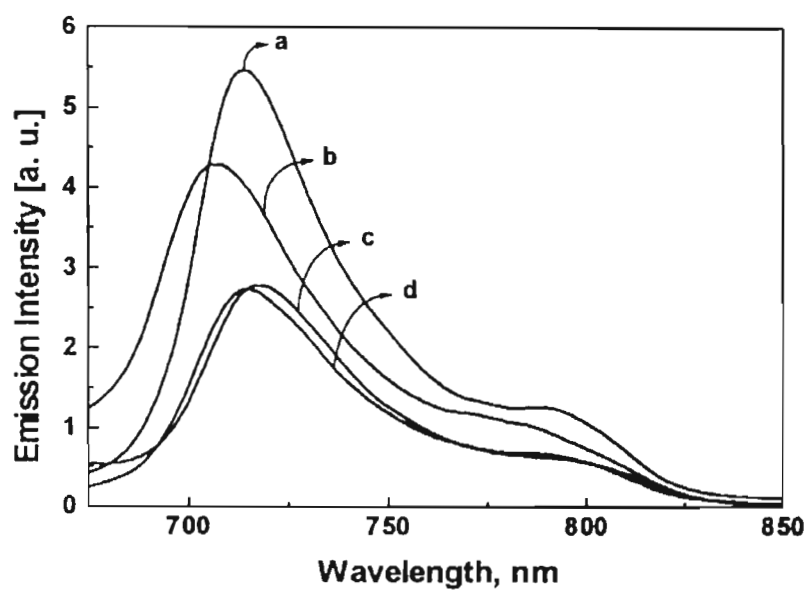


Figure 2.9. Effect of solvent polarity on the fluorescence of **6**: (a) toluene, (b) benzonitrile/25mM TFA, (c) dichloromethane and (d) benzonitrile.

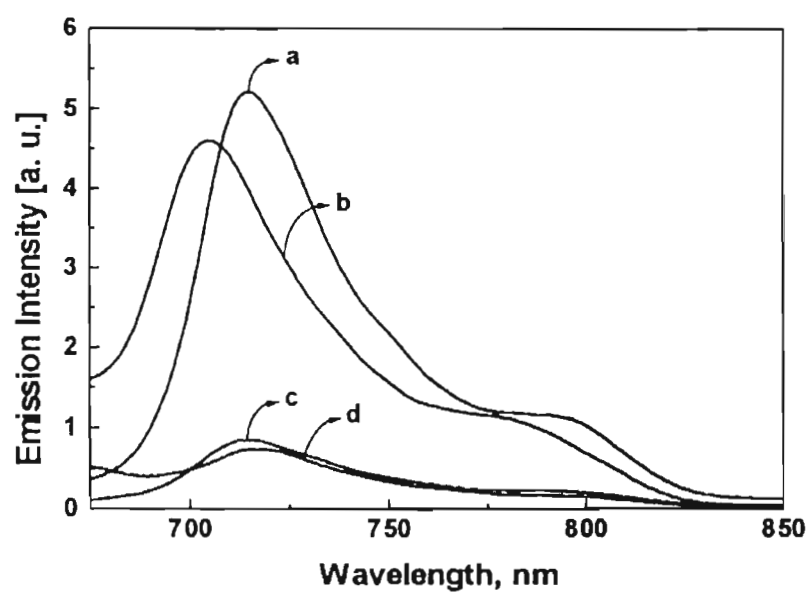


Figure 2.10. Effect of solvent polarity on the fluorescence of **8**: (a) toluene, (b) benzonitrile/25mM TFA, (c) dichloromethane and (d) benzonitrile.



On addition of TFA (25 mM) to benzonitrile solutions of the dyads, an increase in fluorescence intensity was observed (trace 'b' of Figures 2.9 and 2.10). This is essentially due to the protonation of the aniline nitrogen, which inhibits the electron transfer processes. The rates of charge separation and the quantum yields of charge separation are estimated from the fluorescence quantum yields of the dyads and the fluorescence quantum yield as well as life time of model compound using Equations 2.3 and 2.4 respectively.

$$k_{cs} = [(\phi_{ref}/\phi)-1]1/\tau_{ref} \quad (\text{Eq. 2.3})$$

$$\phi_{cs} = k_{cs}/[(1/\tau_{ref}) - k_{cs}] \quad (\text{Eq. 2.4})$$

The large  $k_{cs}$  values observed for the *ortho*-substituted compounds could be attributed to the folding of the aniline group and thereby decreasing the donor-acceptor distance. In the case of other classes of dyads,<sup>14</sup> a specific orientation between the donor and acceptor is required for efficient transfer of electron, but in the fullerene-aniline dyads 7 and 8, the folding of the anilinic group in proximity to anywhere on the surface of C<sub>60</sub> is sufficient for the transfer of electron.

This increase in probability of electron transfer is an additional kinetic gain in the case of the *ortho*-substituted compounds. The existence of long-lived charge separated intermediates was unequivocally proven through pico- and nanosecond laser flash photolysis studies.

### 2.3.6. Transient absorption studies<sup>47</sup>

The excited singlet state of pristine C<sub>60</sub> has an absorption maximum around 920 nm with a lifetime of 1.2 ns and the triplet state has an absorption maximum around 740 nm with a lifetime greater than 100  $\mu$ s. Singlet and triplet excited state

properties of the fullerene-aniline dyads **5-8** and the model compounds **9** and **10** were examined using picosecond and nanosecond laser flash photolysis techniques. The time-resolved transient absorption spectra recorded following 355-nm laser pulse excitation of the model compound **10** and the dyad **5** are shown in Figures 2.11 and 2.12, respectively.

The spectrum recorded immediately after excitation with 355 nm laser pulse shows the formation of the singlet excited state with absorption maximum in the region of 900 nm in the case of both the dyad **5** and the model compound **10**. As the singlet excited state decays, a new absorption band corresponding to the triplet excited state appears with a maximum in the region of 690-740 nm. The triplet excited state of the fullerene-aniline dyad **5** (Figure 2.13) as well as the model compound **10** decay within 50  $\mu$ s to give their respective ground states. The excited state properties of the fullerene-aniline dyad **5** and the model compound **10** in toluene are summarized in Table 2.2.

It should be noted that the photoexcitation of **5** in a polar solvent such as benzonitrile leads to decreased intersystem-crossing yield. The absorption-time profile showing the decay of the singlet excited state of the dyad **5** in different solvents, monitored at 900 nm, is displayed in Figure 2.14. The high dielectric constant of the medium (e.g., benzonitrile relative to toluene) is thermodynamically supportive of an intramolecular electron transfer process and in turn allows this route to compete with the fast intersystem crossing. There are several possibilities for the deactivation of the excited state of the dyads and they are shown in Scheme 2.4.

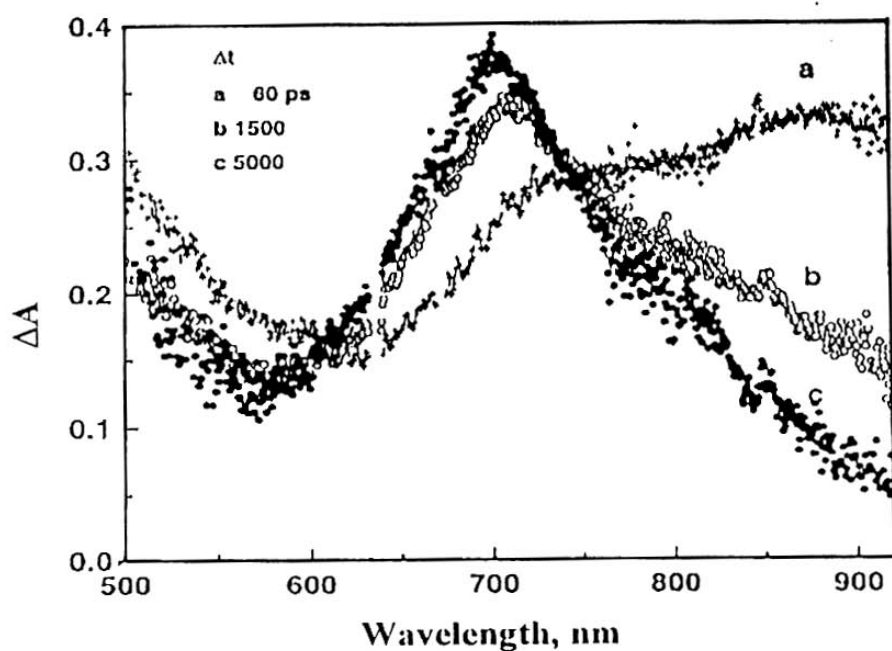


Figure 2.11. Time-resolved transient absorption spectra recorded following 355 nm laser pulse (pulse width 18 ps) excitation of the model compound **10** in toluene at different delay times: (a) 60 ps, (b) 1500 ps and (c) 5000 ps.

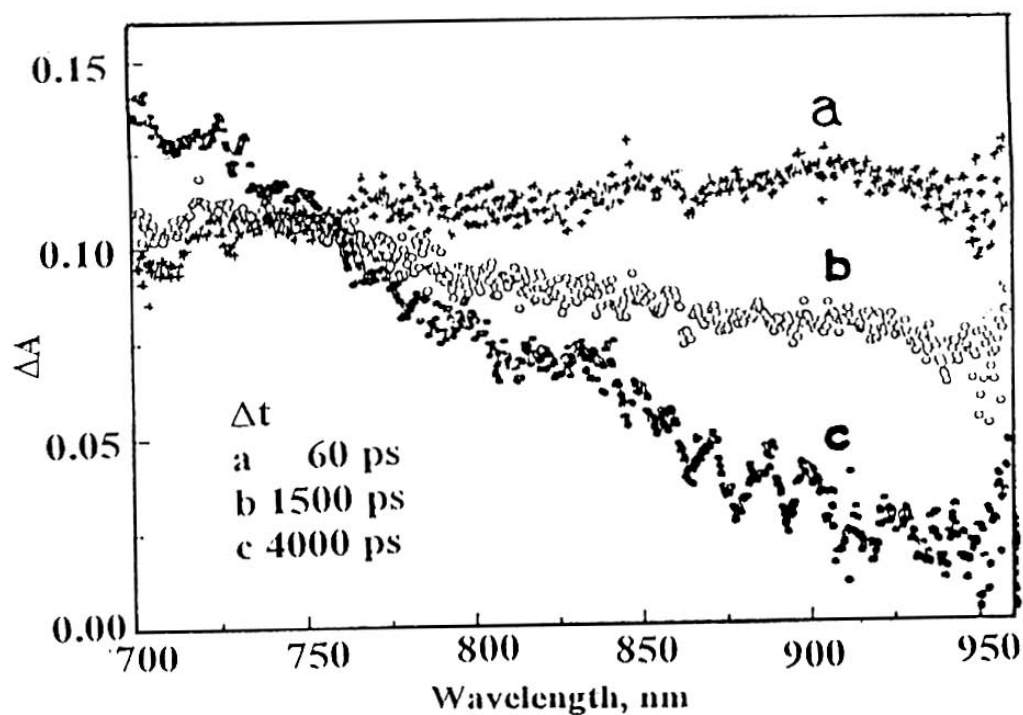


Figure 2.12. Time-resolved transient absorption spectra recorded following 355 nm laser pulse (pulse width 18 ps) excitation of the fullerene-aniline dyad **5** in toluene at different delay times: (a) 60 ps, (b) 1500 ps and (c) 4000 ps.

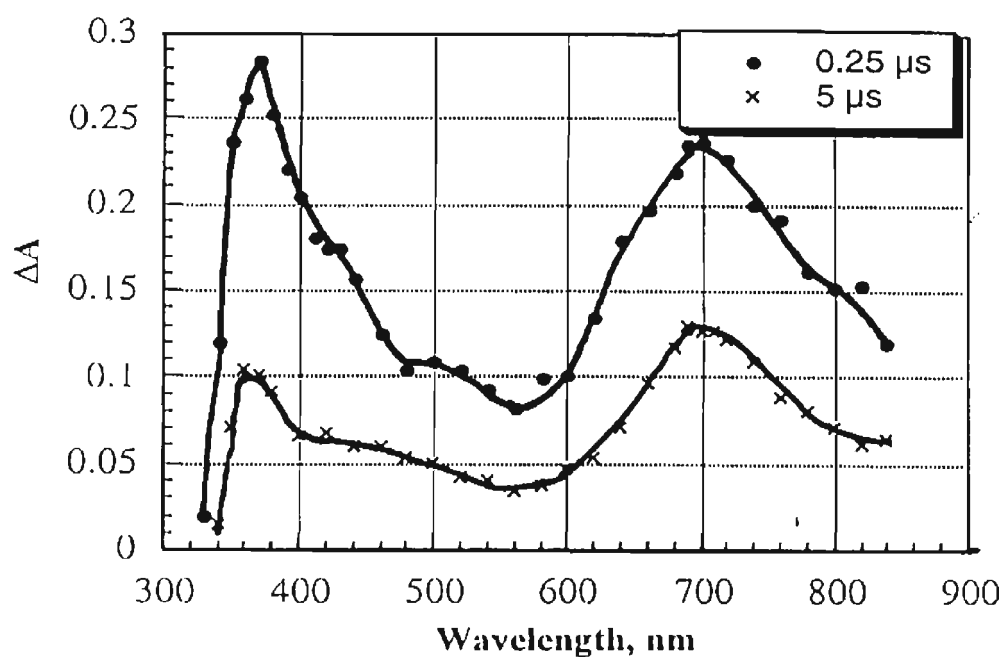


Figure 2.13. Time-resolved difference absorption spectra recorded following 337 nm laser pulse excitation of the fullerene-aniline dyad 5 in toluene at different delay times: (a) 0.25  $\mu\text{s}$  and (b) 5  $\mu\text{s}$ .

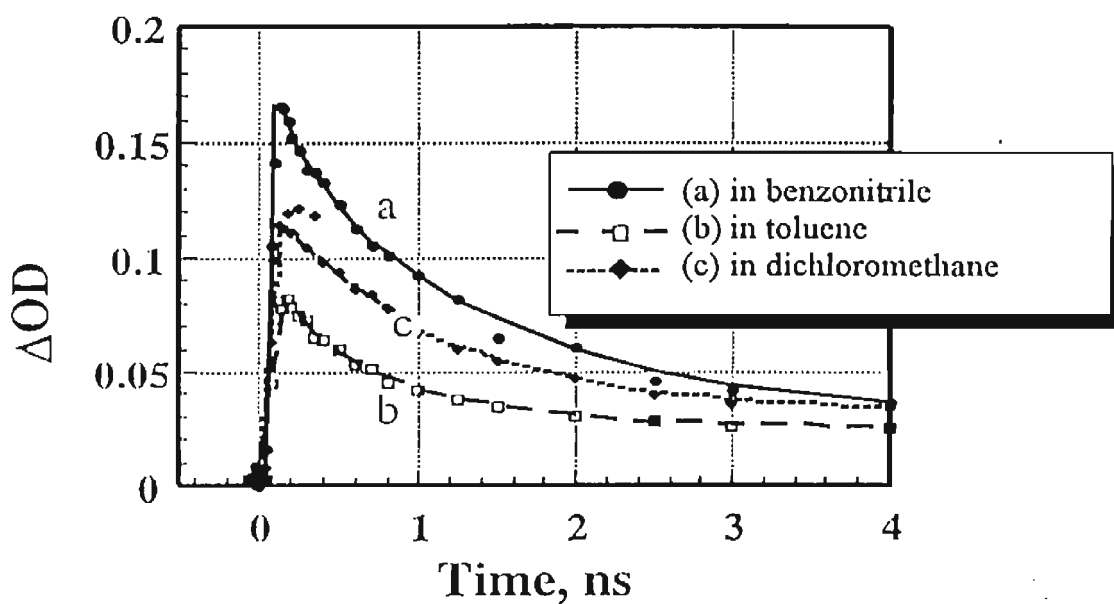
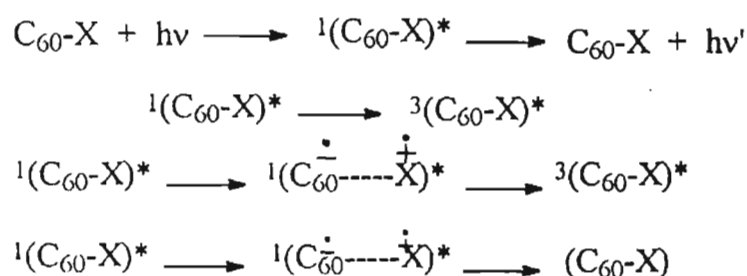


Figure 2.14. Absorption-time profile shows the decay of singlet of the dyad 5 in different solvents at monitoring wavelength of 900 nm.

**Table 2.2.** The excited state properties of the fullerene-aniline dyad **5** and the model compound **10** in toluene

Compound	S <sub>1</sub> , λ <sub>max</sub>	τ (ps)	T <sub>1</sub> , λ <sub>max</sub>	τ (μs)
C <sub>60</sub> <sup>37-39</sup>	920	1200	400, 750	> 100
<b>5</b>	890	1050± 100	690, 370	17± 1
<b>10</b>	880	1250± 100	700	16± 1



**Scheme 2.4**

Nanosecond laser flash photolysis studies of the dyads were carried out in two different solvents of extreme polarity namely, toluene ( $\epsilon = 2.38$ ) and benzonitrile ( $\epsilon = 25.2$ ). The main objectives of these experiments were to investigate the dynamics of the thermodynamically favored electron transfer from aniline to fullerene in dyads **5-8** and characterize the charge-separated intermediates formed. The charge-separated intermediates formed in the present systems are the radical anion of C<sub>60</sub> and the radical cation of aniline. In an earlier study, the radical anion of the dyad **5** was characterized using pulse radiolysis experiments ( $\lambda_{\text{max}}$  at 1080 nm). Since the radical anion of C<sub>60</sub> and functionalized derivatives absorb between 1000-1080 nm, we have

extended our investigations to the NIR region. The transient spectra of the dyads 5-8, in the visible and near-infrared (NIR) region, were monitored using two separate detectors (photomultiplier and diode array, respectively).

Nanosecond transient absorption spectra (350-1100 nm region) of the dyads (5-8) recorded in toluene showed in each case two absorption bands centered around 370 and 700 nm and their spectral features are found to be similar to those of the model compound 10. The spectra of a representative example (6) are shown in Figure 2.15. Based on previous studies (and quenching experiments), these bands were characterized as due to the triplet excited state of the dyads. Lifetimes of the triplet excited state of the dyads in toluene, were estimated by fitting the absorption-time decay curves to first order kinetics and are presented in Table 2.3 (lifetimes range from 13 to 16  $\mu$ s). Quantum yields of the triplet excited states were estimated by a relative method and found to be close to unity for all the dyads (5-8) in toluene (Table 2.3). These results indicate that the intersystem crossing of the dyads is almost quantitative in a nonpolar solvent such as toluene. Absorption-time profiles of optically matched solutions (absorbance at 337 nm = 0.7) of the *para*-substituted dyad 6 (and the *ortho*-substituted dyad 8) in toluene and benzonitrile are shown in Figure 2.16. Interestingly, a drastic decrease in the triplet quantum yield was observed in benzonitrile, for all the dyads (Table 2.3) and this is indicative of decreased intersystem crossing. The decrease in the fluorescence yield (Section 2.3.5.2) and the low triplet yields observed in benzonitrile (relative to toluene), are supportive of an intramolecular electron transfer from the singlet excited state of the dyads.

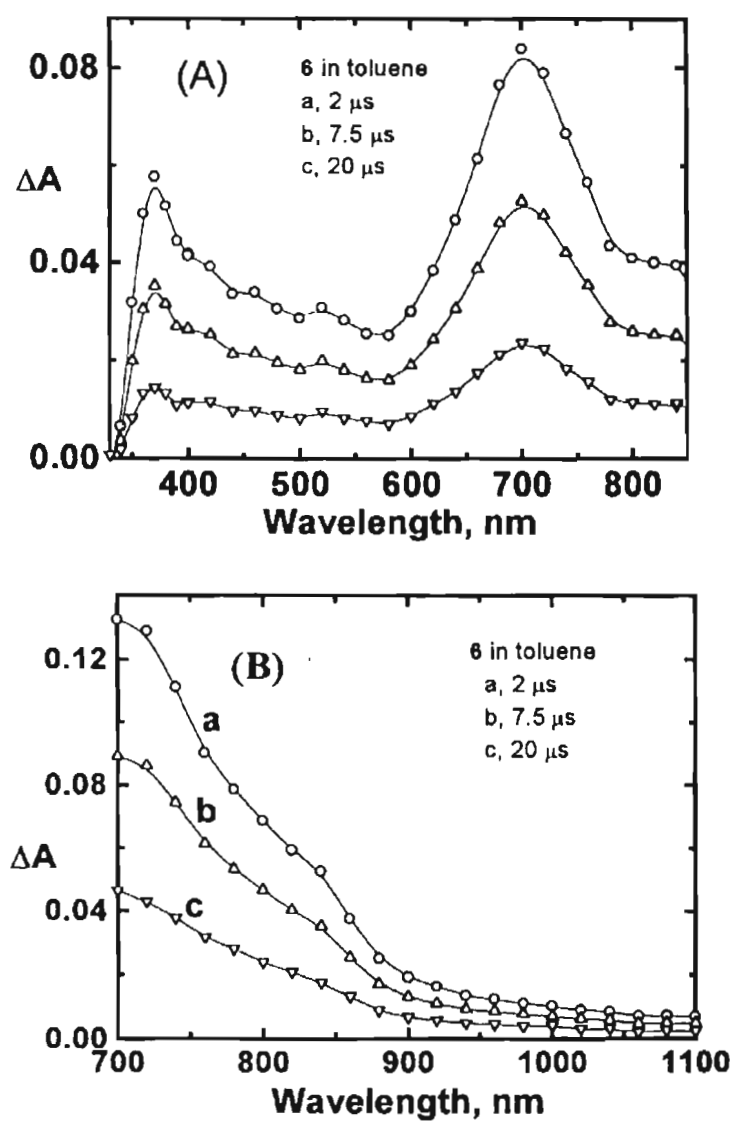


Figure 2.15. Time-resolved difference absorption spectra, recorded following 337 nm laser pulse excitation, of the fullerene-aniline dyad **6** in toluene at different delay times: (A) UV-visible region and (B) infrared region.

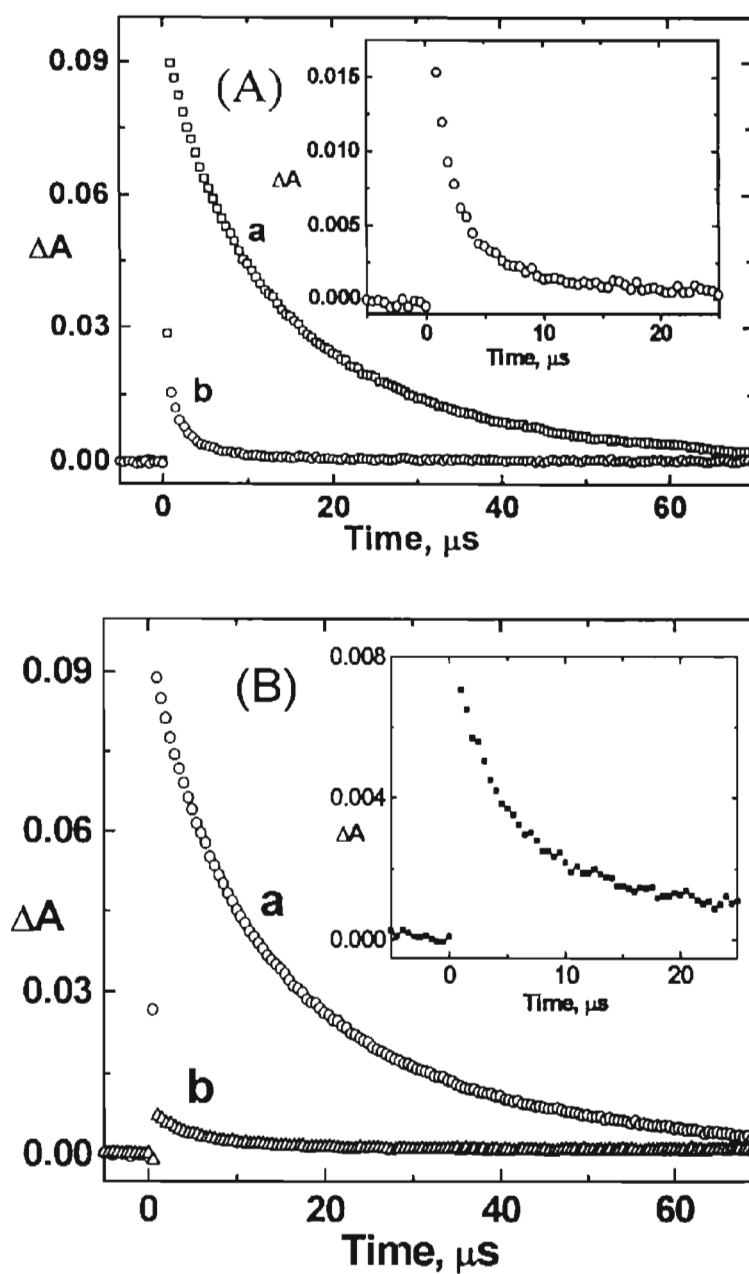


Figure 2.16. Absorption-time decay profile shows the decay of triplet of the optically matched solution of the dyad **6** (A) and **8** (B) in (a) toluene and (b) benzonitrile. Insets show the expanded decay profiles in benzonitrile.



**Table 2.3.** The triplet excited state properties of the fullerene-aniline dyads 5-8

Compound	$\tau$ ( $\mu\text{s}$ ) (toluene)	$\phi_T$ (toluene)	$\tau$ ( $\mu\text{s}$ ) (benzonitrile)	$\phi_T$ (benzonitrile)
5	16.2	0.96	2.4	0.18
6	13.4	0.96	2.2	0.17
7	13.2	0.95	7.4	0.08
8	14.4	0.94	6.6	0.08

Nanosecond transient absorption studies of the dyads were extended to the NIR region in order to characterize the radical anion of  $C_{60}$  (Figure 2.17). The existence of the charge-separated intermediates was not observed (in the nanosecond time scale) for dyad 5 whereas an absorption band around 1000 nm, corresponding to the  $C_{60}$  radical anion, was clearly observed for dyads 6 and 8. In the case of dyad 7, the absorption features in the NIR region are not clear as to unambiguously characterize the anion of  $C_{60}$ .

It is clear from the steady state emission and picosecond laser flash photolysis studies that the forward electron transfer is highly efficient in benzonitrile for all the dyads, under investigation. The enhanced rate of forward electron transfer and the high quantum yield of charge separation (Table 2.1) observed in the case of the *ortho*-substituted dyads is addressed in Section 2.3.5.2. This is attributed to the folding of the aniline group, thereby decreasing the donor-acceptor distances in the *ortho*-substituted dyads. The low triplet quantum yields observed for *ortho*-substituted dyads (Table 2.3) again indicate that the quantum yield of charge separation from the singlet excited state is more than 0.85.

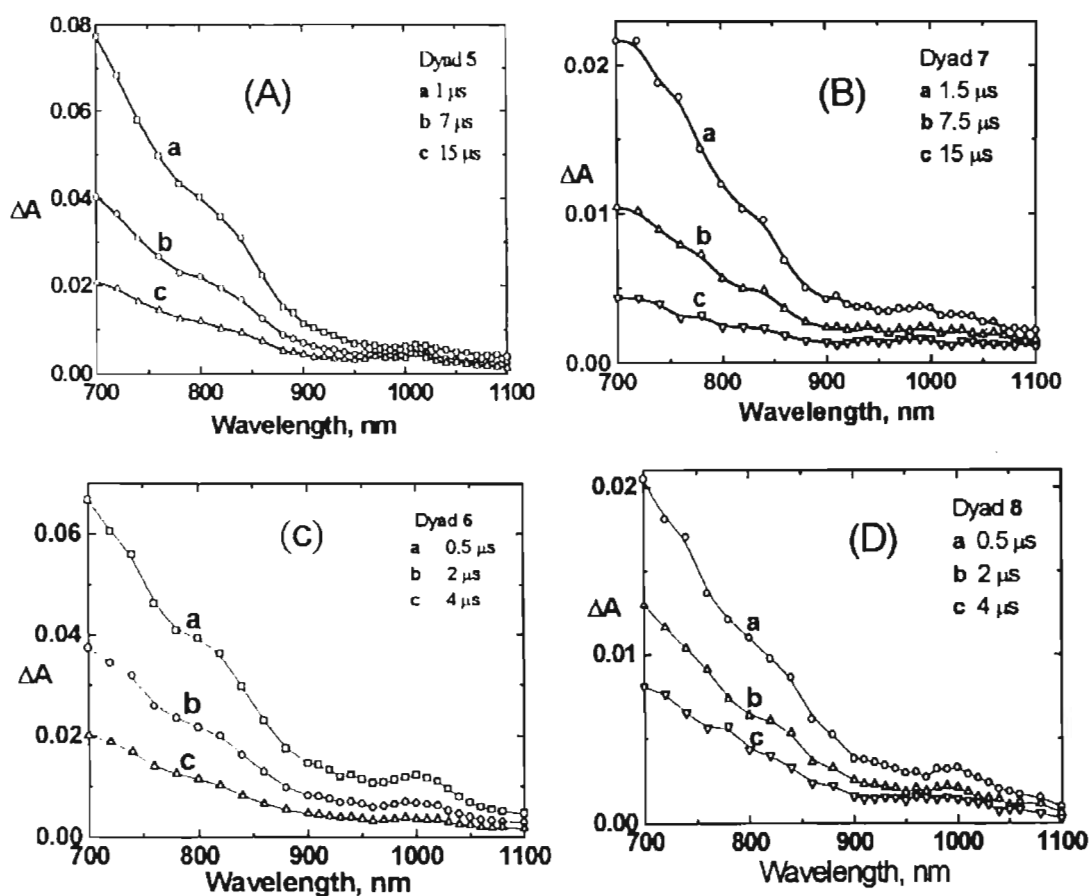


Figure 2.17. Time-resolved difference absorption spectra recorded following 337 nm laser pulse excitation of the various fullerene-aniline dyads in benzonitrile at different delay times: (A) dyad 5; (B) dyad 7; (C) dyad 6 and (D) dyad 8.

The transient absorption corresponding to the radical anion of the  $C_{60}$  is observed clearly in dyad systems 6 and 8. In these systems, the anilinic donor is linked to the *para*- as well as *ortho*- positions of phenyl group of fullerene(1-methyl-2-phenyl)pyrrolidine through three methylene chains. In the other two dyad systems (5 and 7) the donor and acceptor groups are linked together by two methylene groups. The additional methylene group in dyads 6 and 8 may permit a higher degree of freedom and provide extra stability to the radical pairs in polar solvents,

through the conformational rearrangements of fullerene and aniline moieties. Although triplet quantum yields of all the dyads in benzonitrile are less than 0.15, the 700 nm absorption band is more pronounced (Figure 2.17) as compared to the 1000 nm (note that the  $C_{60}$  radical anion does not possess any absorption at 700 nm). Based on the ratio of these two bands and their extinction coefficients, the yield of the anion observed in the nanosecond time scale is estimated to be less than 5%. The low yield of the charge-separated intermediates is due to the fast charge recombination. The estimation of the rate constants for the charge recombination in these dyads is difficult due to the low yield of the anion and the interference from the triplet excited state.

#### 2.4. Conclusions

The orientation dependent electron transfer studies are pertinent in fullerene based systems due to the spherical shape, covered by  $\pi$ -electrons. We have reported examples of remarkably large orientation effects, which can control the photoinduced forward electron transfer in a series of fullerene based D-B-A systems. The difference in orientation is achieved by attaching an anilinic donor to the *ortho*- as well as the *para*- positions of the phenyl groups of fullerene(1-methyl-2-phenyl)pyrrolidine, linked by methylene chains. The marked increase in the rate constants and quantum yields of charge separation observed in the present case for the *ortho*-substituted dyads are attributed to the folding of the anilinic group. The folding of the anilinic group in proximity to anywhere on the surface of  $C_{60}$  allows the transfer of an electron and a specific orientation is not required between the donor and the acceptor. The existence of charge separated intermediates in the case of the dyads 6 and 8 was confirmed using laser flash photolysis experiments.

## 2.5. Experimental Section

### 2.5.1. Starting materials

1,2,3-Triphenylaziridine **24**, mp 99 °C was prepared following a reported procedure.<sup>48</sup> C<sub>60</sub> obtained from SES corporation was used as such. Petroleum ether used was the fraction with bp 60-80 °C.

### 2.5.2. Synthesis of fullerene-aniline dyads 5-8

The general method adopted for the synthesis of the fullerene-aniline dyads is shown in Schemes 2.1 and 2.2. Purity of all these dyads was confirmed by HPLC.<sup>32</sup> The syntheses of N-methyl,N-{(2-bromo)-1-ethyl}aniline (**13**),<sup>29a</sup> N-methyl,N-{(p-formylphenoxy)-1-ethyl}aniline (**17**),<sup>29a</sup> fullerene-aniline dyad (**5**)<sup>29a</sup> and the model compound, N-methylfulleropyrrolidine (**9**)<sup>22</sup> were as per reported procedures.

#### 2.5.2.1. General method for the preparation N-methyl, N-{(ω-hydroxy)-1-alkyl}anilines, **12** and **14**

A mixture of N-methylaniline (0.1 mol), ethylene chlorohydrin or 3-bromo-1-propanol (0.2 mol), potassium carbonate (0.2 mol), and iodine (100 mg) was heated under reflux in 1-butanol (80 mL) for 92 h. On cooling, the solvent was removed under reduced pressure to give a reddish brown liquid.

**Compound 12.** The residual liquid on distillation under reduced pressure gave 13.5 g (90 %) of **12**, bp 171 °C (2 mm); IR (neat)  $\nu_{\max}$  3378, 2968, 2854, 1607, 1512, 1356, 1268, 1193, 1053, 748, 690 cm<sup>-1</sup>; <sup>1</sup>H NMR (CDCl<sub>3</sub>)  $\delta$  2.3-2.4, (1H, s, OH), 2.8-2.9, (3H, s, NCH<sub>3</sub>), 3.3-3.5, (2H, t, NCH<sub>2</sub>), 3.6-3.8, (2H, t, OCH<sub>2</sub>), 6.7-7.4, (5H, m, aromatic); <sup>13</sup>C NMR (CDCl<sub>3</sub>)  $\delta$  38.60, 55.19, 59.76, 112.84, 116.95, 129.06,

149.83; exact mass calcd. for  $C_9H_{13}NO$  151.2040 ( $M^+$ ), found 151.2043 (FAB, high resolution mass spectrometry).



**Compound 14.** The residual liquid on column chromatography on silica gel (100-200 mesh) using a mixture (1:10) of ethyl acetate and petroleum ether (bp 60-80 °C) gave 14.8 g (90 %) of **14**; IR (neat)  $\nu_{max}$  3382, 2944, 2888, 1604, 1510, 1377, 1195, 1060, 750, 693  $cm^{-1}$ ;  $^1H$  NMR ( $CDCl_3$ )  $\delta$  1.5-1.9 (2H, m,  $CH_2$ ), 2.8-2.9 (3H, s,  $NCH_3$ ), 3.0-3.2 (1H, s, OH), 3.3-3.5 (2H, t,  $NCH_2$ ), 3.6-3.8 (2H, t,  $OCH_2$ ), 6.6-7.4 (5H, m, aromatic);  $^{13}C$  NMR ( $CDCl_3$ )  $\delta$  27.86, 36.72, 48.27, 58.86, 111.16, 114.95, 127.51, 147.89; exact mass calcd. for  $C_{10}H_{15}NO$  165.1154 ( $M^+$ ), found 165.1145 (FAB, high resolution mass spectrometry).

#### 2.5.2.2. General method for the preparation N-methyl,N- $\{(\omega$ -bromo)-1-alkyl}aniline (**13** and **15**)

To an ice cold solution of N-methyl,N- $\{(\omega$ -hydroxy)-1-alkyl}anilines (**12** and **14**) (15 mmol) in dichloromethane (20 mL) was added  $PBr_3$  (15 mmol), dropwise over a period of 30 minutes. The reaction mixture was further stirred at room temperature for an additional period of 3 h. The reaction was quenched with ice-cold water and the pH was adjusted to 7-8. The organic portion was extracted with dichloromethane and the solvent was removed under vacuum. The crude product was chromatographed over silica gel (100-200 mesh).

**Compound 13.** Elution of the column with a mixture (1:20) of ethyl acetate and petroleum ether (bp 60-80 °C) gave 2.70 g (85%) of **13**; IR (neat)  $\nu_{max}$  2929, 1605, 1510, 1373, 1351, 1278, 1214, 1175, 1097, 1035, 996, 749, 693  $cm^{-1}$ ;  $^1H$  NMR ( $CDCl_3$ )  $\delta$  2.9-3.0 (3H, s,  $NCH_3$ ), 3.2-3.6 (2H, m,  $NCH_2$ ), 3.6-3.9 (2H, m,  $BrCH_2$ ),

6.6-7.5 (5H, m, aromatic);  $^{13}\text{C}$  NMR ( $\text{CDCl}_3$ )  $\delta$  26.88, 36.90, 52.83, 110.42, 115.43, 127.75, 146.46; exact mass calcd. for  $\text{C}_9\text{H}_{12}\text{NBr}$  213.0153 ( $\text{M}^+$ ), found 213.0142 (FAB, high resolution mass spectrometry).

**Compound 15.** Elution of the column with a mixture (1:20) of ethyl acetate and petroleum ether (bp 60-80 °C) gave 3.06 g (90%) of 15; IR (neat)  $\nu_{\text{max}}$  3037, 2954, 2827, 1605, 1508, 1445, 1369, 1257, 1222, 1109, 1030, 992, 751  $\text{cm}^{-1}$ ;  $^1\text{H}$  NMR ( $\text{CDCl}_3$ )  $\delta$  1.8-2.3 (2H, m,  $\text{CH}_2$ ), 2.95 (3H, s,  $\text{NCH}_3$ ), 3.2-3.6 (4H, m,  $\text{NCH}_2$  and  $\text{BrCH}_2$ ), 6.5-7.4 (5 H, m, aromatic);  $^{13}\text{C}$  NMR ( $\text{CDCl}_3$ )  $\delta$  29.98, 31.29, 38.60, 50.89, 112.35, 116.50, 129.15, 149.02; exact mass calcd. for  $\text{C}_{10}\text{H}_{14}\text{NBr}$  227.0310 ( $\text{M}^+$ ), found 227.0313 (FAB, high resolution mass spectrometry).

#### 2.5.2.3. General method for the preparation of N-methyl-N-((formylphenoxy)-alkyl)anilines (17, 19, 20 and 21)

A suspension of the corresponding bromide (5 mmol), hydroxybenzaldehyde (10 mmol) and potassium carbonate (10 mmol) was refluxed in dry acetone (15 mL) for 12 h. The reaction mixture was cooled, filtered and concentrated under reduced pressure. The crude product was chromatographed over silica gel (100-200 mesh).

**Compound 17.** Elution of the column with a mixture (1:10) of ethyl acetate and hexane gave 1.02 g (80%) of 17; IR (neat)  $\nu_{\text{max}}$  2934, 2759, 1696, 1602, 1476, 1262, 1161, 1028, 798  $\text{cm}^{-1}$ ;  $^1\text{H}$  NMR ( $\text{CDCl}_3$ )  $\delta$  2.9-3.0 (3H, s,  $\text{NCH}_3$ ), 3.6-3.8 (2H, t,  $\text{NCH}_2$ ), 4.0-4.3 (2H, t,  $\text{OCH}_2$ ), 6.4-7.9, (9H, m, aromatic), 9.8 (1H, s, CHO);  $^{13}\text{C}$  NMR ( $\text{CDCl}_3$ )  $\delta$  29.68, 39.17, 51.79, 65.69, 96.15, 112.24, 114.74,

116.95, 129.30, 131.90, 148.69, 163.67, 190.37; exact mass calcd. for  $C_{16}H_{17}NO_2$  255.1259 ( $M^+$ ), found 255.1200 (FAB, high resolution mass spectrometry).

**Compound 20.** Elution of the column with a mixture (1:10) of ethyl acetate and hexane gave 760 mg (60%) of **20**; IR (neat)  $\nu_{max}$  2934, 2762, 2794 1692, 1604, 1500, 1460, 1368, 1292, 1243, 1039, 832  $cm^{-1}$ ;  $^1H$  NMR ( $CDCl_3$ )  $\delta$  3.05 (3H, s,  $NCH_3$ ), 3.7-3.9 (2H, t,  $NCH_2$ ), 4.1-4.3 (2H, t,  $OCH_2$ ), 6.6-7.9 (9H, m, aromatic), 10.4 (1H, s, CHO);  $^{13}C$  NMR ( $CDCl_3$ )  $\delta$  39.02, 51.55, 65.90, 112.06, 112.18, 116.68, 120.77, 124.74, 128.26, 129.18, 135.75, 148.60, 160.87, 189.45; exact mass calcd. for  $C_{16}H_{17}NO_2$  255.1259 ( $M^+$ ), found 255.1266 (FAB, high-resolution mass spectrometry).

**Compound 19.** Elution of the column with a mixture (1:3) of ethyl acetate and petroleum ether (bp 60-80 °C) gave 740 mg (55%) of **19**; IR (neat)  $\nu_{max}$  2949, 2873, 1692, 1601, 1551, 1502, 1480, 1450, 1388, 1356, 1287, 1241, 1195, 1161, 1040, 841  $cm^{-1}$ ;  $^1H$  NMR ( $CDCl_3$ )  $\delta$  2.0-2.4 (2H, m,  $CH_2$ ), 2.95 (3 H, s,  $NCH_3$ ), 3.4-3.8 (2H, t,  $NCH_2$ ), 4.0-4.3 (2H, t,  $OCH_2$ ), 6.7-7.9 (9H, m, aromatic), 10.55 (1H, s, CHO);  $^{13}C$  NMR ( $CDCl_3$ )  $\delta$  26.64, 38.50, 64.92, 65.85, 112.30, 120.71, 128.53, 129.25, 135.95, 156.66, 162.96, 189.50; exact mass calcd. for  $C_{17}H_{19}NO_2$  269.1416 ( $M^+$ ), found 269.1419 (FAB, high resolution mass spectrometry).

**Compound 21.** Elution with a mixture (1:4) of ethyl acetate and hexane gave 1.2 g (90%) of **21**; IR (neat)  $\nu_{max}$  2957, 2887, 2854, 1697, 1606, 1512, 1260, 1219, 1162, 1036, 834  $cm^{-1}$ ;  $^1H$  NMR ( $CDCl_3$ )  $\delta$  2.0-2.4 (2H, m,  $CH_2$ ), 2.95 (3H, s,  $NCH_3$ ), 3.4-3.7 (2H, t,  $NCH_2$ ), 4.0-4.2 (2H, t,  $OCH_2$ ), 6.6-8.0 (9H, m, aromatic), 9.90 (1H, s, CHO);  $^{13}C$  NMR ( $CDCl_3$ )  $\delta$  26.64, 37.89, 38.45, 64.95, 103.88, 112.21, 114.71,

116.35, 129.18, 131.96, 149.14, 163.85, 190.70; exact mass calcd. for  $C_{17}H_{19}NO_2$  269.1416 ( $M^+$ ), found 269.1419 (FAB, high resolution mass spectrometry).

#### 2.5.2.4. General method for the synthesis of the fullerene-aniline dyads (5-8)

A mixture of  $C_{60}$  (0.2 mmol), N-methyl-N-((formylphenoxy)alkyl)-aniline (0.2 mmol) and N-methylglycine (0.2 mmol) in toluene (145 mL) was stirred under reflux for 10 h. The reaction mixture was cooled and removal of the solvent under reduced pressure gave a solid residue, which was chromatographed over silica gel (100-200 mesh) to give the appropriate dyads.

**Dyad 5.**<sup>29a</sup> Elution with a mixture (1:3) of toluene and petroleum ether (bp 60-80 °C) gave 47 mg (33%) of unchanged  $C_{60}$ . Further elution with a mixture (2:3) of toluene and petroleum ether gave 58 mg (44%) of fullerene-aniline adduct, **5**, mp > 400 °C; IR (KBr)  $\nu_{max}$  2932, 2861, 1600, 1507, 1463, 1427, 1249, 1172, 1035, 825, 744  $cm^{-1}$ ;  $^1H$  NMR ( $CDCl_3$ )  $\delta$  2.85 (3H, s,  $NCH_3$ ), 3.0 (3H, s,  $NCH_3$ ), 3.6-3.8 (2H, t,  $NCH_2$ ), 3.95-4.25 (3H, m,  $OCH_2$  and CH (exo)- pyrrolidine ring), 4.8 (1H, s, CH), 4.95 (1H, d, CH (endo),  $J=9.1$  Hz), 6.5-7.8 (9H, m, aromatic);  $^{13}C$  NMR ( $CDCl_3$ )  $\delta$  29.71, 39.16, 39.97, 51.92, 65.15, 68.96, 70.98, 83.13, 112.04, 116.46, 125.29, 128.20, 129.03, 129.14, 129.26, 130.49, 135.74, 135.78, 136.53, 136.77, 139.59, 139.90, 140.11, 140.15, 141.53, 141.67, 141.83, 141.95, 141.99, 142.03, 142.07, 142.12, 142.24, 142.54, 142.67, 142.97, 143.13, 144.38, 144.61, 144.69, 145.14, 145.22, 145.27, 145.33, 145.47, 145.53, 145.77, 146.09, 146.12, 146.20, 146.26, 146.30, 146.33, 146.51, 146.78, 147.29, 148.84, 153.58, 153.62, 154.09, 156.35, 158.70; exact mass calcd. for  $C_{78}H_{22}N_2O$  1002.1732 ( $M^+$ ), found 1002.1725 (FAB, high resolution mass spectrometry)



**Dyad 6.** Elution with a mixture (1:3) of toluene and petroleum ether (bp 60-80 °C) gave 58 mg (40 %) of unchanged C<sub>60</sub> followed by 58 mg (48 %) of **6**, mp > 400 °C; IR (KBr)  $\nu_{\max}$  2940, 2869, 2785, 1606, 1568, 1509, 1473, 1429, 1363, 1336, 1301, 1245, 1176, 1035, 746 cm<sup>-1</sup>; <sup>1</sup>H NMR (CDCl<sub>3</sub>)  $\delta$  2.05 (2H, t, CH<sub>2</sub>), 2.80 (3H, s, NCH<sub>3</sub>), 2.92 (3H, s, NCH<sub>3</sub>), 3.54 (2H, t, anilinic NCH<sub>2</sub>), 4.01(2H, t, OCH<sub>2</sub>), 4.25 (1H, d, CH of pyrrolidine), 4.88 (1H, s, CH of pyrrolidine), 4.98 (1H, d, CH of pyrrolidine), 6.58-6.75 (m), 6.96 (d), 7.13-7.29 (m), 7.63-7.79 (s) (9H, aromatic); <sup>13</sup>C NMR (CDCl<sub>3</sub>)  $\delta$  26.85, 29.74, 38.43, 40.00, 49.37, 65.31, 70.01, 79.14, 83.19, 112.17, 114.55, 116.19, 129.19, 130.49, 135.79, 140.15, 142.12, 142.56, 145.24, 145.48, 145.94, 146.14, 153.66, 154.11, 158.92; exact mass calcd. for C<sub>79</sub>H<sub>24</sub>N<sub>2</sub>O 1017.1967 (M<sup>+</sup>), found 1017.1989 (FAB, high resolution mass spectrometry).

**Dyad 7.** Elution of the column with a mixture (1:3) of toluene and hexane gave 65 mg (45 %) of unchanged C<sub>60</sub> followed by 50 mg (45 %) of the dyad **7**, mp > 400 °C; IR (KBr)  $\nu_{\max}$  2932, 2866, 2786, 1602, 1500, 1455, 1361, 1338, 1247, 1184, 1107, 1036, 749 cm<sup>-1</sup>; <sup>1</sup>H NMR (CDCl<sub>3</sub>)  $\delta$  2.77 (3H, s, NCH<sub>3</sub>), 3.02 (3H, s, NCH<sub>3</sub>), 3.53-3.61 (1H, m, anilinic NCH), 3.64-3.71 (1H, m, anilinic NCH), 3.79-3.85 (1H, m, OCH), 4.21-4.29 (2H, m, OCH and CH of pyrrolidine), 4.95 (1H, d, CH of pyrrolidine ring), 5.52 (1H, s, CH of pyrrolidine ring), 6.70-6.81 (m), 6.68 (d), 7.10 (t), 7.14-7.32 (m), 7.98 (d) (9H, aromatic); <sup>13</sup>C NMR (CDCl<sub>3</sub>)  $\delta$  38.57, 39.84, 51.70, 64.86, 69.01, 69.60, 75.11, 86.54, 111.30, 112.46, 116.91, 121.47, 129.01, 129.26, 129.82, 135.95, 136.43, 139.15, 140.02, 141.70, 141.94, 142.09, 142.43, 142.92, 144.24, 144.44, 144.80, 145.12, 145.26, 145.50, 145.68, 145.99, 147.09, 148.69, 153.62, 156.97; exact mass calcd. for C<sub>78</sub>H<sub>22</sub>N<sub>2</sub>O 1002.1732 (M<sup>+</sup>), found 1002.1713 (FAB, high resolution mass spectrometry).

**Dyad 8.** Elution of the column with a mixture (1:3) of toluene and hexane gave 60 mg (42%) of unchanged C<sub>60</sub> followed by 57 mg (48%) of the dyad **8**, mp > 400 °C; IR (KBr)  $\nu_{\max}$  2939, 2862, 2787, 1607, 1548, 1500, 1453, 1285, 1245, 1190, 1104, 1045, 754 cm<sup>-1</sup>; <sup>1</sup>H NMR (CDCl<sub>3</sub>)  $\delta$  1.89-1.91 (2H, m, CH<sub>2</sub>), 2.82 (3H, s, NCH<sub>3</sub>), 2.96 (3H, s, NCH<sub>3</sub>), 3.51 (2H, t, anilinic NCH<sub>2</sub>), 3.72-3.88 (1H, m, OCH), 3.98-4.11 (1H, m, OCH), 4.31 (1H, d, CH of pyrrolidine), 5.00 (1H, d, CH of pyrrolidine), 5.57 (1H, s, CH of pyrrolidine), 6.65-6.81 (m), 6.90 (d), 7.07-7.32 (m), 7.99 (d) (9H, aromatic); <sup>13</sup>C NMR (CDCl<sub>3</sub>)  $\delta$  26.78, 29.71, 38.62, 40.18, 49.85, 65.78, 69.98, 75.85, 91.32, 111.48, 112.43, 116.41, 121.24, 128.14, 129.06, 134.82, 135.88, 135.92, 135.94, 138.25, 138.27, 138.30, 138.91, 141.29, 141.35, 141.63, 141.88, 142.64, 142.69, 142.74, 144.20, 144.50, 144.62, 145.29, 146.07, 146.82, 147.47, 149.16, 153.82, 153.88, 155.21, 156.81, 157.37; exact mass calcd. for C<sub>79</sub>H<sub>24</sub>N<sub>2</sub>O 1017.1967 (M<sup>+</sup>), found 1017.1987 (FAB, high resolution mass spectrometry).

### 2.5.3. Synthesis of fullero-1,2,5-triphenylpyrrolidine (10)

A mixture of C<sub>60</sub> (72 mg, 0.1 mmol) and 1,2,3-triphenylaziridine (27 mg, 0.1 mmol) in toluene (40 mL) was refluxed for 6 h. The reaction mixture was cooled and removal of the solvent under reduced pressure gave a solid residue, which was chromatographed over silica gel. Elution with petroleum ether (bp 60-80 °C) gave 20 mg (28%) of the unchanged C<sub>60</sub>. Further elution with a mixture (1:4) of toluene and petroleum ether (bp 60-80 °C) gave 30 mg (42%) of the monoadduct **10**, mp > 400 °C; IR (KBr)  $\nu_{\max}$  1601, 1500, 1543, 1450, 1265, 696 cm<sup>-1</sup>; <sup>1</sup>H NMR (CDCl<sub>3</sub>)  $\delta$  6.68-6.82, 7.1-7.4 and 7.72-7.84 (17H, m, methine and aromatic); anal. calcd. for C<sub>80</sub> H<sub>17</sub> N: C, 96.94; H, 1.73;

N, 1.41, found: C, 96.63; H, 1.73; N, 1.21; exact mass calcd. for  $C_{80}H_{18}N$  992.1439 ( $MH^+$ ), found 992.1460 (FAB, high resolution mass spectrometry).

Further elution of the silica gel column with a mixture (3:7) of toluene and petroleum ether gave 20 mg (28%) of the bis-adduct **2**, mp > 400°C; IR (KBr)  $\nu_{max}$  1602, 1569, 1487, 695  $cm^{-1}$ ;  $^1H$  NMR ( $CDCl_3$ )  $\delta$  6.62-6.82, 6.9-7.82 and 7.9-8.02 (34 H, m, methine and aromatic); anal. calcd. for  $C_{100}H_{34}N_2$ : C, 95.02; H, 2.71; N, 2.21, found: C, 95.80. H, 2.51; N, 1.93; exact mass calcd. for  $C_{100}H_{35}N_2$  1264.3201( $MH^+$ ), found 1264.3242 (FAB, high resolution mass spectrometry).

#### 2.5.4. Instrumental techniques

All melting points are uncorrected and were determined on a Aldrich melting point apparatus. IR spectra were recorded on a Perkin Elmer Model 882 IR spectrometer and UV-visible spectra on a Shimadzu 2100 or GBC 918 spectrophotometer.  $^1H$  NMR and  $^{13}C$  NMR spectra were recorded either on a JEOL EX-90 MHz spectrometer or a Bruker DPX-300 MHz spectrometer. The emission spectra were recorded on a Spex-Fluorolog, F112-X equipped with a 450 W, Xe lamp and a Hamamatsu R928 photomultiplier tube. The excitation and emission slits were 1 and 4, respectively. A 570-nm long pass filter was placed before the emission monochromator in order to eliminate the interference from the solvent. Solvent spectra were recorded in each case and subtracted. Quantum yields of fluorescence were measured by a relative method using optically dilute solutions (absorbance adjusted to 0.1 at 470 nm). N-Methylfulleropyrrolidine dissolved in toluene ( $\phi_f = 6.0 \times 10^{-4}$ ) was used as reference.<sup>29,43,44</sup>

Picosecond laser flash photolysis experiments<sup>47</sup> were performed using 355 nm laser pulses from a mode-locked, Q-switched Quantel YG-501 DP Nd:YAG laser system (out put 1.5 mJ/pulse, pulse width ~18 ps). The white continuum picosecond probe pulse was generated by passing the fundamental output through a D<sub>2</sub>O/H<sub>2</sub>O mixture. The output was fed to a spectrograph (HR-320, ISDA Instruments, Inc.), with fiber optic cables and was analyzed with a dual diode array detector (Princeton Instruments, Inc.), interfaced with an IBM-AT computer. Time zero in these experiments corresponds to the end of the excitation pulse. All the lifetimes and rate constants reported in this study are at room temperature (297 K) and have an experimental error of  $\pm 10\%$ . The deaerated dye solution was continuously flowed through the sample cell during the measurements.

Nanosecond laser flash photolysis experiments<sup>47</sup> were performed with a Laser Photonics PRA/Model UV-24 nitrogen laser system (337 nm, 2 ns pulse width, 2-4 mJ/pulse) with front face excitation geometry. A typical experiment consisted of a series of 2-3 replicate shots per single measurement. The average signal was processed with an LSI-11 microprocessor interfaced with a VAX computer.

## 2.6. References

1. Deisenhofer, J.; Michel, H. *Angew. Chem. Int. Ed. Engl.*, **1989**, *28*, 829.
2. Hüber, R. *Angew. Chem. Int. Ed. Engl.*, **1989**, *28*, 848.
3. Balzani, V.; Maggi, L.; Scandola, F. *Supramolecular Photochemistry*, Balzani, V. (Ed.), Reidel, Holland, **1987**, pp 1-28.
4. Grabowski, Z.; Dobkowski, J. *Pure. Appl. Chem.*, **1983**, 245.
5. Wang, Y.; Crawford, M. C.; Eisenthal, K. B. *J. Am. Chem. Soc.*, **1982**, *104*, 5874.
6. Paddon-Row, M. N.; Oliver, A. M.; Warman, J. M.; Smit, K. J.; De Haas, M. P.; Oevering, H.; Verhoeven, J. W. *J. Phys. Chem.*, **1988**, *92*, 6958.
7. Moore, T. A.; Gust, D.; Mathis, P.; Mialocq, J. C.; Chachaty, C.; Bensasson R. V.; Land, E. J.; Doizi, D.; Liddell, P. A.; Nemeth, G. A.; Moore, A. L. *Nature (London)*, **1984**, *307*, 630.
8. Gust, D.; Moore, T. A.; Moore, A. L.; Lee, S. -J.; Bittersmann, E.; Kuttrull, D. K.; Rehms, A. A.; DeGraziano, J. M.; Ma, X. C.; Gao, F.; Belford, R. E.; Trier, T. T. *Science*, **1990**, *248*, 199.
9. Curtis, J. C.; Bernstein, J. S.; Mayer, T. J. *Inorg. Chem.*, **1985**, *24*, 385.
10. Norton, K. A.; Hurst, J. K. *J. Am. Chem. Soc.*, **1982**, *104*, 5960.
11. Connolly, J. S.; Bolton, J. R. In *Photoinduced Electron Transfer, Part D*, Fox, M. A.; Channon, M. (Eds.), Elsevier: Amsterdam, **1988**, pp 303-393.
12. Wasielewski, M. R. In *Photoinduced Electron Transfer, Part A*, Fox, M. A.; Channon, M. (Eds.), Elsevier: Amsterdam, **1988**, pp 161-206
13. Osuka, A.; Morikawa, S.; Maruyama, K.; Hirayama, S.; Minami T. *J. Chem. Soc., Chem. Commun.*, **1987**, 359.
14. Crawford, M. K.; Wang, Y.; Eisenthal, K. B. *Chem. Phys. Lett.*, **1981**, *79*, 529.
15. Mataga, N. *Pure. Appl. Chem.*, **1984**, *56*, 1255.
16. Yang, N. -C.; Neoh, S. B.; Naito, T.; Ng, L. -K.; Chernoff, D. A.; McDonald, D. B. *J. Am. Chem. Soc.*, **1980**, *102*, 2806.

17. Komatsu, K.; Kagayama, K.; Murata, Y.; Sugita, N.; Kobayashi, K.; Nagase, S.; Wan, T. S. M. *Chem. Lett.*, **1993**, 2163.
18. Vasella, A.; Uhlmann, P.; Waldraff, C. A. A.; Diederich, F.; Thilgen, C.; *Angew. Chem. Int. Ed. Engl.*, **1992**, *31*, 1388.
19. Hoke, S. H.; Molstad, J.; Dilettato, D.; Jay, M. J.; Carlson, D.; Kahr, B.; Cooks, R. G. *J. Org. Chem.*, **1992**, *57*, 5069.
20. Prato, M.; Maggini, M.; Scorrano, G.; Lucchini, V. *J. Org. Chem.*, **1993**, *58*, 3613.
21. Zhang, X.; Willems, M.; Foote, C. S.; *Tetr. Lett.*, **1993**, *34*, 8187.
22. Maggini, M.; Scorrano, G.; Prato, M. *J. Am. Chem. Soc.*, **1993**, *115*, 9798.
23. Sacrifitci, N. S.; Smilowitz, L.; Heeger, A. J.; Wudl, F. *Science*, **1992**, *258*, 1474.
24. Meier, M. S.; Poplawska, M. *J. Org. Chem.*, **1993**, *58*, 4524.
25. Akasaka, T.; Ando, W.; Kobayashi, K.; Nagase, S. *J. Am. Chem. Soc.*, **1993**, *115*, 10366.
26. Wudl, F.; Hirsch, K. C.; Khemani, T.; Suzuki, T.; Allemand, P.-M.; Koch, A.; Eckert, H.; Srdanov, G.; Webb, H. M. ACS Symp. Ser. (Fullerenes), **1992**, *481*, 161.
27. Belik, P.; Gugel, A.; Spickerman, J.; Mullen, K. *Angew. Chem. Int. Ed. Engl.*, **1993**, *32*, 78.
28. Hirsch, A.; Lamparth, I.; Karfunkel, H. R. *Angew. Chem. Int. Ed. Engl.* **1994**, *33*, 437.
29. a) Thomas, K. G.; Biju, V.; George, M. V.; Guldi, D. M.; Kamat, P. V. *J. Phys. Chem.*, **1998**, *102*, 5341. b) Kamat, P. V.; Guldi, D. M.; Liu, D.; Thomas, K. G.; Biju, V.; Das, S.; George, M. V. *Fullerenes*, Vol. 4, Kadish and Ruoff (Eds.), The Electrochemical Society, Pennington, NJ, **1997**. c) Kamat, P. V.; Guldi, D. M.; Biju, V.; Thomas, K. G.; George, M. V. *Fullerenes*, Vol. 6, Kadish and Ruoff (Eds.), The Electrochemical Society, Pennington, NJ, **1998**.
30. Huisgen, R.; Scheer, W.; Huber, H. *J. Am. Chem. Soc.*, **1967**, *89*, 1753.
31. Heine, H. W.; Peavy, R.; Durretaki, A. J. *J. Org. Chem.*, **1966**, *31*, 3924.
32. Confirmed on a Cosmosil Buckprep HLPC column.

33. Evaluated using the Sybyl force field method of PC SPARTAN software obtained from Wavefunction, Inc.; 18401, Von Karman, Suite 370, Irvine, CA 92612, USA.
34. Prato, M.; Maggini, M. *Acc. Chem. Res.*, **1998**, *31*, 519.
35. Bensasson, R. V.; Bienvenüe, E.; Fabre, C.; Janot, J. -M.; Land, E. J.; Leach, S.; Leboulaire, V.; Rassat, A.; Roux, S.; Seta, P. *Chem. Eur. J.*, **1998**, *4*, 270.
36. Catalan, J.; Elguero, J. *J. Am. Chem. Soc.*, **1993**, *115*, 9249.
37. Sun, Y. -P. In *Molecular and Supramolecular Photochemistry*, Vol. 1, *Organic Photochemistry*, Ramamurthy, V. and Schanze, K. S. (Eds.), Marcel Dekker, New York, **1997**, pp. 325-390.
38. Foote, C. S. In *Topics in Current Chemistry; Electron Transfer 1*, Matty, J. (Ed.), Springer-Verlag, Berlin, **1994**, pp 347.
39. Kamat, P. V.; Asmus, K. -D. *Interface*, **1996**, *5*, 22.
40. Zhou, F.; Jehoulet, C.; Bard, A. J. *J. Am. Chem. Soc.*, **1992**, *114*, 11004.
41. Dubois, D. K.; Kadish, K. M.; Flanagan, S.; Haufler, R. E.; Chibante, L. P. E.; Wilsson, L. F. *J. Am. Chem. Soc.*, **1992**, *114*, 3978.
42. Arbogast, J. W.; Foote, C. S.; Kao, M. *J. Am. Chem. Soc.*, **1992**, *114*, 2277.
43. Guldi, D. M.; Maggini, M.; Scarrano, G.; Prato, M. *J. Am. Chem. Soc.*, **1997**, *119*, 974.
44. Sariciftci, N. S.; Wudl, F.; Heeger, A. J.; Maggini, M.; Scarrano, G.; Prato, M.; Bourassa, J.; Ford, F. C. *Chem. Phys. Lett.*, **1995**, *247*, 510.
45. Williams, R. M.; Koeberg, M.; Lawson, J. M.; An, Y. -Z.; Rubin, Y.; Paddon-Row, M. N.; Verhoeven, J. M. *J. Org. Chem.*, **1996**, *61*, 5055.
46. Bell, T. D. M.; Smith, T. A.; Ghiggino, K. P.; Ranasinghe, M. G.; Shephard, M. J.; Paddon-Row, M. N. *Chem. Phys. Lett.*, **1997**, *268*, 223.
47. Transient absorption studies were done in collaboration with Dr. Prashant V. Kamat, Dr. D. M. Guldi and Dr. K. George Thomas at the Radiation Laboratory, University of Notre Dame, Indiana, USA.
48. Taylor, T.W.J.; Owen, J. S.; Whitaker, D. *J. Chem. Soc.*, **1938**, 206.

## Chapter 3

### Photoinduced Intramolecular Electron Transfer Processes in Clusters of Fullerene-Aniline and Bis(fullerene)-Aniline Dyads

#### 3. 1. Abstract

Synthesis of bis(fullerene) derivatives was achieved through cycloaddition reactions of  $C_{60}$  with appropriate azomethine ylides. Fullerene derivatives 1-5 form stable, optically transparent clusters in 75-95% (v/v) acetonitrile-toluene mixtures. Intermolecular interactions between the clusters of fullerene derivative 5 and electron donors were investigated using steady state fluorescence spectroscopy and a strong quenching of the fluorescence was observed with increase in quencher concentrations. Ground and excited state properties of the clusters of the dyads 1 and 3 and the model compounds 2 and 4 were compared with their corresponding monomeric forms. Clustering of the dyads and the model compounds resulted in red shifted emission maxima with different quantum yields for the associated emission of the singlet excited states. The large quenching of fluorescence, noticed for the dyad clusters is attributed to an electron transfer process from the appended aniline function, which is known to be a good electron donor, to the electron accepting fullerene cluster. Both, singlet and triplet excited states of fullerene derivatives 1-4, exhibited similar absorption features in toluene solutions. However, the growth of a broad absorption with a lifetime of  $\sim 3$  ns was observed following the excitation of clusters of the dyad 1 in acetonitrile-toluene mixtures. Charge transfer interaction between the photoexcited fullerene and aniline moieties led to the production of radical anion of 1 which was independently confirmed by the presence of an absorption band of the fullerene radical anion in the NIR region (1010 nm).



### 3. 2. Introduction

Design of molecular systems which can spontaneously self assemble and generate three-dimensionally extended structures such as in clusters are of interest in "chemical nanotechnology".<sup>1</sup> Fullerene and its derivatives are known to form clusters in solutions which are optically transparent and thermodynamically stable.<sup>2-8</sup> Recent studies of molecular systems based on  $C_{60}$ ,<sup>4-37</sup> particularly the dyads and triads,<sup>11-25</sup> indicate that they may serve as building blocks for optoelectronic and photovoltaic devices and systems mimicking photosynthesis.<sup>28-29</sup> In this context, several fullerene based donor-acceptor systems containing porphyrins,<sup>11-16</sup> phthalocyanines,<sup>17</sup> ruthenium complexes,<sup>18,19</sup> ferrocenes<sup>20,21</sup> and anilines,<sup>22-25,26</sup> as donors have been synthesized and the photoinduced electron transfer processes in these dyads, in homogeneous solutions, have been studied.

The photoactive molecules based on fullerenes, when incorporated in solid matrices, show optical limiting and photoconducting behaviour.<sup>28-37</sup> The enhanced photoconductivity observed by doping fullerenes and their derivatives in polymers is attributed to an efficient intermolecular charge transfer process. For device applications, it is desirable to have detailed mechanistic understanding of the various inter- and intramolecular interactions and the electron transfer behaviour in solid state. Several reports are available on photoinduced electron transfer processes of dyads in solutions. In these systems, the solute-solvent interactions play a decisive role in the stabilization of the charge-separated species. Such interactions are absent in the solid state and hence studies in solutions cannot be taken as a model for electron transfer behaviour in solids. Photophysical and electron transfer studies related to

clusters could provide information, bridging the solution and solid state properties, in molecular systems.

### 3. 2.1. Clusters of fullerenes

It has been recently reported that fullerenes, C<sub>60</sub> and C<sub>70</sub>, as well as the water soluble derivatives of C<sub>60</sub> bearing charged functional groups form optically transparent microscopic clusters (aggregates) in solutions at room temperature.<sup>5,6,8</sup> Clustering in this class of molecules is mainly associated with the strong three-dimensional hydrophobic interactions between fullerene units. Details of the conditions<sup>2-4</sup> for the formation of the clusters as well as their spectroscopic<sup>2-6</sup> and size distribution studies<sup>4</sup> are well documented. More recently, it has been observed that the radiolytic reductions of fullerene clusters depend on their surface potential.<sup>6</sup> There are no reports on the electron transfer processes in clusters of fullerene based systems and such studies would be helpful for a molecular level understanding of their properties in solid state devices. With this view, we have recently initiated studies on the photophysical and electron transfer properties of the clusters of a few fullerene based dyads.<sup>7</sup> Clusters of these dyads can be visualized as self assembled antenna systems containing hydrophobic fullerene as the central core with appended anilinic groups. Photoinduced electron transfer in such self-assembled systems can provide useful information about the dynamics of electron transfer in aggregates. In the present study, we have investigated the possibility of cluster formation in a monofunctionalized dyad 1<sup>25</sup> and a novel bis(buckminsterfullerene)-aniline dyad 3 (Chart 3.1). The detailed photophysical properties and photoinduced intramolecular electron transfer processes in clusters of the dyads

are also presented. The photophysical properties and photoinduced intramolecular electron transfer processes in clusters of the dyads are compared with those of the two model compounds 2 and 4 (Chart 3.1), which do not possess the anilinic donor groups. Intermolecular electron transfer processes

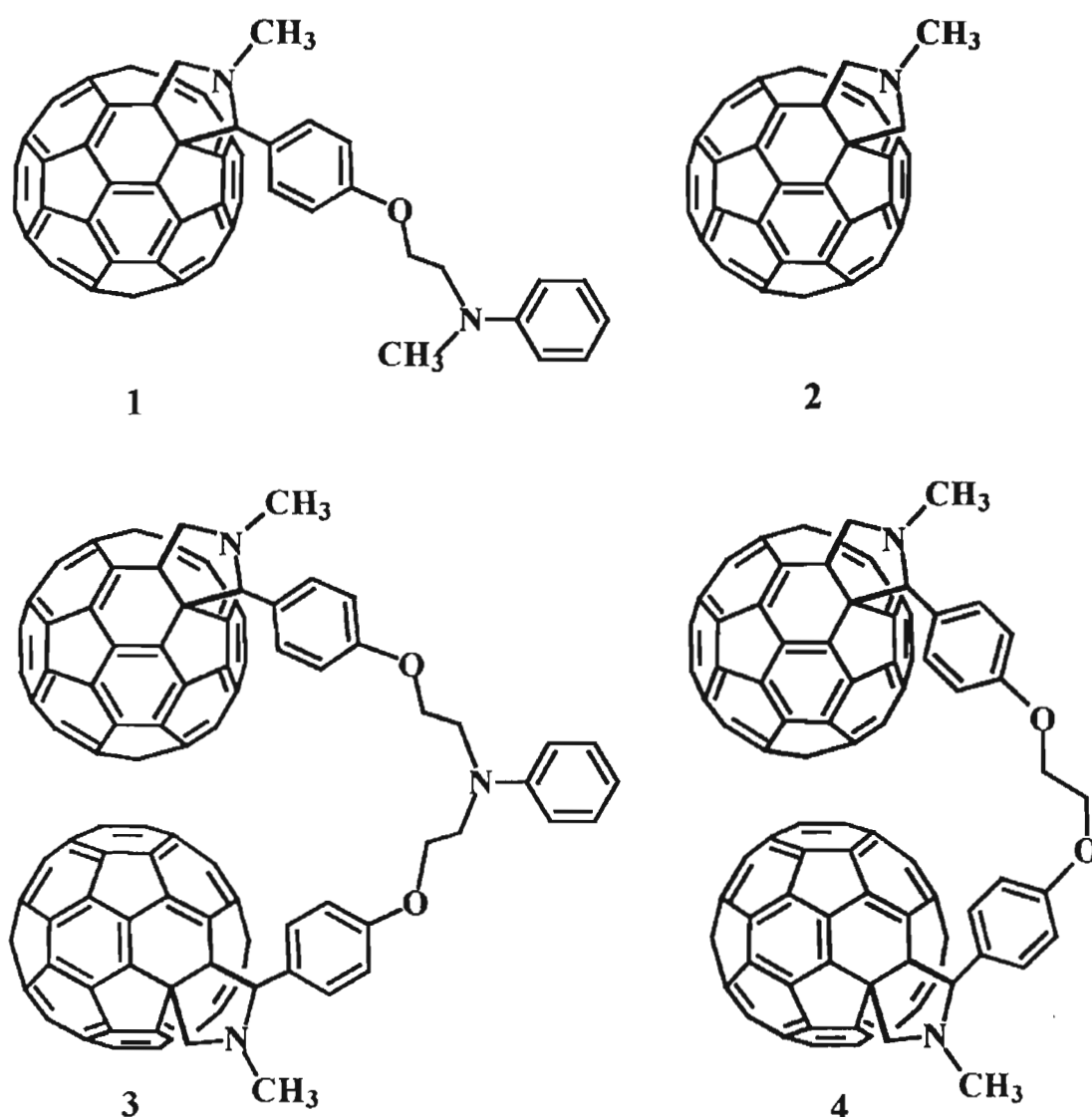


Chart 3.1

between the clusters of **5** and electron donors like N,N-dimethylaniline and 10-methylphenothiazine (Chart 3.2) were also investigated.

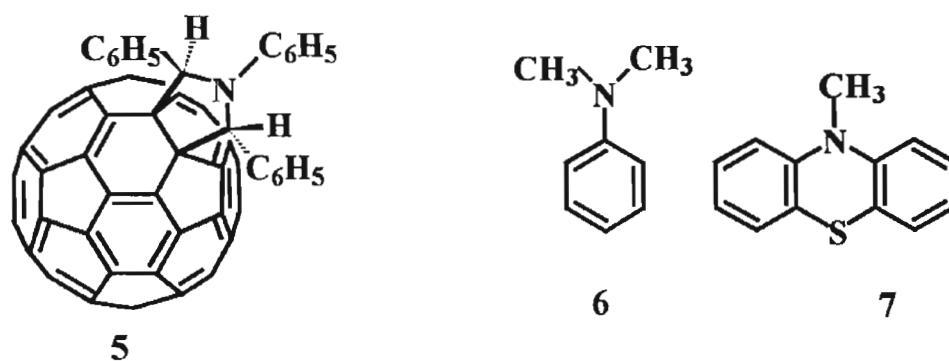
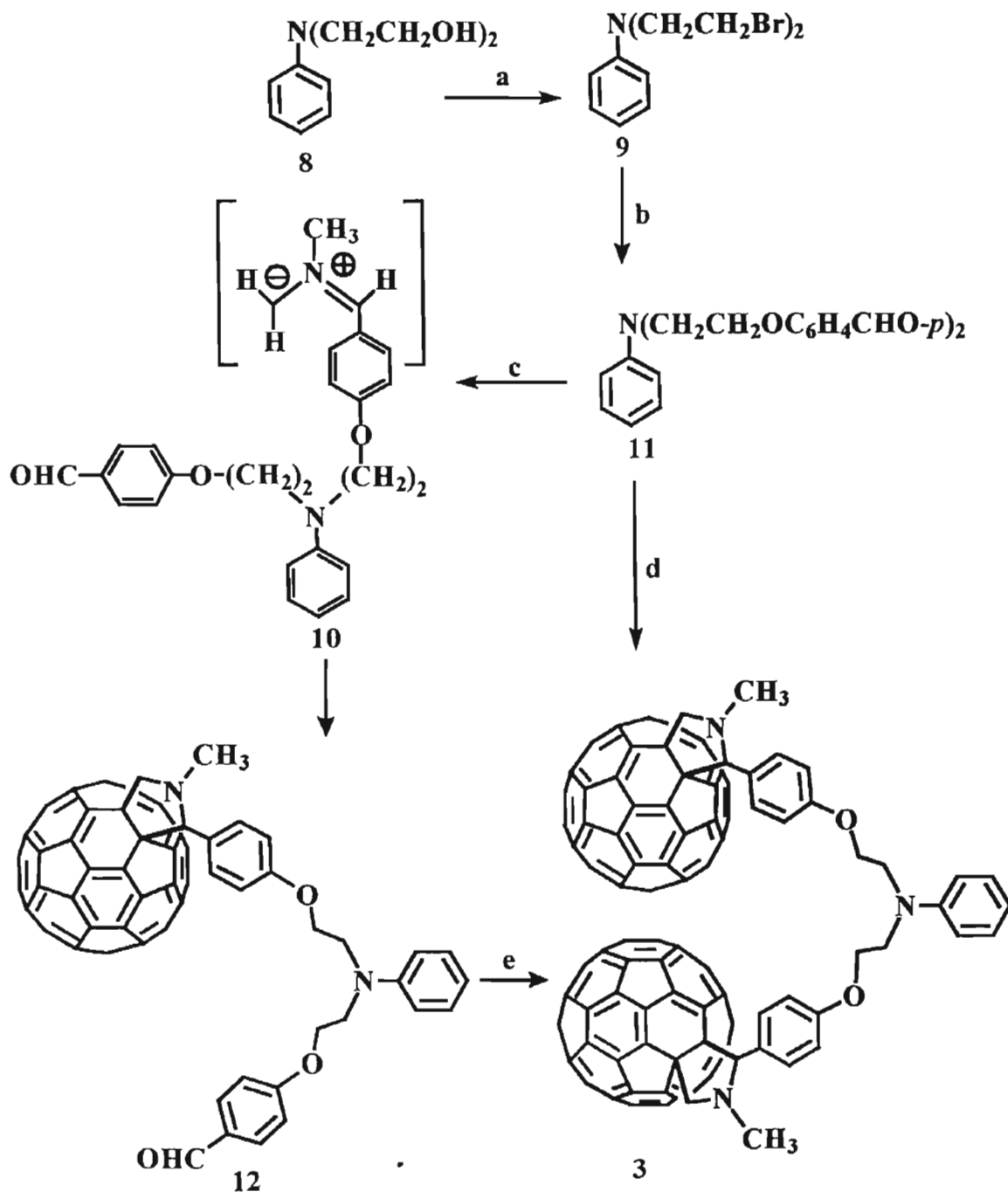


Chart 3.2

### 3.3. Results and Discussion

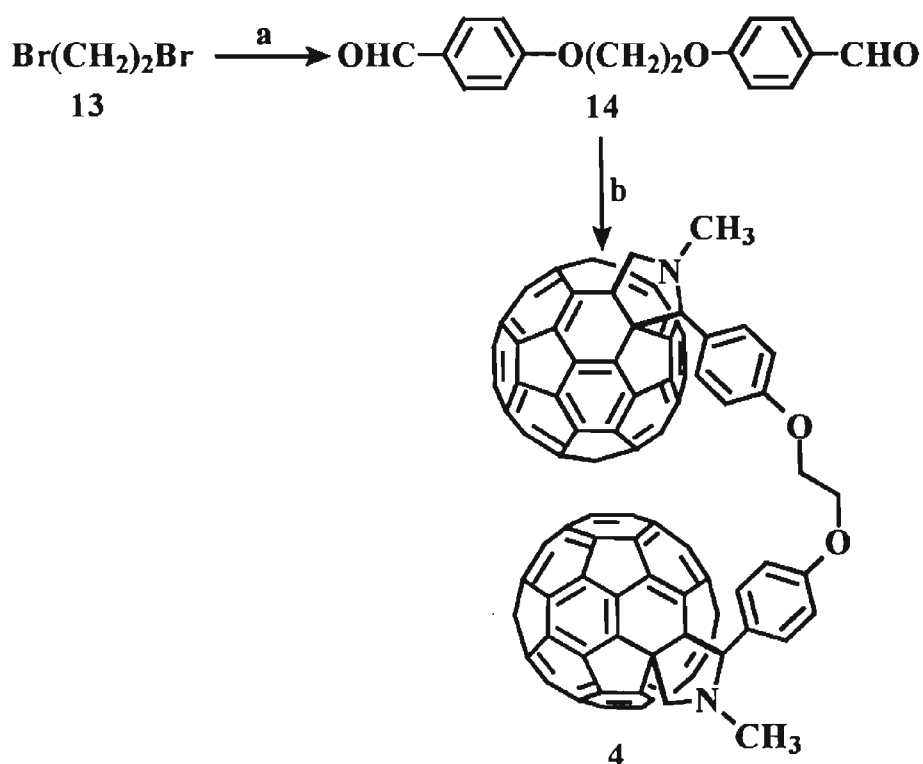
#### 3.3.1. Synthesis

The details of the synthesis of the fullerene-aniline dyad, **1** were reported in Chapter 2. The model compound, N-methylfulleropyrrolidine, **2** was prepared as per a reported procedure.<sup>38</sup> The general method adopted for the synthesis of bis(fullerene)-aniline dyad, **3** and the model compound, **4** are shown in Schemes 3.1 and 3.2, respectively. The starting material for the synthesis of **3**, namely N,N-di(2-hydroxy-1-ethyl)aniline **8** was prepared in a 85 % yield by adopting methods similar to those reported in the literature.<sup>38-42</sup> Purity of all these dyads was confirmed by HPLC.<sup>43</sup>



a)  $\text{PBr}_3/\text{CH}_2\text{Cl}_2$ ; b)  $\text{K}_2\text{CO}_3/p\text{-OHC}_6\text{H}_4\text{CHO/acetone}$ , reflux;  
 c), d) and e)  $\text{C}_{60}$ , N-methylglycine, heat

Scheme 3.1



a)  $K_2CO_3/p\text{-OH-C}_6\text{H}_4\text{CHO/acetone}$ , reflux; b)  $C_{60}$ , N-methylglycine, toluene, heat

**Scheme 3.2**

### 3.3.2. Steady state absorption properties

The absorption spectra of the fullerene-aniline dyad **1**<sup>25</sup> and its model compound **2** as well as the bis(fullerene)-aniline dyad **3** and its model compound **4** in toluene are shown in Figures 3.1-3.4, respectively. The absorbance of all the C<sub>60</sub> compounds under investigation obey the Beer-Lambert Law in toluene, in the spectral region 400-750 nm and concentrations up to 50  $\mu\text{M}$ , ruling out the possibility for the formation of other absorbing species. Dyads **1** and **3** as well as the model compounds **2**<sup>27,38</sup> and **4** possess a sharp band at 430 nm, which is characteristic of all monofunctionalized [6,6]-closed fullerene adducts, and a weak band around 700 nm. Representative examples, indicating these bands clearly, are

shown in the inset of Figure 3.1. A detailed assignment of the 700 nm band in the case of the dyad **1** is given in Section 2.3.4 and attributed as the sum of a forbidden transition<sup>27</sup> and a charge-transfer transition.<sup>25</sup> Similar results were also observed for the dyad **3**. A partial disappearance of the 700 nm band was observed by adding trifluoroacetic acid (25 mM), indicating the presence of a ground state charge transfer interaction. These changes were completely reversed by adding pyridine (30 mM). The absorption spectrum of the bis(fullerene) model compound **4** was found to be unaffected by the addition of TFA (up to 250 mM), ruling out the possibility of a ground state charge transfer interaction.

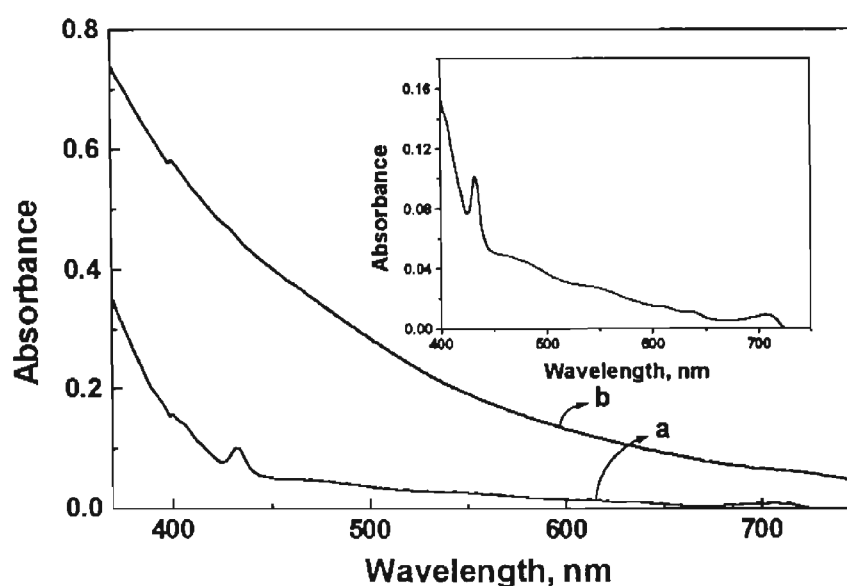


Figure 3.1. Absorption spectra of **1** (19  $\mu\text{M}$ ) in (a) toluene and (b) 75% v/v acetonitrile-toluene. Inset shows the expanded absorption spectrum of **1** (19  $\mu\text{M}$ ) in toluene.

As in the case of  $\text{C}_{60}$  and  $\text{C}_{70}$ ,<sup>2-4,8</sup> the dyads and the model compounds exist as monomers in toluene and a solvent-induced clustering was observed in acetonitrile-toluene mixtures containing more than 70% (v/v) of acetonitrile. Clusters of  $\text{C}_{60}$  and  $\text{C}_{70}$  prepared through this “fast method”<sup>2-4</sup> were found to be

stable. In the present study, we have adopted a similar method for the preparation of the clusters by injecting toluene solutions of 1-5 into acetonitrile. Formation of the

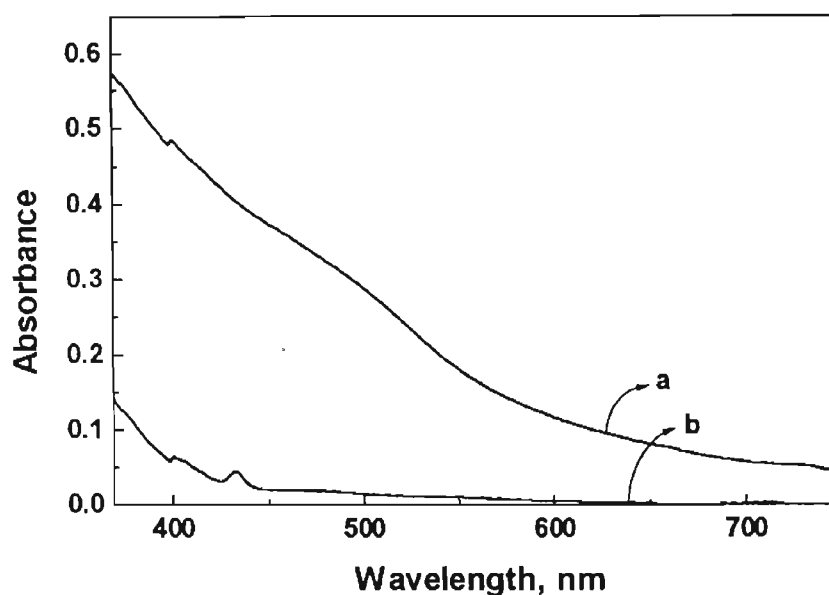


Figure 3.2. Absorption spectra of 2 ( $12 \mu\text{M}$ ) in (a) 75% v/v acetonitrile-toluene and (b) toluene.

clusters of the dyads and the model compounds was investigated, in detail, by monitoring their absorption properties as a function of substrate concentration and more importantly by varying the content of a polar solvent, namely acetonitrile in toluene. In the former case, substrate concentration is varied by injecting different volumes of toluene solutions ( $\sim 0.5 \text{ mM}$ ) of the fullerene derivatives into acetonitrile or toluene-acetonitrile mixtures, in such a way that the solvent composition remains the same (1:3). In each case the absorption spectrum was recorded and observed that the Beer-Lambert law is obeyed up to  $10 \mu\text{M}$  concentration, above which there is a substantial enhancement in the molar extinction coefficient (Figures 3.1-3.4) up to  $20 \mu\text{M}$ . When the concentration exceeded  $20 \mu\text{M}$ , precipitation was observed. In the latter case, when the ratio of acetonitrile in toluene-acetonitrile mixture was



varied at constant substrate concentration, the solutions were found to obey the Beer-Lambert law up to 60% (v/v) of acetonitrile. A sudden increase in the absorptivity was observed on further increasing the acetonitrile content up to 95% (v/v), above which precipitation takes place. It should be noted that the hydrophobic nature of the fullerene moiety prevents their dissolution in polar solvents. The absorption spectra in the 400-750 nm region transformed into featureless and broad absorption onset by increasing the acetonitrile content (75-95% (v/v)) with significant increase in molar extinction coefficients (Figures 3.1-3.4), despite the same substrate concentration. This sudden enhancement in the absorption is attributed to the formation of clusters. Similar absorption properties were observed during formation the clusters of  $C_{60}$ ,<sup>2,4</sup>  $C_{70}$ <sup>2,4</sup> and some charged derivatives of  $C_{60}$ ,<sup>5,8</sup> which were further characterized on the basis of light scattering experiments and TEM techniques.

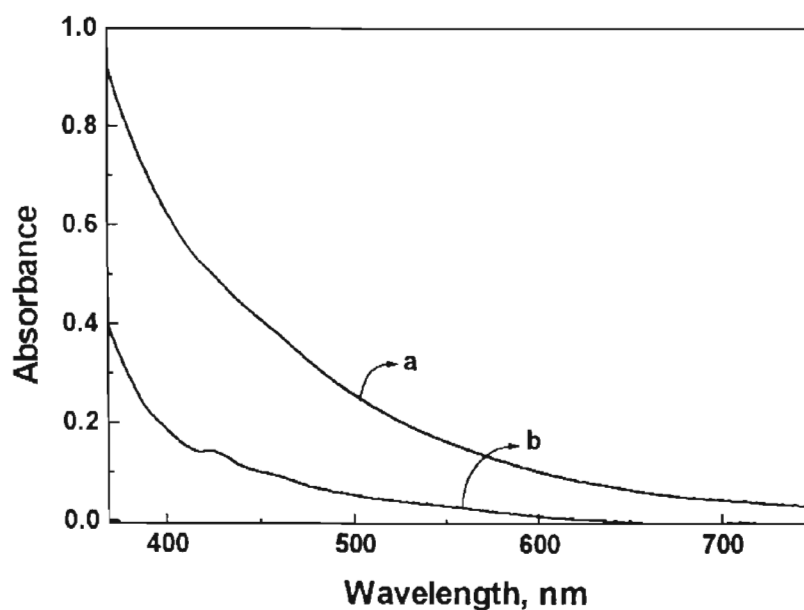


Figure 3.3. Absorption spectra of **3** (50  $\mu$ M) in (a) 75% v/v acetonitrile-toluene and (b) toluene.

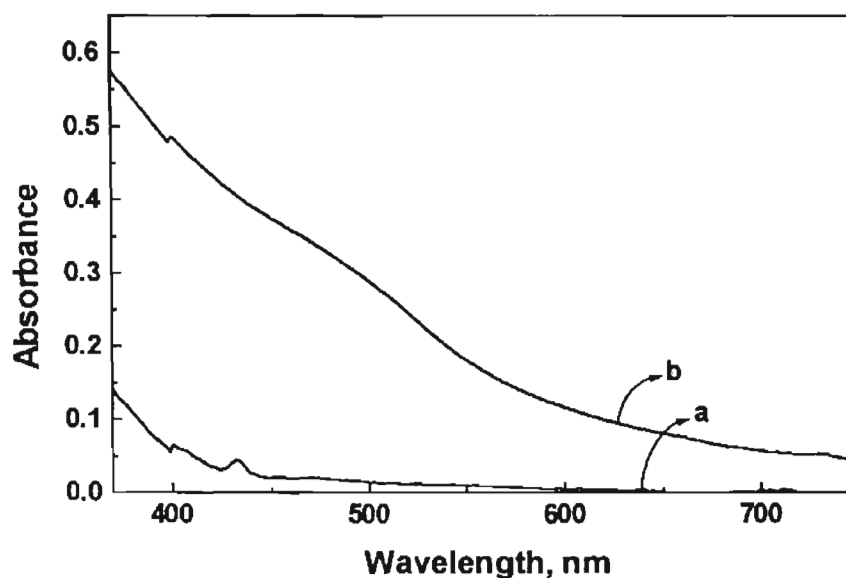


Figure 3.4. Absorption spectra of **4** (50  $\mu\text{M}$ ) in (a) toluene and (b) 75% v/v acetonitrile-toluene.

These optically transparent clusters are found to be quite stable at room temperature and were reverted back to their monomeric forms by diluting with toluene or by adding nanomolar quantities of trifluoroacetic acid. Spectral properties of the monomers and clusters of the dyads and the model compounds are summarized in Table 3.1.

### 3.3.3. Steady state emission properties

In this section, we have undertaken a detailed investigation of the emission properties of the clusters of  $\text{C}_{60}$  derivatives 1-5 and these results are compared with those of the monomeric forms. The emission properties of the monomeric forms of the fullerene-aniline dyad **1** and the bis(fullerene) derivatives are discussed in Section 2.3.5.2 and Section 3.3.3.2, respectively.

#### 3.3.3.1. Emission characteristics of the clusters of the fullerene-aniline dyad **1**

We have systematically investigated the effect of clustering on the emission spectral properties of the dyad **1** and the model compounds **2**. In general, clustering

leads to a bathochromic shift of ~25 nm in their emission maxima, for both the compounds under investigation (Table 3.1). As a representative example, the normalized emission spectra of the monomeric and the clustered form of the fullerene derivative, **2** are shown in Figure 3.6.

Based on the electron donating ability of aniline and the electron accepting properties of the fullerene core, we have further examined the possibility of an electron transfer process in the dyad clusters. Clusters of the C<sub>60</sub>- aniline dyad **1** and the model compound **2** exhibit emission in the same spectral region with maximum around 740 nm and their emission properties are compared using optically matched solutions (absorbance at 470 nm, the wavelength of excitation, was adjusted to 0.35). Interestingly, a substantial decrease in the fluorescence quantum yield was observed for clusters of the dyad **1** (Figure 3.7). Relative fluorescence yields of the dyad **1** and model compound **2** are summarized in Table 3.1. A possible explanation for the quenching of fluorescence may be due to a thermodynamically favoured electron transfer in a polar medium (acetonitrile-toluene mixture) compared to toluene. Earlier, we have systematically investigated the effect of solvent polarity on the emission properties of the fullerene-aniline dyad **1** and the results are summarized in Section 2.3.5.2. These studies indicate that even in a highly polar solvent such as benzonitrile, only ~ 50% quenching of fluorescence is observed.

In the present case, a large bathochromic shift in emission maximum with a substantial decrease in the fluorescence quantum yield is observed as a result of clustering of the dyads. The clusters of the dyads may be considered as a self assembled three dimensional antenna systems possessing the fullerene moiety as a central core with anchored aniline groups in various directions.

**Table 3.1.** Spectral profiles of monomers and clusters of the dyads (**1** and **3**) and the model compounds (**2** and **4**)

compound	Solvent <sup>a</sup>	$\epsilon$ (at 470 nm) M <sup>-1</sup> cm <sup>-1</sup>	$\lambda_{\text{max}}(\text{em.})$ nm	relative emission intensity <sup>b,c</sup>
<b>1</b>	Toluene	0.24 x 10 <sup>4</sup>	713	-
<b>1</b>	Toluene-acetonitrile (1:7)	1.86 x 10 <sup>4</sup>	738	19
<b>2</b>	Toluene	0.40 x 10 <sup>4</sup>	714	-
<b>2</b>	Toluene-acetonitrile (1:7)	2.96 x 10 <sup>4</sup>	737	100
<b>3</b>	Toluene	0.43 x 10 <sup>4</sup>	722, 776	-
<b>3</b>	Toluene-acetonitrile (1:7)	1.90 x 10 <sup>4</sup>	737	32
<b>4</b>	Toluene	0.56 x 10 <sup>4</sup>	725, 776	-
<b>4<sup>c</sup></b>	Toluene-acetonitrile (1:7)	2.71 x 10 <sup>4</sup>	750	-

<sup>a</sup> solvent ratios are based on volume/volume(v/v); <sup>b</sup> emission intensities (at 738 nm) were measured by matching the optical density (0.35) of clusters; <sup>c</sup> a shift in emission maximum was observed for the clusters of **4** and hence intensity was not compared.

A possible self-assembled structure of the dyad is shown in Chart 3.3. Dynamic light scattering studies<sup>44</sup> using **1** in a mixture (3:1) of acetonitrile and toluene reveal that the size distribution of the clusters is over a narrow range (120-200 nm) and the mean diameter is around 170 nm (Figure 3.5). Similar values are reported in the literature for the clusters of C<sub>60</sub>.<sup>4,45</sup> A higher probability of interaction between the fullerene moiety and the anilinic donor groups, exists in the

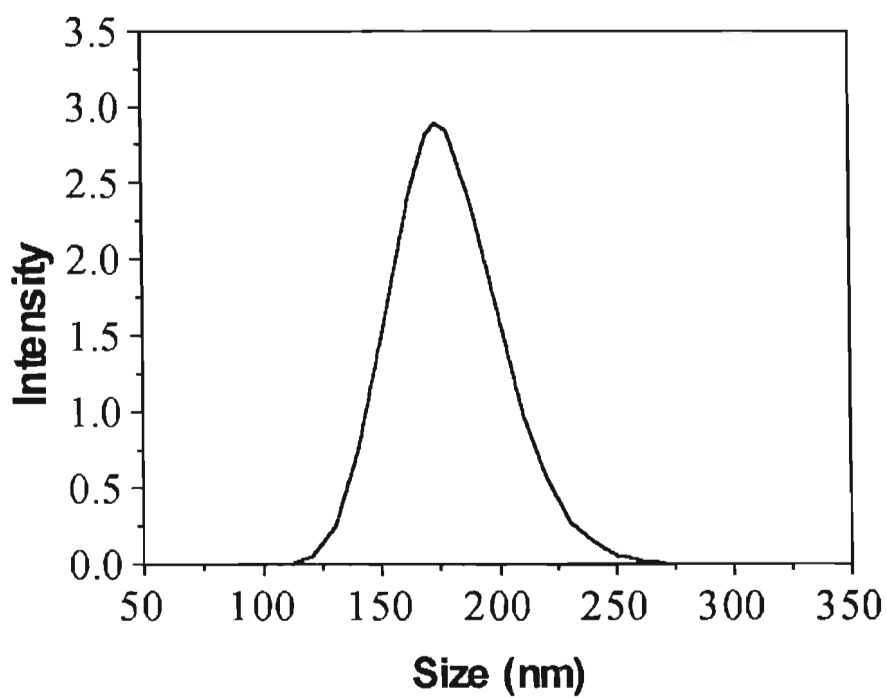


Figure 3.5. Size distribution of clusters of the dyad 1 in a mixture (3:1) of acetonitrile and toluene.

micro-heterogeneous domains of the clusters than in a homogeneous system. The transfer of an electron from the covalently linked aniline moiety to the photoexcited fullerene cluster leads to the quenching of the excited singlet-state of the cluster.

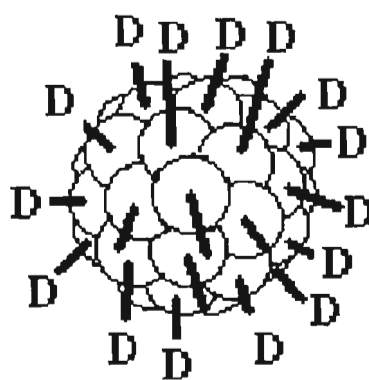


Chart 3.3. Possible self assembled structure of the dyad 1

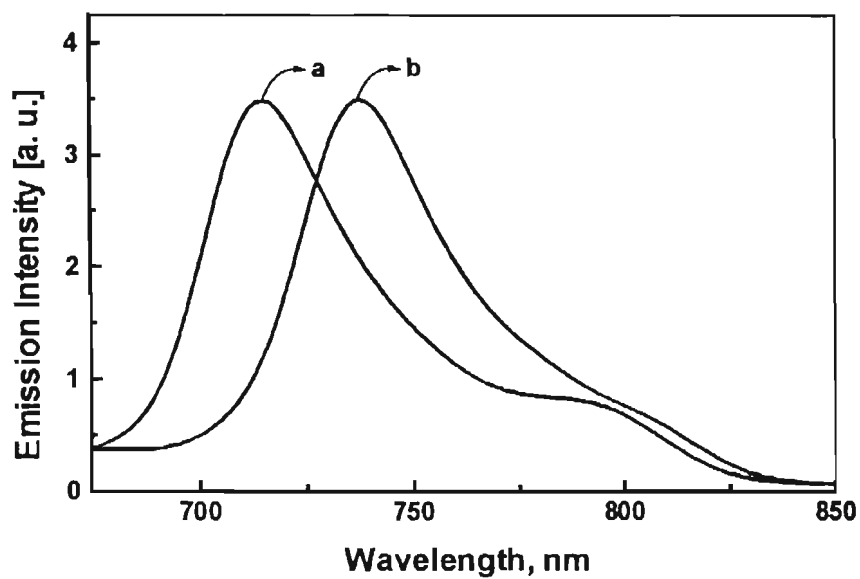


Figure 3.6. Normalized emission spectra of **2** in (a) toluene and (b) 12.5% (v/v) toluene-acetonitrile.

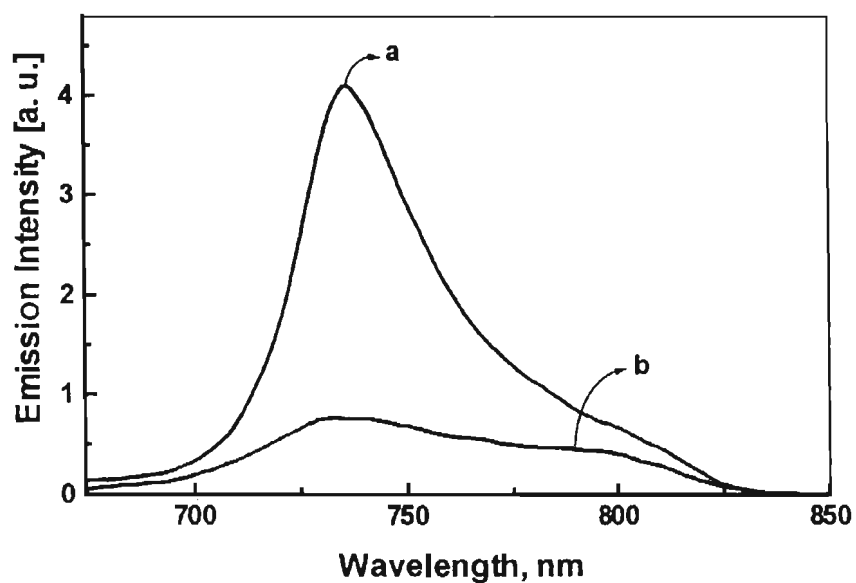


Figure 3.7. Emission spectra of the optically matched solutions of the dyad and the model compound in 12.5% (v/v) toluene-acetonitrile: (a) **2** and (b) **1** [absorbance of 0.35 at the excitation wavelength (470 nm)].

### 3.3.3.2. Emission characteristics of the monomers of bis(fullerene) derivatives

The normalized emission spectra of the bis(C<sub>60</sub>) derivatives **3** and **4** in toluene, where they exist in monomeric forms, are shown in Figure 3.8. Compared to the monofullerene derivatives (trace 'a' of Figure 3.8), the spectral features of the bis(C<sub>60</sub>) derivatives are quite different (traces 'b' and 'c' of Figure 3.8). Apart from the band around 720 nm, both the bis(C<sub>60</sub>) derivatives possess an additional band around 775 nm. Preliminary studies indicate that the relative intensities of both these bands are unaffected by varying the temperature (5 - 40 °C) and solvent polarity (toluene to benzonitrile). Also, the excitation spectra of the bis(C<sub>60</sub>)-aniline dyad, **3** and the model compound **4** obtained by following emission at 710, 740 and 775 nm are similar in nature and match closely to the absorption features of the corresponding monomeric forms. More detailed studies on the emission properties of a series of bis(C<sub>60</sub>) derivatives, linked together with methylene groups of varying length, are required to understand the emission behaviour of bisfullerenes.

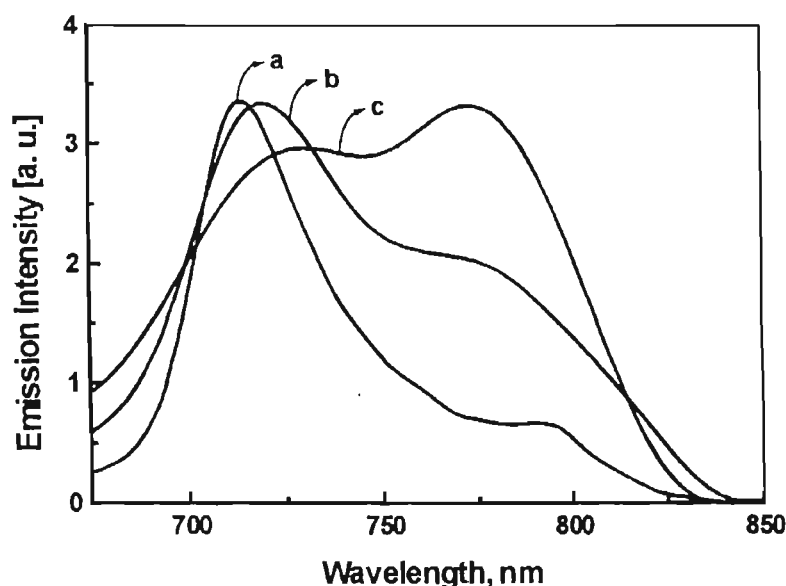


Figure 3.8. Normalized emission spectra of the monomeric forms of the dyads in toluene: (a) **1**, (b) **3**, (c) the model compound **4**.

### 3.3.3.3. Emission characteristics of the clusters of bis(fullerene) derivatives

We have also investigated the effect of clustering on the emission spectral properties of the bis(C<sub>60</sub>) derivatives and the possibility of an electron transfer in the clusters of the bis(C<sub>60</sub>)-aniline dyad **3**. As observed in the case of the fullerene-aniline dyad **1** (Section 3.3.3.1), the bis(fullerene) derivatives also exhibit a bathochromic shift in their emission maxima on clustering (Figure 3.9). Clusters of the bis(C<sub>60</sub>)-aniline dyad **3** exhibit an emission maximum around 740 nm, whereas the emission spectrum of the clusters of the model compound **4** is further red-shifted to 750 nm. Earlier, we had observed that the clusters of the model compound **2**<sup>7</sup> exhibit an emission maximum around 740 nm and therefore, this was used as a standard for investigating the possibility of an electron transfer in the clusters of the bis(C<sub>60</sub>)-aniline dyad **3**. The emission properties of the bis(C<sub>60</sub>)-aniline dyad **3** and the model compound **2** are compared using optically matched solutions (absorbance at 470 nm was adjusted to 0.35). A large decrease in the fluorescence intensity was observed for the clusters of the bis(C<sub>60</sub>)-aniline dyad **3** (Figure 3.9) and the relative fluorescence yields are summarized in Table 3.1. A possible self-assembled structure of the bis(C<sub>60</sub>)-aniline dyad **3** is shown in Chart 3.4.<sup>6,44</sup> Photoexcitation of the bis(C<sub>60</sub>)-aniline clusters brings

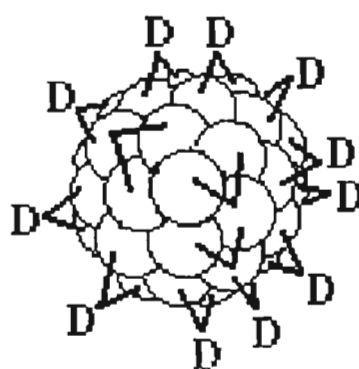


Chart 3.4. Possible self assembled structure of the dyad **3**



about an electron transfer from the anchored aniline to fullerene core resulting in the quenching of their excited singlet state.

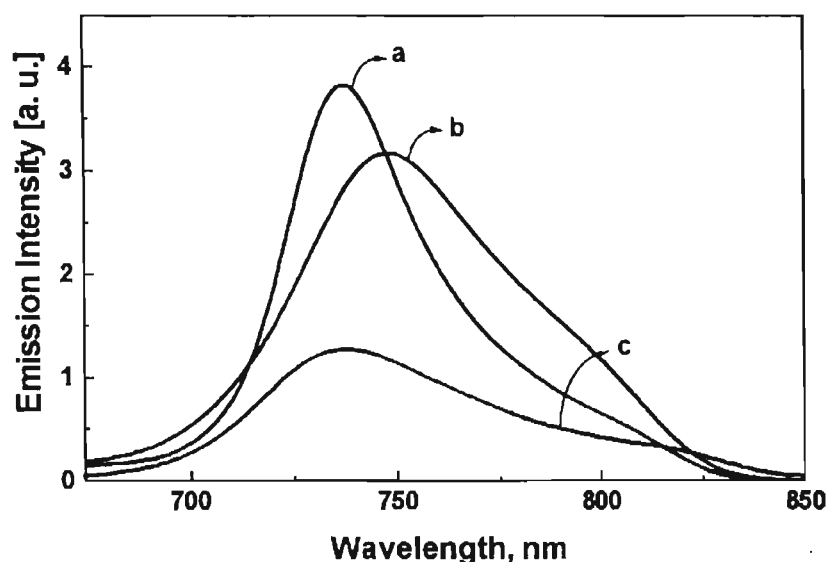


Figure 3.9. Emission spectra of the optically matched solutions of the clusters of the dyads and the model compounds in 12.5% (v/v) toluene-acetonitrile: (a) **2**, (b) **4** and (c) **3**. [absorbance of 0.35 at the excitation wavelength (470 nm)].

#### 3.3.3.4. Fluorescence quenching of the clusters of **5** by electron donors

Earlier, we have found that the emission spectral features and  $\phi_f$  of the model compound, 1,2,5-triphenylpyrrolidinofullerene, **5** are more or less unaffected by the change in solvent polarity. Results of fluorescence quenching of the monomeric form of **5**, on adding electron donors such as N,N-dimethylaniline, in a mixture (1:1) of toluene and acetonitrile are presented in Section 2.3.5.1. In the present study, we have found that the model fullerene derivative **5** forms stable and optically transparent clusters in 95% (v/v) acetonitrile-toluene mixtures and a fast method<sup>2-4</sup> was adopted for the preparation of the clusters. Typically, the clusters are prepared by a fast injection of 100  $\mu$ L toluene solution of the **5** (2 mM) into 3.5 mL of acetonitrile. In this section, we have investigated the intermolecular interaction

between these clusters and various electron donors such as N,N-dimethylaniline (DMA) and 10-methylphenothiazine (MP). The absorption spectral features of the clusters remain unaffected on addition of electron donors, ruling out the possibility of the disruption of the clusters, in presence of the donors. A marked decrease in the fluorescence yield of the clusters of **5** was observed with increase of quencher concentration (Figures 3.10 and 3.11). Interestingly, a lower donor concentration is sufficient to quench the fluorescence of the clusters of **5**, compared to the monomers in 1:1 toluene and acetonitrile mixture (for details, see Section 2.3.5.1.). Intermolecular interactions with the donor systems may be more efficient in the case of clusters and the transfer of an electron from the donor leads to the quenching of the excited singlet state of the clusters. The Stern-Volmer plots (for details, see Section 2.3.5.1.) for fluorescence quenching

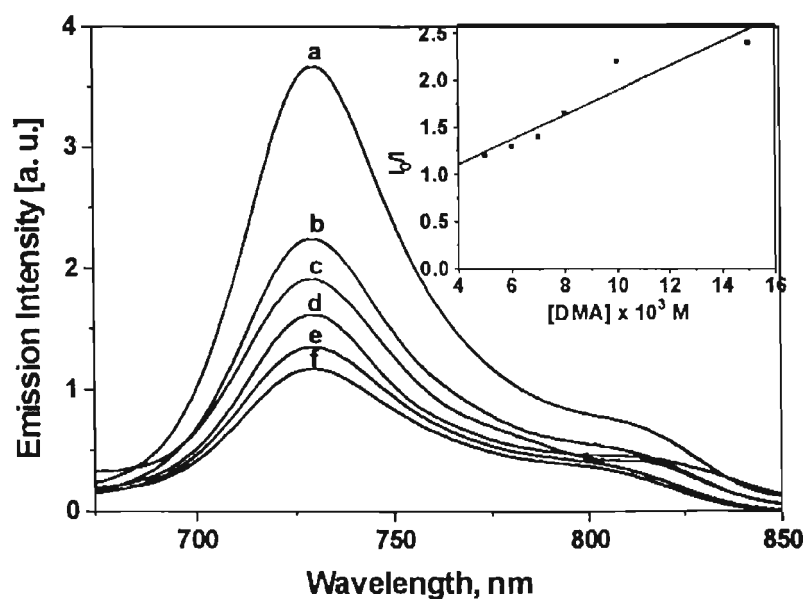


Figure 3.10. Effect of addition of N,N-dimethylaniline (DMA) on the fluorescence of the clusters of **5** in 95% (v/v) acetonitrile-toluene: [DMA] (a) 0, (b) 5, (c) 6, (d) 7, (e) 10 and (f) 15 mM.

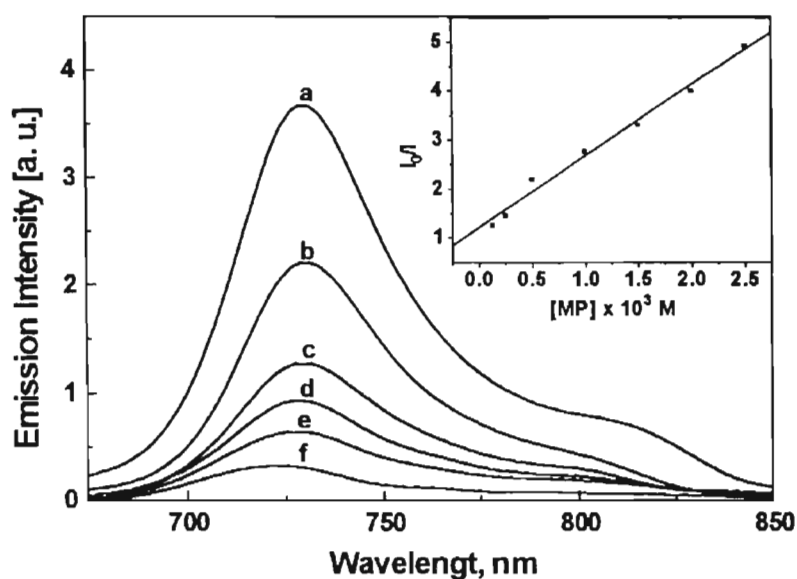


Figure 3.11. Effect of addition of 10-methylphenothiazine (MP) on the fluorescence of the clusters of **5** in 95 % (v/v) acetonitrile-toluene: [MP] (a) 0, (b) 0.125, (c) 0.5, (d) 1.0, (e) 2.0 and (f) 5.0 mM.

are given in the insets of Figures 3.10 and 3.11 and the Stern-Volmer constants ( $K_{sv}$ ) were estimated as  $474 \text{ M}^{-1}$  for *N,N*-dimethylaniline and  $676 \text{ M}^{-1}$  for 10-methylphenothiazine.

#### 3.3.4. Dynamics of photoinduced charge transfer in dyad clusters

The dynamics of photoinduced electron transfer in clusters of dyad **1** was further probed, in detail, using picosecond and nanosecond laser flash photolysis experiments. These results were compared with photoinduced electron transfer in dyad **1** in homogeneous solutions. In nonpolar solvents such as toluene, fullerene derivatives possess a broad absorption around 920 nm, which is a characteristic of the singlet excited state (Section 2.3.6).

The excited singlet state behavior of the fullerene clusters in acetonitrile/toluene mixture was significantly different than that observed in toluene.

The difference absorption spectra recorded immediately after the laser pulse excitation for the clusters in acetonitrile/toluene mixtures lack any prominent absorption bands in this spectral region. On the other hand, the cluster solutions of dyad **1** as well as model compound **2**, exhibit a slow absorption growth throughout the entire UV-VIS-NIR region which continues up to several nanoseconds. Time-resolved transient absorption spectra shown in Figure 3.12 indicate the growth of such a broad absorption band. Close packing of the fullerene moieties in these clusters facilitates excited state interactions, which in turn results in the excited state charge transfer complexation. Such excited state interactions are likely to dominate in the case of the dyad **1** in which fullerene and aniline moieties can participate in a photoinduced charge transfer. The spectral changes noted for the cluster of dyad, are different from those of the triplet excited state, but they are similar to those reported for a charge-separated radical pair in a rigidly spaced fullerene-aniline system.

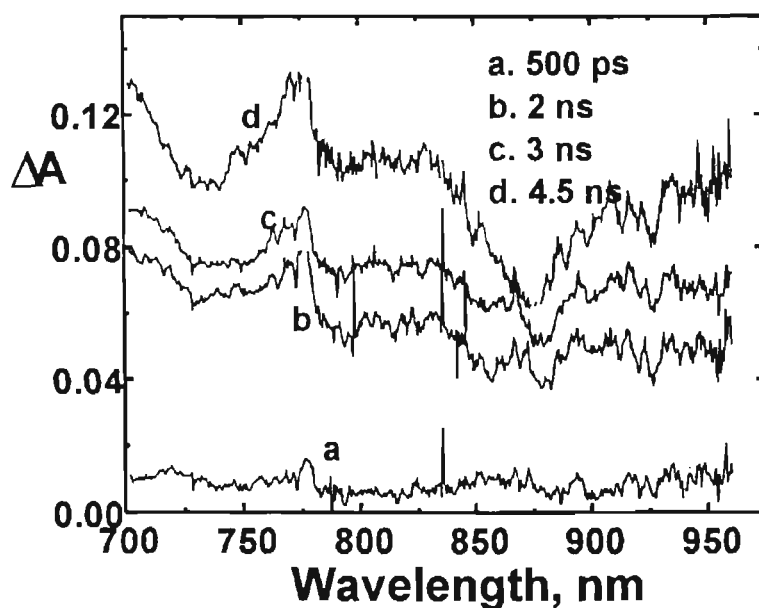


Figure 3.12. Time-resolved Difference absorption spectra recorded after 532 nm laser pulse excitation of **1** in 12.5% (v/v) toluene-acetonitrile

These results, thus, indicate the possibility of an intramolecular electron transfer between the singlet excited fullerene and the aniline. The broad nature of the 700-800 nm spectral band prevented us from resolving the contribution that arise from the charge separated pair and the triplet excited state.

It is well established that the triplet excited state of  $C_{60}$  and its derivatives possess absorption having maximum around 700 nm and extends to the NIR region. Similarly, the radical anion of fullerene derivatives possesses characteristic band in the NIR region. In an earlier study we have characterized the triplet excited state of **1** ( $\lambda_{\text{max}}$  at 700 nm) using flash photolysis and the radical anion spectrum was generated by pulse radiolysis ( $\lambda_{\text{max}}$  at 1010 nm).

Nanosecond laser flash photolysis studies of the clusters in the visible and near infrared (NIR) region were performed in order to characterize charge separation products, namely the radical anion of  $C_{60}$ . The time-resolved absorption spectra recorded, in the visible and NIR region, following the 337-nm laser pulse excitation of the clusters of dyad **1** in deoxygenated acetonitrile-toluene (3:1) mixtures, are shown in Figures 3.13 and 3.14, respectively. The transient absorption spectra (in the 450-1100 nm region) possess two peaks; one centered around 700 nm and the other around 1010 nm. Interestingly, the decays of these absorption bands are significantly different. The absorption band in the 450-850 nm region decays completely in 10  $\mu\text{s}$ . On the other hand, a long-lived component of remarkably longer lifetime of several hundred microseconds was observed in the NIR region (inset of Figure 3.14). The absorption-time decay profiles of the clusters of the dyad recorded at 700 and 1010 nm are shown in Figure 3.15. Clustered dyad exhibits monoexponential decay at 700 nm with a lifetime of about 1.85  $\mu\text{s}$ ,

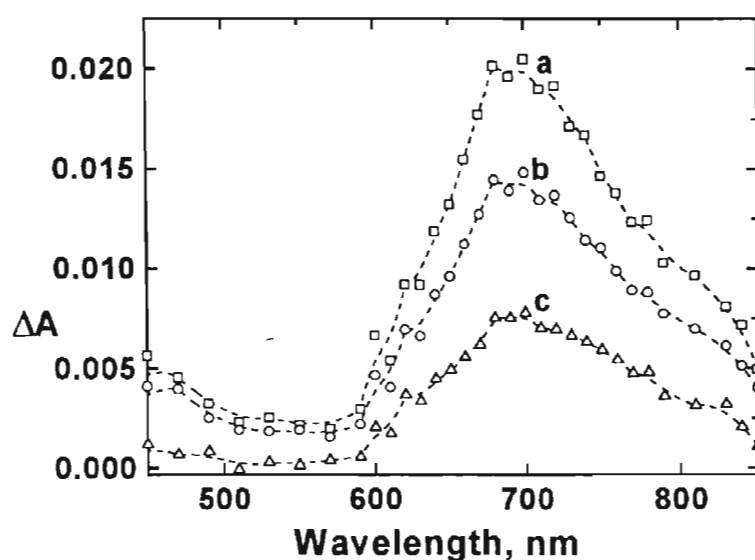


Figure 3.13. Time resolved difference absorption spectra of the clusters of dyad 1 ( $30\mu\text{M}$ ), recorded in the visible region, in deoxygenated acetonitrile-toluene (3:1) mixtures: (a) 0.5; (b) 1.0 and (c) 2.0  $\mu\text{s}$ .

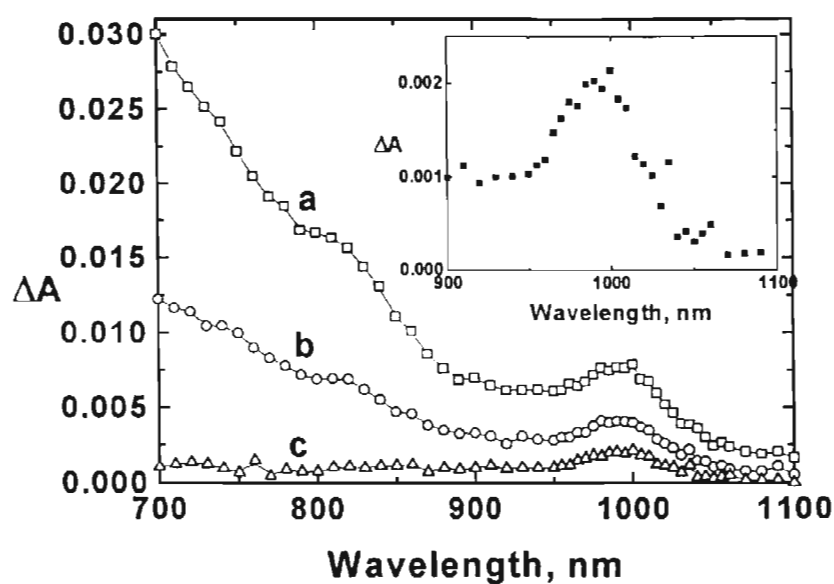


Figure 3.14. Time resolved difference absorption spectra of the clusters of dyad 1 ( $30\mu\text{M}$ ), recorded in the NIR region in deoxygenated acetonitrile-toluene (3:1) mixtures: (a) 1.0; (b) 2.5 and (c) 10  $\mu\text{s}$ . Inset shows the expanded absorption spectrum after 10  $\mu\text{s}$ .

whereas the decay at 1010 nm is biexponential in nature, with lifetimes of 1.45  $\mu\text{s}$  and 60  $\mu\text{s}$ . Based on previous studies, the transient absorption at 700 nm can be attributed to decay of triplet excited state of the clustered dyad. Biexponential decay curve observed in the NIR region can be ascribed to the contribution from two different species absorbing in this region, namely the triplet excited state ( $\tau = 1.45 \mu\text{s}$ ) and the radical anion of  $\text{C}_{60}$  ( $\tau = 60 \mu\text{s}$ ).

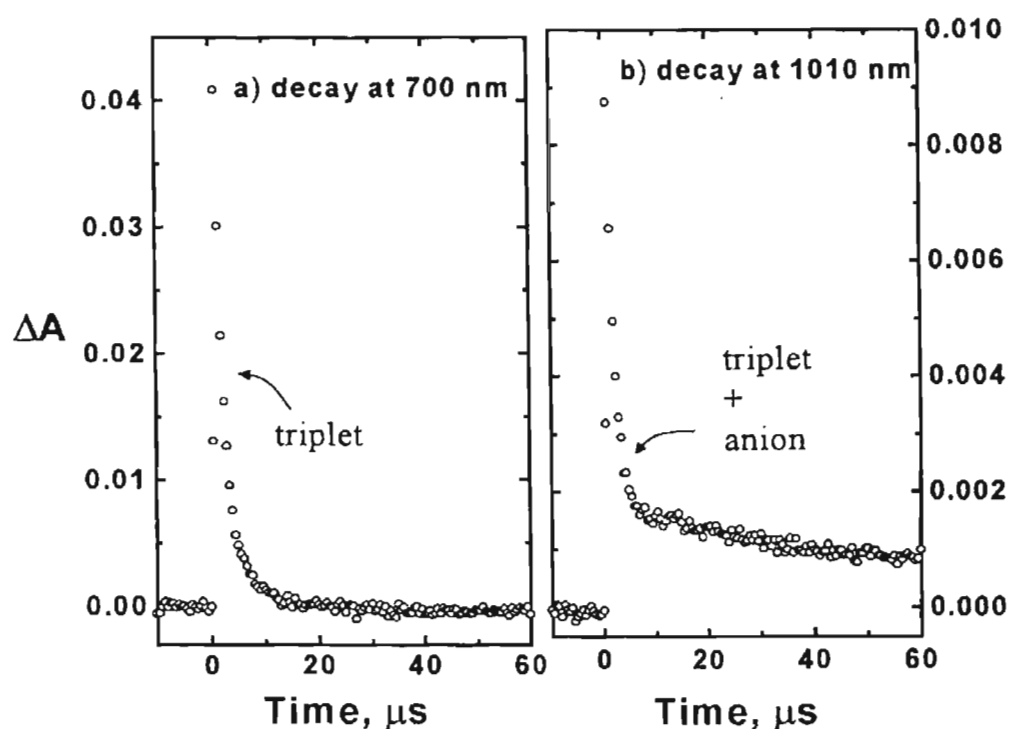


Figure 3.15. Absorption-time decay profile recorded of the clusters of dyad 1 ( $30 \mu\text{M}$ ) in deoxygenated acetonitrile-toluene (3:1) mixtures; (a) 700 nm and (b) 1010 nm.

Based on the steady state fluorescence and time-resolved studies, a possible mechanism illustrating various photochemical events is given in Scheme 3.3. There are two competing processes from the singlet excited state of the cluster dyads. They are mainly the intersystem crossing to the triplet excited state and the electron transfer from the anchored anilinic donor group to the photoexcited fullerene cluster.

We have further studied the effect of increasing the concentration of the dyad clusters (in acetonitrile-toluene (3:1)) on the recombination processes (traces b-d in Figure 3.16). Interestingly, the lifetime of the triplet excited state remains almost constant ( $1.4 \mu\text{s}$ - $1.8 \mu\text{s}$ ) whereas the lifetime of radical anion varied on increasing the concentration of the dyad clusters. Lifetime of the cluster dyads at a lower concentration ( $30 \mu\text{M}$ ) is about  $60 \mu\text{s}$  (trace b; Figure 3.16). On increasing the concentration of the dyad clusters to  $4.5 \mu\text{M}$  (trace c; Figure 3.16), radical anion is found more stable ( $\tau_2 = \sim 160 \mu\text{s}$ ). The scattering of the data points at higher dyad concentrations prevented us from detailed kinetic analysis of the radical anion in

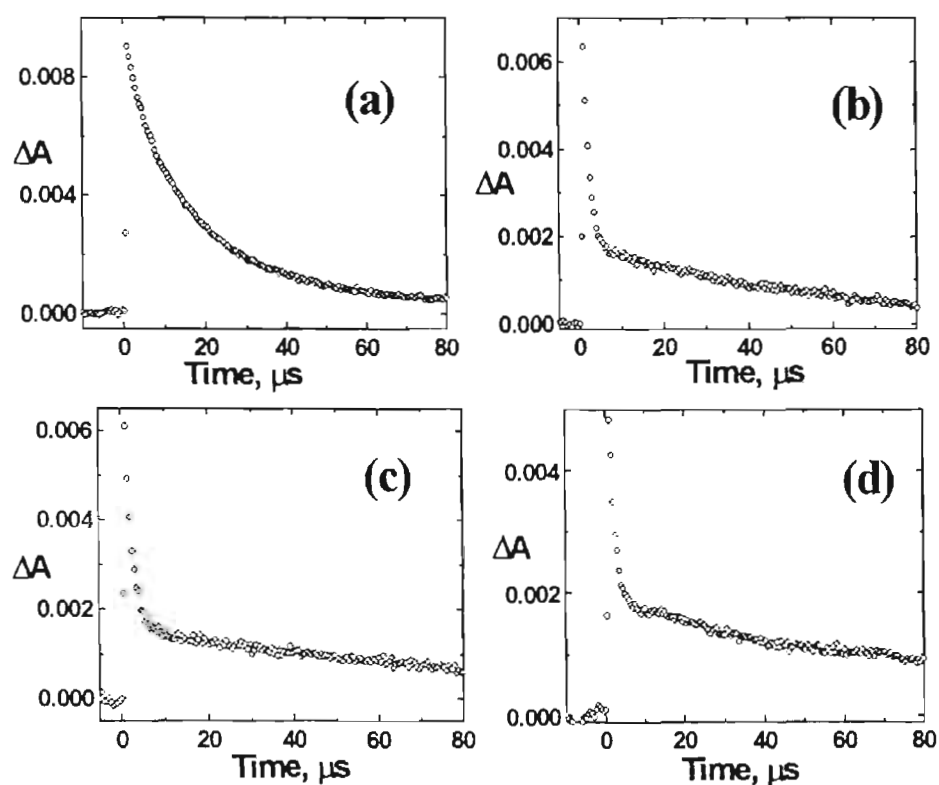
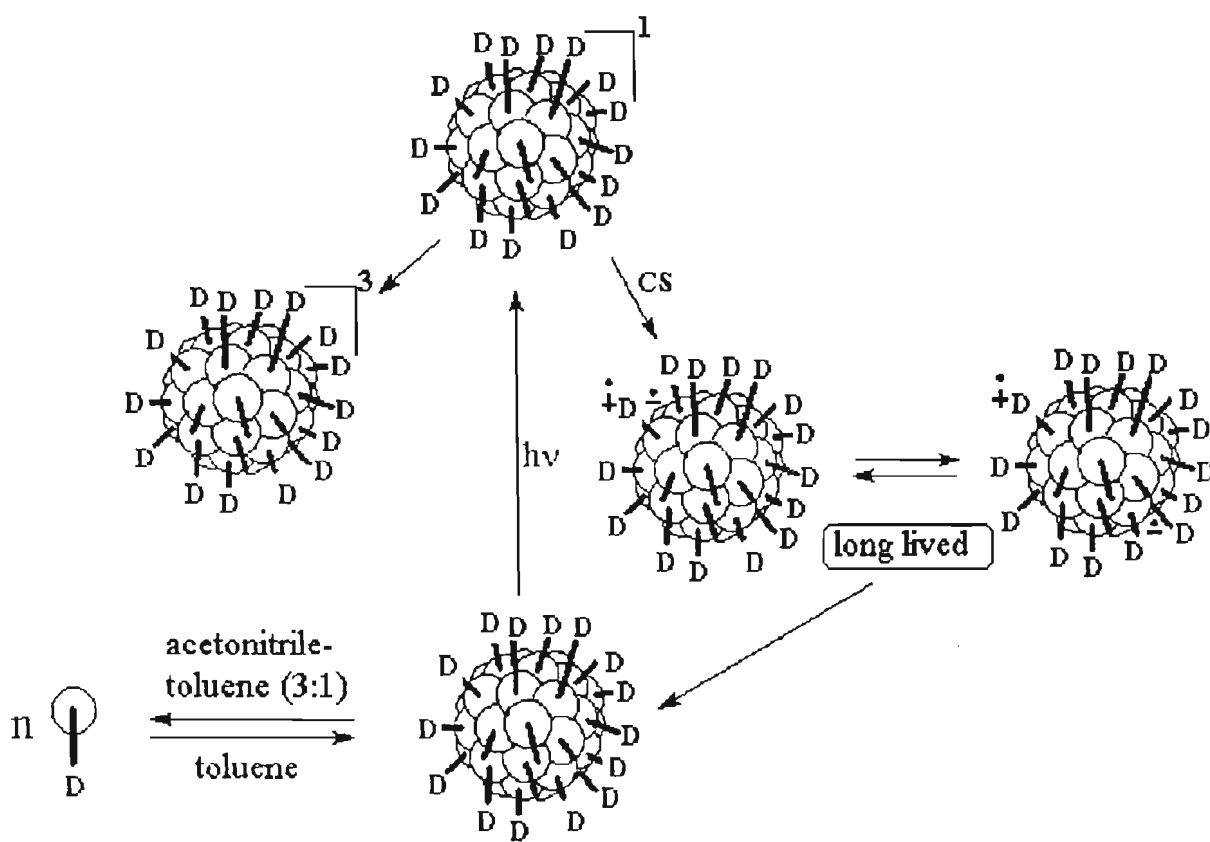


Figure 3.16. Absorption-time decay profile at 1010 nm recorded in deoxygenated toluene (trace a) and in deoxygenated acetonitrile-toluene (3:1) solutions (trace b-d) : [1] (a) 30; (b) 30; (c) 4.5 and (d) 60  $\mu\text{M}$ .



the longer time scale. On further increasing the concentration of the dyad cluster (60  $\mu\text{M}$ ), a decrease in the lifetime of the  $\text{C}_{60}$  radical anion (45  $\mu\text{s}$ ) is observed (trace d; Figure 3.16)

The interesting aspect of the study is the stabilization of the charge-separated intermediates. In the present study, the experiments were carried out in acetonitrile-toluene (3:1) mixtures and the high polarity of the medium (dielectric constant  $\epsilon$  of  $\text{CH}_3\text{CN}$  is 38.0) can also play an important role in stabilization of the charge separated state. In order to distinguish between the effect of polarity and clustering, we have systematically investigated the effect of



Scheme 3.3

solvent polarity on the photophysical properties of dyad **1** and extended to solvents having dielectric constants comparable with acetonitrile. Solvents of wide range of polarity, namely toluene ( $\epsilon = 2.38$ ), benzonitrile ( $\epsilon = 25.2$ ) (Section 2.3.6) and nitrobenzene ( $\epsilon = 34.8$ ), were selected and the time resolved transient absorption spectra, in the visible and NIR regions, were recorded. Time resolved absorption spectra of the dyad in toluene as well as benzonitrile were recorded following the 337.1-nm pulse excitation ( $N_2$  laser) and reported in Section 2.3.6. The experiments using nitrobenzene as solvent were carried out following the 532-nm laser pulse excitation (YAG laser), in order to avoid the direct excitation of the solvent. However, the time-resolved absorption spectra recorded in solvents of high dielectric constant like benzonitrile (and nitrobenzene) did not show any spectral evidence for the presence of charge-separated radical pair, in the nanosecond time scale. The polarity of solvent may play a major role in promoting the forward electron transfer, but the charge recombination processes may also be fast, so that the charge separated intermediates not observed on a nanosecond time scale.

Based on the photochemical studies of dyads in homogenous solutions, one can conclude that the remarkably longer lifetime of charge separated state for clusters is essentially due to the stabilization of the transferred electron in cluster framework. The hopping of the transferred electron to second fullerene molecule in the cluster is likely to increase the distance of separation of radical pair which in turn retards the charge recombination process (Scheme 3.3). Accordingly, it is safe to postulate that the added electrons are fully delocalized within the entire cluster network, while the positive charges are quite localized at the aniline functions. Based on this hypothesis one can propose that the back electron transfer should

occur mainly in a bimolecular fashion between two individual clusters. The present studies indicate that the clustering in the fullerene based dyads can be used as a useful strategy for circumventing the back electron transfer.

### 3.4. Conclusions

Fullerene based dyads (1 and 3) as well as the model systems 2 and 4, form optically transparent microscopic clusters (aggregates) in 75-95% (v/v) acetonitrile-toluene mixtures at room temperature. The manifold increase in molar extinction coefficients during clustering makes them promising candidates for the design of solar energy harvesting devices. Clustering in this class of molecules is mainly associated with the strong three-dimensional hydrophobic interactions between the fullerene units. Based on the steady state and time resolved studies, it is further concluded that the electron transfer processes are more facile in the clusters of the dyads than in homogeneous medium. The remarkably high stability of the charge-separated intermediates in the clustered dyads is attributed to the hopping of the electrons between the fullerene molecules. The results of the electron transfer studies in the clusters indicate that they are promising as models for studying the photoinduced electron transfer and resemble more close by to real solid state systems.

### 3.5. Experimental Section

#### 3.5.1. Synthesis of the bis(fullerene)-aniline dyad, 3

##### 3.5.1.1. Preparation of N,N-di (2-bromo-1-ethyl)aniline, 9

Phosphorus tribromide (2.7 g, 10 mmol) was added dropwise to an ice cold solution of 8 (1.8 g, 10 mmol) in dichloromethane (20 mL) over a period of 30 min. The reaction mixture was stirred at room temperature for 24 h, quenched with ice-cold water and the pH was adjusted to 7-8. The organic portion was extracted with dichloromethane

and the solvent was removed under reduced pressure. The crude product was chromatographed on silica gel (100-200 mesh) using petroleum ether (bp 60-80 °C) to give 2.4 g (80%) of **9**, mp 48-49 °C; IR (KBr)  $\nu_{\max}$  2929, 1605, 1510, 1373, 1351, 1278, 1214, 1175, 1095, 1035, 996, 749 693  $\text{cm}^{-1}$ ;  $^1\text{H}$  NMR ( $\text{CDCl}_3$ )  $\delta$  3.2-3.6 (4H, m,  $\text{CH}_2$ ), 3.6-3.9 (4 H, m,  $\text{CH}_2$ ), 6.6-7.5 (5H, m, aromatic);  $^{13}\text{C}$  NMR ( $\text{CDCl}_3$ )  $\delta$  28.25, 53.33, 112.12, 117.99, 129.73, 145.64; exact mass calcd. for  $\text{C}_{10}\text{H}_{13}\text{NBr}_2$  ( $\text{MH}^+$ ) 305.9473, found 305.9488 (FAB, high resolution mass spectrometry).

### 3.5.1.2. Preparation of the dialdehyde, **11**

A suspension of N,N-di(2-bromo-1-ethyl)aniline, **9** (1.50 g, 5 mmol), *p*-hydroxybenzaldehyde (2.4 g, 20 mmol) and potassium carbonate (1.4 g, 10 mmol) was refluxed in acetone (20 mL) for 12 h. The reaction mixture was cooled, filtered and concentrated under reduced pressure. The crude product was chromatographed on silica gel (100-200 mesh) using a mixture (3:7) of ethyl acetate and petroleum ether (bp 60-80 °C) to give 1.2 g (60%) of N,N-di{2-(*p*-formylphenoxy)-1-ethyl}aniline, **11**, mp 40-41 °C; IR (KBr)  $\nu_{\max}$  3073, 2934, 2759, 1696, 1602, 1496, 1262, 1161, 1028 798  $\text{cm}^{-1}$ ;  $^1\text{H}$  NMR ( $\text{CDCl}_3$ )  $\delta$  3.8-4.0 (4H, t,  $\text{NCH}_2$ ), 4.17-4.35 (4H, t,  $\text{OCH}_2$ ), 6.4-7.9 (13 H, m, aromatic), 9.8 (2H, s, CHO);  $^{13}\text{C}$  NMR ( $\text{CDCl}_3$ )  $\delta$  50.54, 65.57, 111.85, 114.47, 114.65, 116.98, 129.33, 129.72, 129.90, 131.60, 146.69, 163.31, 190.01; exact mass calcd. for  $\text{C}_{24}\text{H}_{23}\text{NO}_4$  ( $\text{MH}^+$ ) 390.1705, found 390.1721 (FAB, high resolution mass spectrometry).

### 3.5.1.3. Synthesis of the buckminsterfullerene-aniline dyad aldehyde, **12**

A mixture of **11** (38 mg, 0.1 mmol), N-methylglycine (18 mg, 0.2 mmol) and  $\text{C}_{60}$  (144 mg, 0.2 mmol) was heated under argon in toluene (144 mL) for 10 h. The reaction mixture was cooled and removal of the solvent under reduced pressure

gave a solid residue, which was chromatographed over silica gel (100-200 mesh). Elution with a mixture (1:1) of toluene and petroleum ether (bp 60-80 °C) gave 60 mg (42%) of unchanged C<sub>60</sub> followed by 11 mg (5%) of the bisadduct, **3** and 53 mg (40%) of the dyad aldehyde **12**.

**Dyad aldehyde 12.** mp > 400 °C; IR (KBr)  $\nu_{\max}$  2792, 1645, 1588, 1542, 1504, 1465, 1412, 1176, 736, 578 cm<sup>-1</sup>; <sup>1</sup>H NMR (CDCl<sub>3</sub>)  $\delta$  2.78 (3H, s, NCH<sub>3</sub>), 3.86-3.88 (4H, m, NCH<sub>2</sub>), 4.16-4.25 (5H, m, OCH<sub>2</sub> and CH of pyrrolidine ring), 4.87 (1H, s, CH of pyrrolidine ring), 4.97 (1H, d, CH of pyrrolidine ring), 6.56-6.96 (m), 7.43-7.80 (m) (13H, aromatic), 9.86 (1H, s, CHO); <sup>13</sup>C NMR (CDCl<sub>3</sub> + CS<sub>2</sub>)  $\delta$  39.95, 50.80, 51.09, 65.27, 65.69, 68.96, 69.97, 83.09, 97.24, 111.85, 114.46, 114.76, 116.92, 129.60, 130.38, 130.54, 131.99, 135.74, 139.90, 140.18, 141.42, 141.52, 141.56, 142.27, 142.57, 142.70, 143.55, 144.41, 144.71, 144.75, 145.20, 145.29, 145.46, 145.53, 145.70, 145.94, 146.30, 146.39, 146.50, 146.98, 147.31, 148.65, 148.76, 153.56, 158.63, 190.67; exact mass calcd. for C<sub>86</sub>H<sub>28</sub>N<sub>2</sub>O<sub>3</sub> (MH<sup>+</sup>) 1136.2100, found 1136.2070 (FAB, high resolution mass spectrometry).

#### 3.5.1.4. Synthesis of the bis(buckminsterfullerene)-aniline dyad, **3**

A mixture of **11** (38 mg, 0.1 mmol), N-methylglycine (18 mg, 0.2 mmol) and C<sub>60</sub> (144 mg, 0.2 mmol) was heated under argon in toluene (144 mL) for 20 h. The reaction mixture was cooled and removal of the solvent under reduced pressure gave a solid residue, which was chromatographed over silica gel (100-200 mesh). Elution with a mixture (1:1) of toluene and petroleum ether (bp 60-80 °C) gave 55 mg (38%) of unchanged C<sub>60</sub>, followed by 40 mg (35%) of the dyad **3** and 7 mg (5%) of the dyad aldehyde **12**.

**Dyad 3.** mp > 400 °C; IR (KBr)  $\nu_{\max}$  2947, 2924, 2877, 2783, 1606, 1509, 1465, 1429, 1355, 1337, 1302, 1243, 1175, 1120, 1117, 1032, 907, 834, 731  $\text{cm}^{-1}$ ;  $^1\text{H}$  NMR ( $\text{CDCl}_3$ )  $\delta$  2.65-2.75 (6 H, m,  $\text{NCH}_3$ ), 3.60-4.90 (14 H, m,  $\text{NCH}_2$ ,  $\text{OCH}_2$  and pyrrolidine ring protons), 6.55-7.67 (13 H, m, aromatic);  $^{13}\text{C}$  NMR ( $\text{CDCl}_3 + \text{CS}_2$ )  $\delta$  30.17, 39.25, 39.70, 53.24, 53.82, 67.40, 68.10, 69.00, 80.73, 81.35, 96.24, 111.95, 112.15, 112.34, 113.89, 116.78, 117.27, 127.09, 128.93, 129.57, 130.06, 131.20, 134.42, 135.67, 139.97, 141.23, 141.94, 144.50, 145.06, 145.60, 147.26, 147.63, 148.11, 150.85, 151.84, 153.16, 157.21, 158.38, 158.66, 159.95; mass spectrum showed a ( $\text{M}-60^+$ ) peak at 1164 (observed by MALDI and FAB mass spectrometry).

### 3.5.2. Synthesis of the model compound, 4

The model compound 4 was prepared through the pathways shown in Scheme 3.2.

#### 3.5.2.1. Preparation of the bisaldehyde, 14

A suspension of 1,2-dibromoethane (1.86 g, 10 mmol), *p*-hydroxybenzaldehyde (2.45 g, 20 mmol) and potassium carbonate (2.80 g, 20 mmol) was heated under reflux in acetone (20 mL) for 12 h. The reaction mixture was cooled, filtered and concentrated under reduced pressure. The crude product was chromatographed over silica gel (100-200 mesh) and elution with chloroform gave 2.3 g (85%) of 14, mp 128-129 °C; IR (KBr)  $\nu_{\max}$  2989, 2957, 2835, 1693, 1607, 1574, 1509, 1460, 1429, 1389, 1300, 1252, 1215, 1162, 1055, 1007, 965  $\text{cm}^{-1}$ ;  $^1\text{H}$  NMR ( $\text{CDCl}_3$ )  $\delta$  4.40 (4H, s,  $\text{OCH}_2$ ), 7.00 (2H, d, aromatic), 7.85 (2H, d, aromatic), 9.90 (2H, s, CHO);  $^{13}\text{C}$  NMR ( $\text{CDCl}_3$ )  $\delta$  66.44, 114.80, 130.35, 131.87, 163.31, 190.55; exact mass calcd. for  $\text{C}_{16}\text{H}_{14}\text{O}_4$  ( $\text{MH}^+$ ) 271.0970, found 271.0996 (FAB, high resolution mass spectrometry).

### 3.5.2.2. Synthesis of 4

A mixture of the bisaldehyde, **14** (34 mg, 0.125 mmol), N-methylglycine (22 mg, 0.25 mmol) and C<sub>60</sub> (180 mg, 0.25 mmol) in toluene (180 mL) was stirred at reflux for 20 h. On cooling the reaction mixture, the solvent was removed under reduced pressure. The solid residue was chromatographed over silica gel (100-200 mesh) using a mixture (1:2) of petroleum ether (bp 60-80 °C) and toluene to give 80 mg (44%) of unchanged C<sub>60</sub>, followed by 60 mg (45%) of the model compound **4**, mp > 400 °C; IR (KBr)  $\nu_{\max}$  3074, 2967, 2877, 2747, 1694, 1605, 1493, 1389, 1270, 1162, 1132, 1069, 1067, 1048, 963, 919, 831, 741 cm<sup>-1</sup>; <sup>1</sup>H NMR (CDCl<sub>3</sub>)  $\delta$  2.30-2.95 (6 H, m, NCH<sub>3</sub>), 3.5-4.8 (10 H, m, OCH<sub>2</sub> and pyrrolidine ring protons), 6.65-7.75 (8H, m, aromatic); <sup>13</sup>C NMR (CDCl<sub>3</sub> + CS<sub>2</sub>)  $\delta$  39.46, 39.71, 68.57, 68.69, 68.90, 69.37, 79.45, 81.20, 112.32, 115.98, 117.30, 127.39, 128.57, 128.95, 129.63, 130.24, 131.14, 134.61, 136.64, 141.15, 141.61, 142.93, 144.11, 144.51, 144.64, 144.85, 145.16, 145.61, 145.72, 146.74, 147.10, 147.63, 148.42, 151.27, 151.70, 152.53, 154.23, 156.34, 158.31, 158.44, 159.61. The mass spectrum of **4** showed a (M-C<sub>60</sub><sup>+</sup>) peak at 1045 (MALDI and FAB, high resolution mass spectrometry).

**3.5.3. Methods:** All melting points are uncorrected and were determined on a Aldrich melting point apparatus. IR spectra were recorded on a Perkin Elmer Model 882 IR spectrometer and the UV-Visible spectra on a Shimadzu 2100 or GBC 918 spectrophotometer. <sup>1</sup>H NMR and <sup>13</sup>C NMR spectra were recorded on a JEOL EX-90 or Bruker DPX-300 MHz spectrometer. Mass spectra were recorded on a JEOL JM AX 505 HA mass spectrometer. The emission spectra were recorded on a Spex-Fluorolog, F112-X equipped with a 450W Xe lamp and a Hamamatsu R928 photomultiplier tube. The excitation and emission slits were 1 and 4, respectively.

A 570 nm long pass filter was placed before the emission monochromator in order to eliminate the interference from the solvent. Solvent spectra were recorded in each case and subtracted. Quantum yields of fluorescence were measured by a relative method using optically dilute solutions.

Picosecond laser flash photolysis experiments were performed using 355 nm laser pulses from a mode-locked, Q-switched Quantel YG-501 DP Nd:YAG laser system (output 1.5 mJ/pulse, pulse width ~18 ps). The white continuum picosecond probe pulse was generated by passing the fundamental output through a D<sub>2</sub>O/H<sub>2</sub>O mixture. The output was fed to a spectrograph (HR-320, ISDA Instruments, Inc.), with fiber optic cables and was analyzed with a dual diode array detector (Princeton Instruments, Inc.), interfaced with an IBM-AT computer. Time zero in these experiments corresponds to the end of the excitation pulse. All the lifetimes rate constants and quantum yields reported in this studies are at room temperature (297 K) and have an experimental error of  $\pm 10\%$ . The deaerated dye solution was continuously flowed through the sample cell during the measurements.

Nanosecond laser flash photolysis experiments were performed with a Laser Photonics PRA/Model UV-24 nitrogen laser system (337 nm, 2 ns pulse width, 2-4 mJ/pulse) with front face excitation geometry. A typical experiment consisted of a series of 2-3 replicate shots per single measurement. The average signal was processed with an LSI-11 microprocessor interfaced with a VAX computer.



### 3.6. Reference

1. Antonietti, M.; Goltner, C. *Angew. Chem. Int. Ed. Engl.*, **1997**, *36*, 910.
2. Sun, Y. -P.; Bunker, C. E. *Nature (London)*, **1993**, *365*, 398.
3. Sun, Y. -P.; Bunker, C. E. *Chem. Mater.*, **1994**, *6*, 578.
4. Sun, Y. -P.; Ma, B.; Bunker, C. E.; Liu, B. *J. Am. Chem. Soc.*, **1995**, *117*, 12705.
5. Guldi, D. M.; Hungerbuhler, H.; Asmus, K. -D. *J. Phys. Chem.*, **1995**, *99*, 13487.
6. Guldi, D. M. *J. Phys. Chem. A.*, **1997**, *101*, 3895.
7. Thomas, K. G.; Biju, V.; Guldi, D. M.; Kamat, P. V.; George, M. V. *J. Phys. Chem.*, **1999**, 0000.
8. Sun, Y. -P. In *Molecular and Supramolecular Photochemistry, Vol. 1, Organic Photochemistry*, Ramamurthy, V.; Schanze, K. S. (Eds.), Marcel Dekker, New York, **1997**, 325.
9. Foote, C. S. In *Topics in Current Chemistry; Electron Transfer 1*, Matty, J. (Ed.), Springer-Verlag, Berlin, **1994**, 347.
10. Imahori, H.; Sakata, Y. *Adv. Mater.*, **1997**, *9*, 537.
11. Liddell, P. A.; Kuciauskas, D.; Sumida, J. P.; Nash, B.; Nguyen, D.; Moore, A. L.; Moore, T. A.; Gust, D. *J. Am. Chem. Soc.*, **1997**, *119*, 1400.
12. Kuciauskas, D.; Lin, S.; Seely, G. R.; Moore, A. L.; Moore, T. A.; Gust, D.; Drovetskaya, T.; Reed, C. A.; Boyd, P. D. W. *J. Phys. Chem.*, **1996**, *100*, 15926.
13. Liddell, P. A.; Sumida, J. P.; Macpherson, A. N.; Noss, L.; Seely, G. R.; Clark, K. N.; Moore, A. L.; Moore, T. A.; Gust, D. *Photochem. Photobiol.*, **1994**, *60*, 537.
14. Baran, P. S.; Monaco, R. R.; Khan, A. U.; Schuster, D. I.; Wilson, S. R. *J. Am. Chem. Soc.*, **1997**, *119*, 8363.
15. Imahori, H.; Hagiwara, K.; Asoki, M.; Akiyama, T.; Taniguchi, S.; Okada, T.; Shirakawa, M.; Sakata, Y. *J. Am. Chem. Soc.*, **1996**, *118*, 11771.

16. Imahori, H.; Yamada, K.; Hasegawa, M.; Taniguchi, S.; Okada, T.; Sakata, Y. *Angew. Chem. Int. Ed. Engl.*, **1997**, *36*, 2626.
17. Linssen, T. G.; Durr, K.; Hanack, M.; Hirsch, A. *J. Chem. Soc. Chem. Commun.*, **1995**, 103.
18. Sariciftci, N. S.; Wudl, F.; Heeger, A. J.; Maggini, M.; Scorrano, G.; Prato, M.; Bourassa, J.; Ford, F. C. *Chem. Phys. Lett.*, **1995**, *247*, 510.
19. Maggini, M.; Guldi, D. M.; Mondini, S.; Scorrano, G.; Paolucci, F.; Ceroni, P.; Roffia, S. *Chem. Eur. J.*, **1998**, *4*, 1992.
20. Guldi, D. M.; Maggini, M.; Scorrano, G.; Prato, M. *J. Am. Chem. Soc.*, **1997**, *119*, 974.
21. Guldi, D. M.; Maggini, M.; Scorrano, G.; Prato, M. *Res. Chem. Intermed.*, **1997**, *23*, 575.
22. Williams, R. M.; Koeberg, M.; Lawson, J. M.; An, Y. -Z. Rubin, Y.; Paddon-Row, M. N.; Verhoeven, J. W. *J. Org. Chem.*, **1996**, *61*, 5055.
23. Williams, R. M.; Zwier, J. M.; Verhoeven, J. W. *J. Am. Chem. Soc.*, **1995**, *117*, 4093.
24. Lawson, J. M.; Oliver, A. M.; Rothenfluh, D. F.; An, Y. -Z.; Ellis, G. A.; Ranasinghe, M. G.; Khan, S. I.; Franz, A. G.; Ganapathi, P. S.; Shephard, M. J.; Paddon-Row, M. N.; Rubin, Y. *J. Org. Chem.* **1996**, *61*, 5032.
25. Thomas, K. G.; Biju, V.; George, M. V.; Guldi, D. M.; Kamat, P. V. *J. Phys. Chem.*, **1998**, *102*, 5341.
26. Armaroli, N.; Diederich, F.; Dietrich-Buchecker, C. O.; Flamigni, L.; Marconi, G.; Nierengarten, J. -F.; Sauvage, J. -P. *Chem. Eur. J.*, **1998**, *4*, 406.
27. Bensasson, R. V.; Bienvenue, E.; Fabre, C. Janot, J. -M.; Land, E. J.; Leach, S.; Leboultaire, V.; Rassat, A.; Roux, S.; Sata, P. *Chem. Eur. J.*, **1998**, *4*, 270.
28. Wang, Y.; West, R.; Yuan, C. -H. *J. Am. Chem. Soc.*, **1993**, *115*, 3844.
29. Wang, Y. *Nature (London)*, **1992**, *356*, 585.

30. Sariciftci, N. S.; Smilowitz, L.; Heeger, A. J.; Wudl, F. *Science*, **1992**, *258*, 1474.
31. Yu, G.; Gao, J.; Hummelen, J. C.; Heeger, A. J. *Science*, **1995**, *270*, 1789.
32. Tutt, L. W.; Kost, A. *Nature (London)*, **1992**, *356*, 225.
33. Maggini, M.; Scorrano, G.; Prato, M.; Brusatin, G.; Innocenzi, P.; Guglielmi, M.; Renier, A.; Signorini, R.; Meneghetti, M.; Bozio, R. *Adv. Mater.*, **1995**, *4*, 404.
34. Signorini, R.; Zerbetto, M.; Bozio, R.; Maggini, M.; Faveri, C. D.; Prato, M.; Scorrano, G. *Chem. Commun.*, **1996**, 1891.
35. Sauve, G.; Dimitrijevic, N. M.; Kamat, P. V. *J. Am. Chem. Soc.*, **1995**, *99*, 1199.
36. Watanabe, A.; Ito, O. *J. Chem. Soc. Chem. Commun.*, **1994**, 1285.
37. Kraabel, B.; Lee, C. H.; McBranch, L. D.; Moses, D.; Sariciftci, N. S.; Heeger, A. J. *Chem. Phys. Lett.*, **1993**, *213*, 389.
38. Maggini, M.; Scarrano, G.; Prato, M. *J. Am. Chem. Soc.*, **1993**, *115*, 9798.
39. Robello, D. R. *J. Polym. Sci. A: Polym. Chem.*, **1990**, *28*, 1.
40. Desai, R. D. *J. Indian Inst. Sci.*, **1924**, *7*, 235.
41. Liang, K.; Law, K. -Y.; Whitten, D. G. *J. Phys. Chem. B*, **1997**, *101*, 540.
42. Schultz, R. A.; White, B. D.; Dishong, D. M.; Arnold, K. A.; Gokel, G. W. *J. Am. Chem. Soc.*, **1985**, *107*, 6659.
43. Confirmed on a Cosmosil Buckprep HPLC column.
44. Dynamic light scattering studies (Coulter Scientific Instruments), employing the dyad **1** in a mixture (3:1) of acetonitrile and toluene at 20 °C, were carried out by Dr. K. George Thomas at the University of Notre Dame, Indiana, USA.
45. Nath, S.; Pal, H.; Palit, D. K.; Sapre, A. V.; Mittal, J. P. *J. Phys. Chem.*, **1998**, *102*, 10158.

## Chapter 4

### Effect of Varying the Donor Strength on Photoinduced Electron Transfer Processes in C<sub>60</sub>-based Dyads

#### 4.1. Abstract

Two series of fullerene based D-B-A systems, containing donor groups of varying oxidation potentials, have been synthesized. The first series consists of fullerene-based systems possessing heteroaromatic donor groups such as phenothiazine and phenoxazine (1-3 in Chart 4.1) and the second one consists of substituted anilines such as *p*-anisidine and *p*-toluidine as donor groups (5 and 6 in Chart 4.2). Theoretical calculations suggest that the lowest energy conformation in each of these dyads is the extended one. The photoinduced electron transfer processes in these systems were compared with those in an unsubstituted fullerene-aniline dyad 7 and a model compound 4. In contrast to the unsubstituted fullerene-aniline dyad, an efficient intramolecular electron transfer is observed in the case of fullerene-heteroaromatic dyads and fullerene-*p*-anisidine as well as fullerene-*p*-toluidine dyads, even in a nonpolar solvent such as toluene. This effect is more predominant in polar solvents such as benzonitrile. An increase in the rate constant and quantum yield for charge separation ( $k_{cs}$  and  $\phi_{cs}$ ) was observed for both classes of dyads, with decrease in the oxidation potential of the donor groups. Flash photolysis studies revealed the formation of charge separated intermediates through intramolecular electron transfer in these cases.

## 4.2. Introduction

Donor-bridge-acceptor (D-B-A) systems can serve as building blocks in artificial photosynthetic systems<sup>1-5</sup> and in the construction of molecular level electronic devices.<sup>6-9</sup> Matching of the energetics of donor and acceptor is very critical in the design of D-B-A systems with maximum charge separation. Linked porphyrin-quinone D-B-A systems have been investigated as models to test the redox properties of the donor-acceptor pairs on the charge separation and recombination processes.<sup>1-5</sup> Wasielewski and coworkers have studied the dependence of the rate of photoinduced charge separation and charge recombination on the free energy of the reaction, in a series of porphyrin-quinone systems, linked together by a rigid triptycene group.<sup>10-13</sup> The existence of the Marcus inverted region has been experimentally proved by varying the redox properties of the donor-acceptor pairs in these systems as well as from the earlier work of Miller et al.<sup>14</sup> on thermal electron transfer reactions.

Photophysical studies and redox properties have shown that C<sub>60</sub> is an ideal acceptor of electrons.<sup>15-19</sup> Intermolecular electron transfer processes between amines, having a wide range of oxidation potential, and the triplet state of C<sub>60</sub> have been investigated by Foote and coworkers.<sup>20</sup> In a recent paper, Luo et al.<sup>21</sup> have studied the photoinduced electron transfer between N,N-dimethylaniline and a series of functionalized pyrrolidinofullerenes, containing electron donating and withdrawing groups. They have concluded that substitution effects play an important role in the electron transfer processes in these systems.

Photoinduced electron transfer processes in linked fullerene-based dyads<sup>22-34</sup> containing donors such as anilines,<sup>22-25</sup> ferrocenes,<sup>26</sup> porphyrins,<sup>27-31</sup>

carotenes<sup>32,33</sup> and ruthenium complexes<sup>34,35</sup> have been investigated by various groups of workers. Although, there are several reports on the design and studies of fullerene-based dyads, there have been no reports on any systematic investigation on photoinduced intramolecular electron transfer processes as a function of the donor strength. Heteroaromatic groups such as 10-methylphenothiazine and 10-methylphenoxazine are reported to be excellent electron donors in photoinduced electron transfer reactions owing to their low ionization potential<sup>36-39</sup> and the ability to form extremely stable radical cations.<sup>40-44</sup> In the present investigation, we have synthesized two series of fullerene-based dyads containing donor groups of varying oxidation potentials. The first series consists of fullerene-based dyads possessing heteroaromatic groups such as phenothiazine and phenoxazine as donors (Chart 4.1) and the second one consists of substituted anilines such as *p*-anisidine and *p*-toluidine

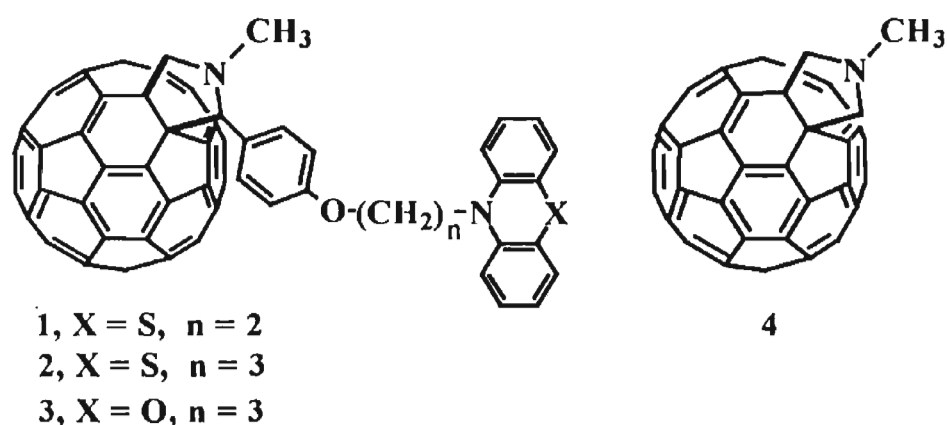


Chart 4.1

as donor groups (Chart 4.2). The distance between the donor and acceptor groups in these systems is kept more or less constant by using the same bridging unit. The free energy of charge separation in such systems mainly depends upon the oxidation potentials of the donor groups. The reported values ( $E_{1/2}$  vs SCE) in acetonitrile

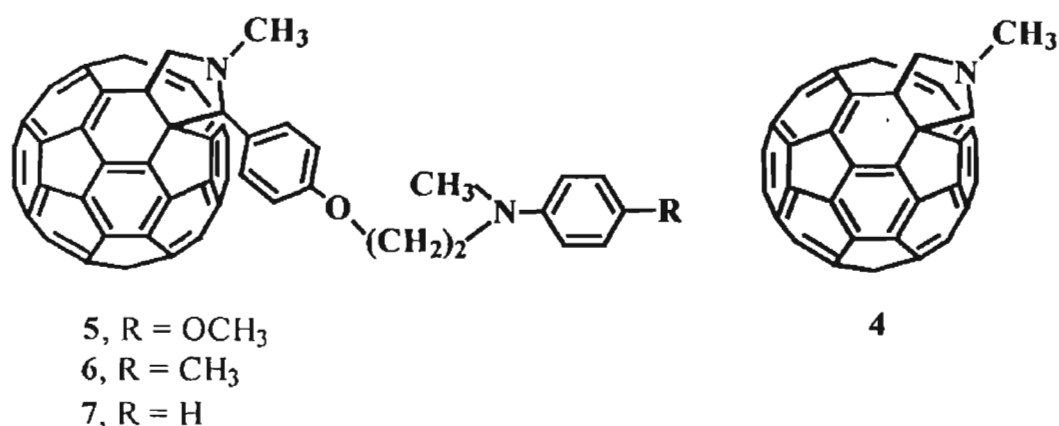


Chart 4.2

for N-methylphenoxazine,<sup>37,45</sup> N-methylphenothiazine,<sup>37</sup> N,N-dimethyl-*p*-anisidine<sup>46</sup> and N,N-dimethyl-*p*-toluidine<sup>46</sup> are 329, 423, 490, 650 mV, respectively. The electron transfer processes in the second series of compounds are compared with a fullerene-aniline dyad 7 (Chapter 2) possessing the same bridging unit (the oxidation potential,  $E_{1/2}$  vs SCE, of N,N-dimethylaniline is 810 mV in acetonitrile).<sup>37,45</sup>

### 4.3. Results and discussion

#### 4.3.1. Synthesis and characterization

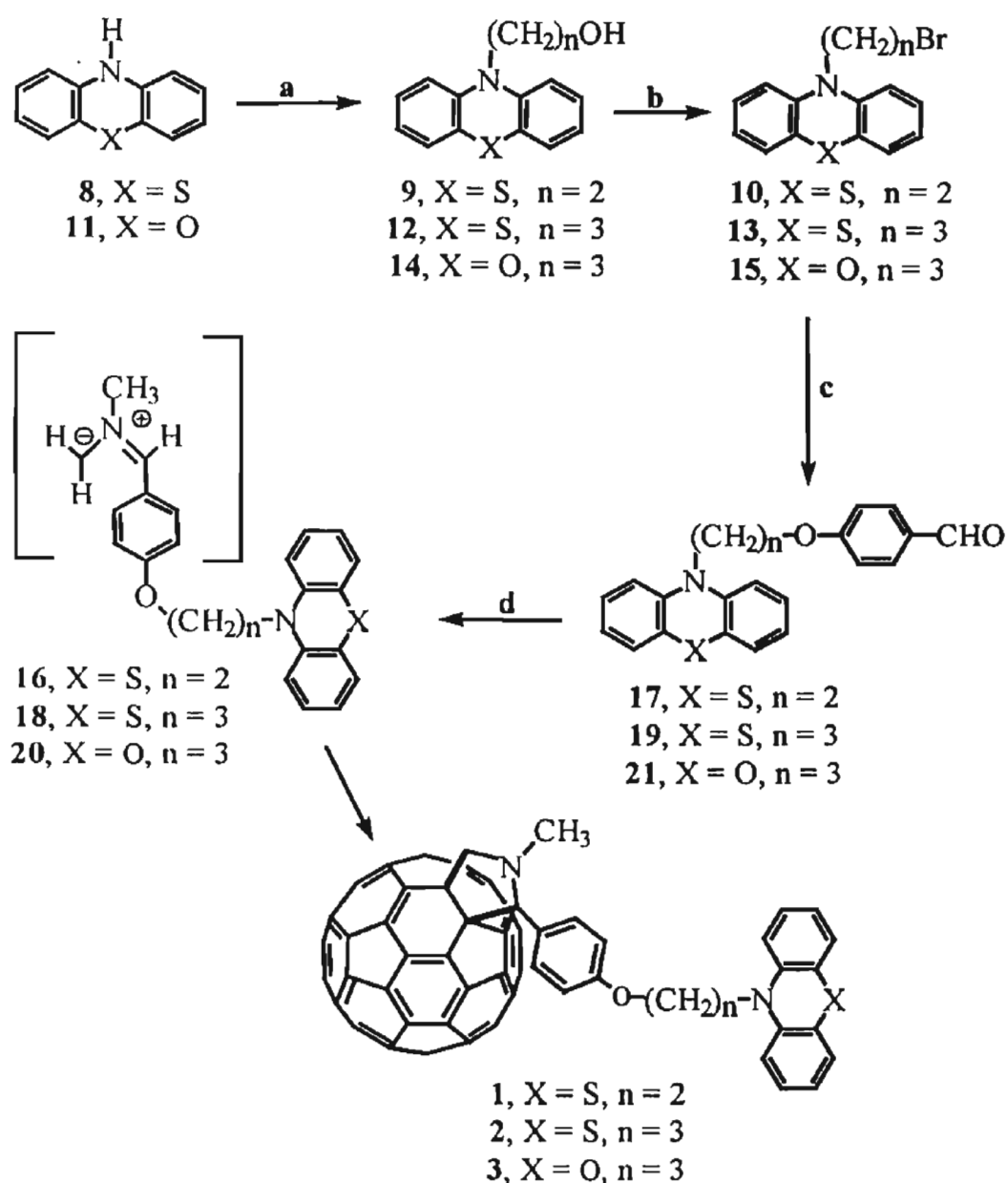
Synthesis of N- $\{\omega$ -(*p*-formylphenoxy)-alkyl}heteroaromatics, 17, 19 and 21 were achieved through the sequence of reactions shown in Schemes 4.1. The preparation of N- $\{(\omega$ -hydroxy)-1-alkyl}heteroaromatics, 9, 12 and 14 was carried out by following reported procedures<sup>47</sup> and they were converted to the corresponding N- $\{(\omega$ -bromo)-1-alkyl}heteroaromatics, 10, 13 and 15, respectively by treating with phosphorous tribromide. The bromo-derivatives were further treated with *p*-hydroxybenzaldehyde to yield the required aldehydes (N- $\{ \omega$ -(*p*-formylphenoxy)-alkyl}heteroaromatics, 17, 19 and 21).

Syntheses of N-methyl,N-{2-(*p*-formylphenoxy)-1-ethyl}anilines, **30** and **31** were achieved through the sequence of reactions shown in Scheme 4.2. N-methyl, N-{(2-hydroxy)-1-ethyl}-*p*-anisidine (**24**) and N-methyl,N-{(2-hydroxy)-1-ethyl}-*p*-toluidine (**28**) were prepared and converted to N-methyl, N-{(2-bromo)-1-ethyl}-*p*-anisidine (**25**) and N-methyl,N-{(2-bromo)-1-ethyl}-*p*-toluidine (**29**), respectively by treating with phosphorous tribromide. The bromo- derivatives were further reacted with *p*-hydroxybenzaldehyde to yield the required aldehydes (N-methyl, N-{2-(*p*-formylphenoxy)-1-ethyl}-*p*-anisidine, **30** and N-methyl,N-{2-(*p*-formylphenoxy)-1-ethyl}-*p*-toluidine, **31**, respectively.

The syntheses of the fullerene-heteroaromatic dyads **1-3**, as well as the fullerene-aniline dyads, **5** and **6** were achieved through a 1,3-dipolar cycloaddition reaction of the appropriate azomethine ylide, generated through the thermal reaction of the corresponding aldehyde and N-methylglycine, with C<sub>60</sub> (Schemes 4.1 and 4.2). The crude reaction product, in each case, was chromatographed over silica gel (100-200 mesh) to give the appropriate dyads in a 45-50% yield.

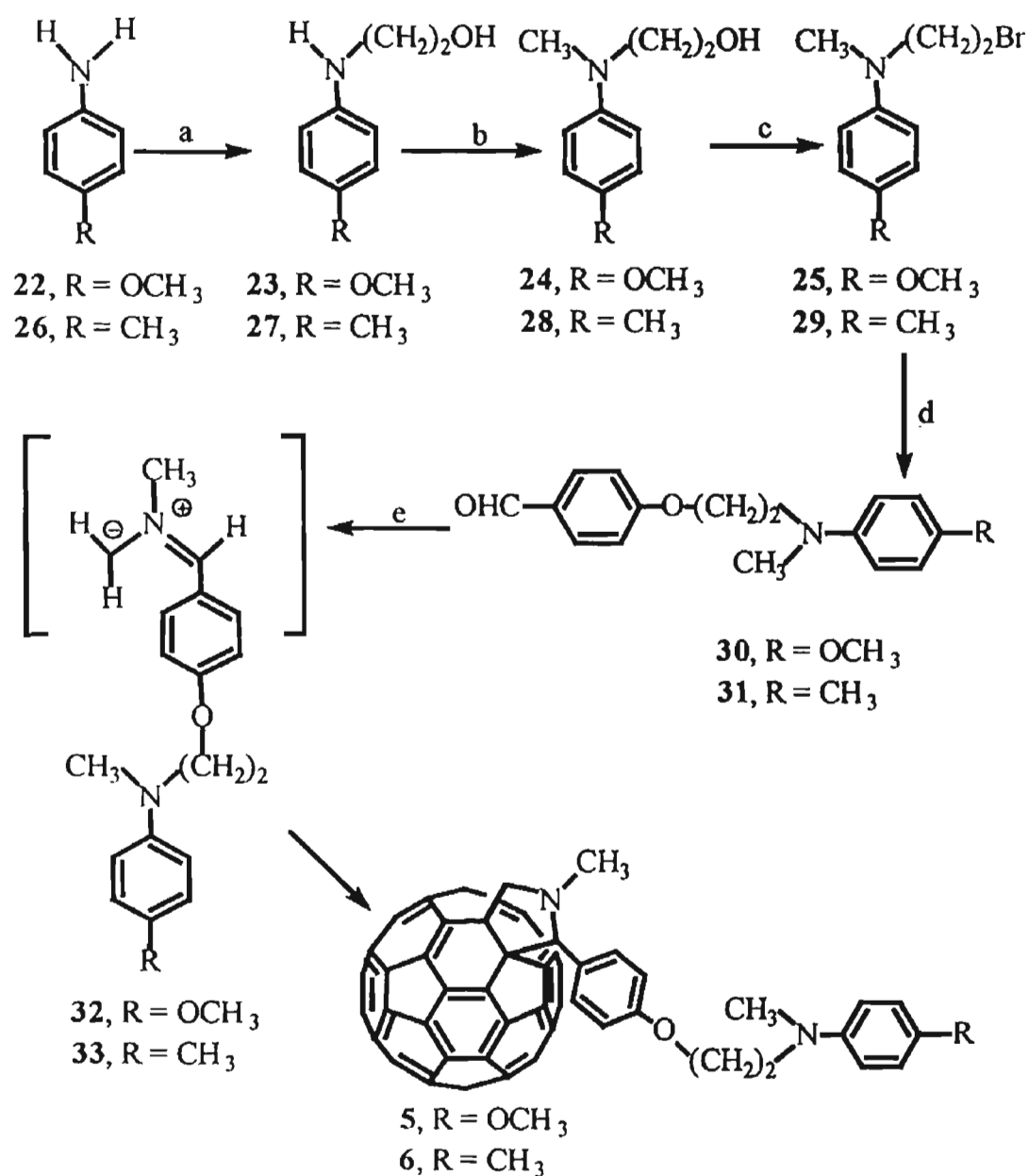
All new compounds were fully characterized on the basis of analytical results and spectral data. Detailed experimental procedure for the synthesis, purification and characterization of the dyads and their precursors are given in Section 4.4.1. Purity of all the dyads was confirmed by HPLC analysis.<sup>48</sup>





(a)  $X(\text{CH}_2)_n\text{OH}$  ( $X = \text{Cl}/\text{Br}$ ,  $n = 2/3$ ),  $\text{K}_2\text{CO}_3$ ,  $\text{I}_2$ , *o*-dichlorobenzene, reflux;  
 (b)  $\text{PBr}_3$ ,  $\text{CH}_2\text{Cl}_2$ , room temperature; (c) *p*-OH  $\text{C}_6\text{H}_4\text{CHO}$ ,  $\text{K}_2\text{CO}_3$ , acetone, reflux; (d) N-methylglycine,  $\text{C}_{60}$ , toluene, heat.

**Scheme 4.1**



(a) Cl(CH<sub>2</sub>)<sub>2</sub>OH, K<sub>2</sub>CO<sub>3</sub>, I<sub>2</sub>, n-butanol, reflux; (b) CH<sub>3</sub>I, K<sub>2</sub>CO<sub>3</sub>, I<sub>2</sub>, CH<sub>3</sub>CN, reflux; (c) PBr<sub>3</sub>, CH<sub>2</sub>Cl<sub>2</sub>, room temperature; (d) *p*-OH C<sub>6</sub>H<sub>4</sub>CHO, K<sub>2</sub>CO<sub>3</sub>, acetone, reflux; (e) N-methylglycine, C<sub>60</sub>, toluene, heat.

**Scheme 4.2**

### 4.3.2. Computational studies

Molecular-modeling studies using the sybyl force field method<sup>49</sup> suggest that the energy-minimized conformations of fullerene-heteroaromatic dyads 1-3 as well as that of fullerene-*p*-anisidine (5) and fullerene-*p*-toluidine (6) dyads are the extended ones. As representative examples, the lowest-energy conformations of the fullerene-phenothiazine dyad 2, the fullerene-phenoxazine dyad 3 and the fullerene-*p*-anisidine dyad 5 are shown in Figures 4.1, 4.2 and 4.3, respectively. In the case of the fullerene-heteroaromatic dyads, the edge to edge distance between the heteroaromatic nitrogen atom and C<sub>60</sub> is found to be 9.45 Å for 1 and 9.96 Å for 2. The edge to edge distance between the anilinic nitrogen and C<sub>60</sub> is found to be nearly the same (9.5 Å) for the fullerene-*p*-anisidine and the fullerene-*p*-toluidine dyads and for the unsubstituted fullerene-aniline dyad 7 (Section 2.3.2).

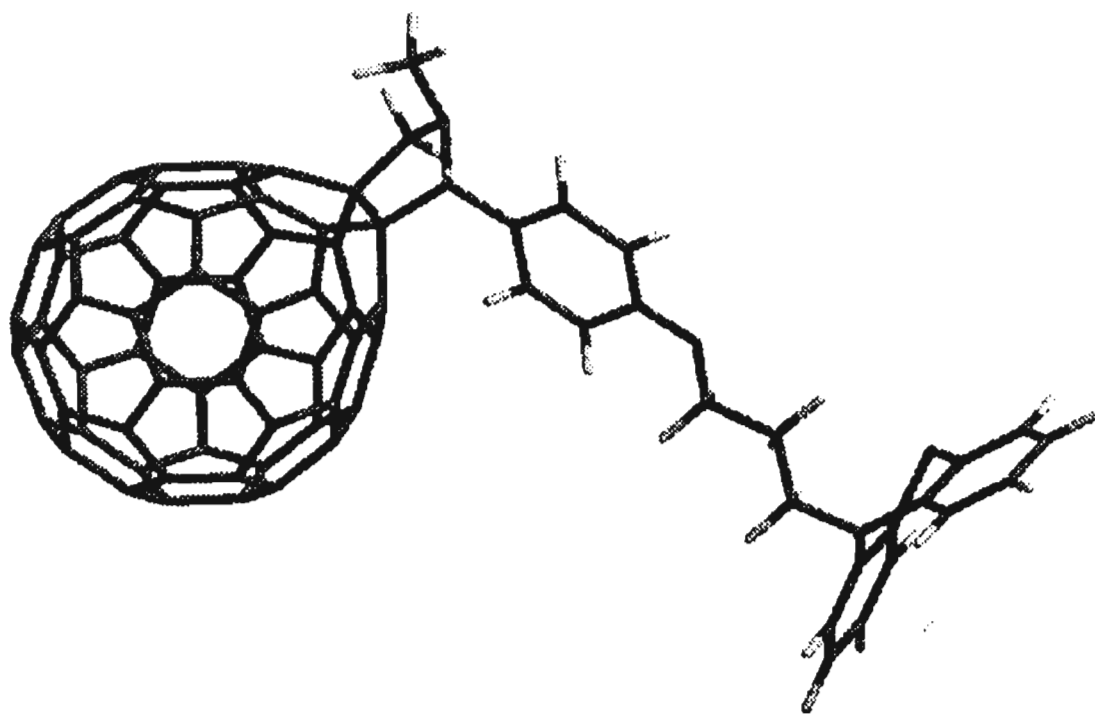


Figure 4.1. The minimum energy configuration of the dyad 2 obtained using molecular mechanics calculations.

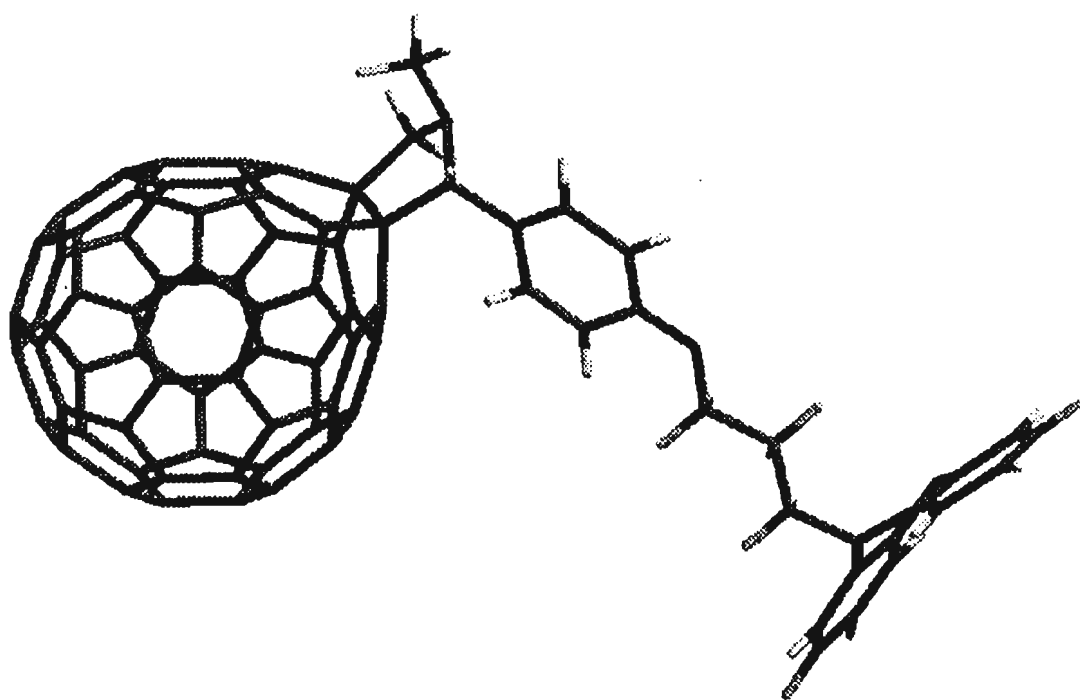


Figure 4.2. The minimum energy configuration of the dyad 3 obtained using molecular mechanics calculations.

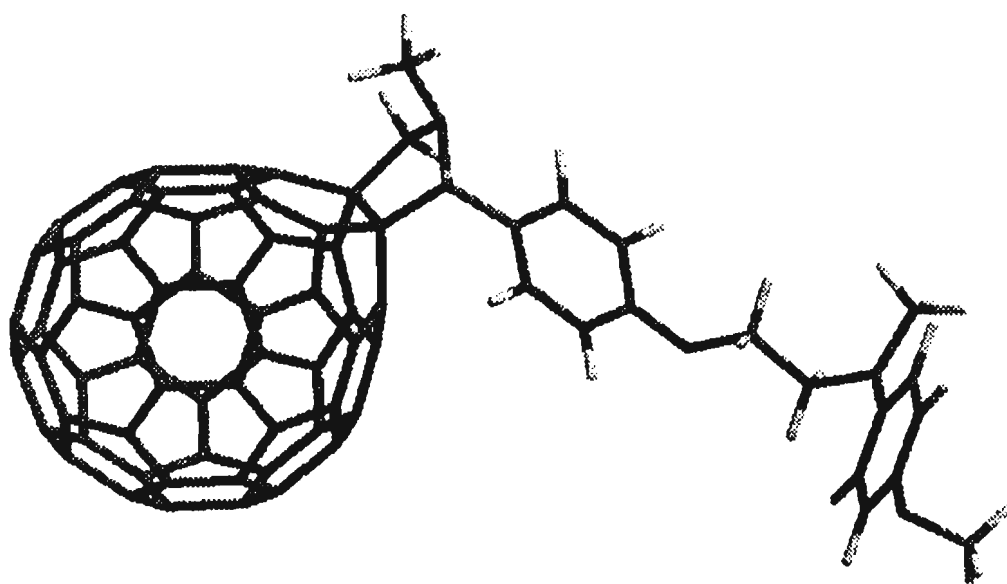


Figure 4.3. The minimum energy configuration of the dyad 5 obtained using molecular mechanics calculations.

### 4.3.3. Steady state absorption properties

The visible absorption spectral features of the fullerene-heteroaromatic dyads 1-3 as well as those of the fullerene-*p*-anisidine (5) and the fullerene-*p*-toluidine (6) dyads are similar to those of the fullerene-aniline dyad 7, reported in Section 2.3.4.<sup>24</sup> Representative absorption spectrum of the fullerene-heteroaromatic dyad 2 in toluene is shown in Figure 4.4. The sharp band around 430 nm is considered as characteristic of all [6-6] closed ring fullerene compounds.<sup>50</sup> Detailed discussions dealing with the 430 as well as 700 nm bands, of fullerene-aniline dyads, are given in Section 2.3.4. The fullerene-aniline dyads possess a weak charge transfer band<sup>24</sup> around 700 nm, merged with a weak forbidden band and were characterized by observing the spectral changes on adding trifluoroacetic acid (TFA). Similar results were also observed in the case of the fullerene-*p*-anisidine and the fullerene-*p*-toluidine dyads. It is reported that heteroaromatic groups such as N-methylphenothiazine and N-methylphenoxazine

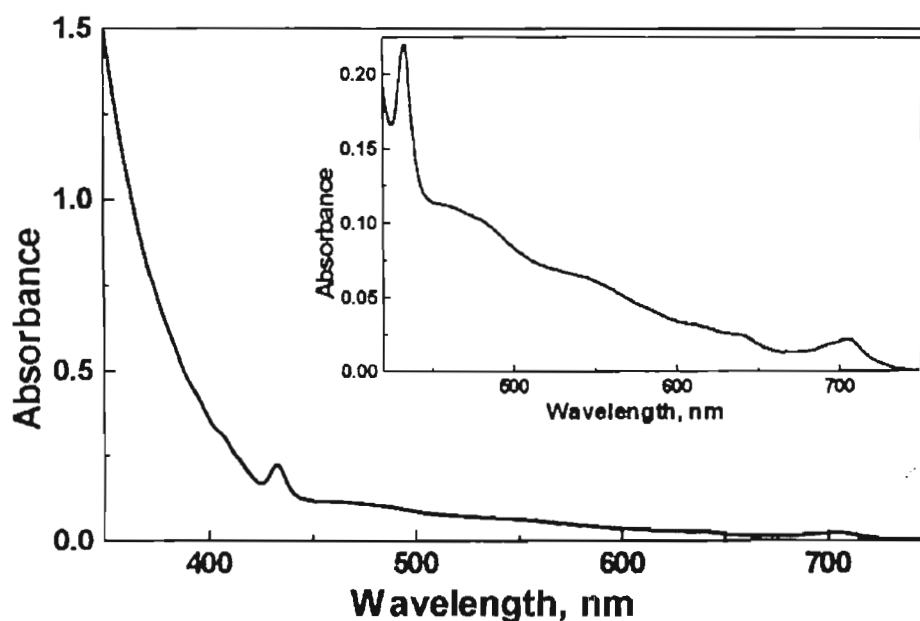


Figure 4.4. Absorption spectrum of the fullerene-phenothiazine dyad 2 in toluene (50 mM)

undergo direct oxidation<sup>51</sup> in presence of acids and this limits us from examining the effect of TFA on the ground state of the fullerene-heteroaromatic dyads.

#### 4.3.4. Steady state emission properties

The emission spectral properties of the fullerene-heteroaromatic dyads, 1-3 and those of the fullerene-*p*-anisidine and the fullerene-*p*-toluidine dyads, 5 and 6 were investigated in solvents of wide ranging polarity (Tables 4.1 and 4.2). The emission maxima and spectral profiles of all these dyads are found to be similar to those of the model pyrrolidinofullerene 4.<sup>22,52</sup> The emission spectra of the dyads of both the series, recorded in toluene, are compared with that of the model compound 4 and the spectral details are shown in Figures 4.5 and 4.6. In Section 2.3.5, we had stated that the quantum yield of fluorescence of fullerene-aniline dyads in toluene are nearly identical to that of the model compound 4, indicating the absence of an electron transfer process. Interestingly, in the present study, a reduction in the quantum yield of fluorescence is observed for the fullerene-heteroaromatic dyads, 1-3 as well as for the fullerene-*p*-anisidine and the fullerene-*p*-toluidine dyads, 5 and 6, even in a nonpolar solvent such as toluene. This effect is more pronounced in the case of the fullerene-phenoxazine dyad 3 and the fullerene-*p*-anisidine dyad 5 (trace c in Figure 4.5 and trace d in Figure 4.6, respectively). A substantial decrease in the quantum yield of fluorescence was observed with increase in the solvent polarity for the fullerene-heteroaromatic dyads 1-3 as well as for the fullerene-aniline dyads 5 and 6 and representative examples are shown in Figures 4.7 and 4.8. The reduction in fluorescence yield is attributed to the quenching of the excited singlet state of fullerene through an intramolecular electron transfer from the appended donor group. This was further confirmed by studying the effect of

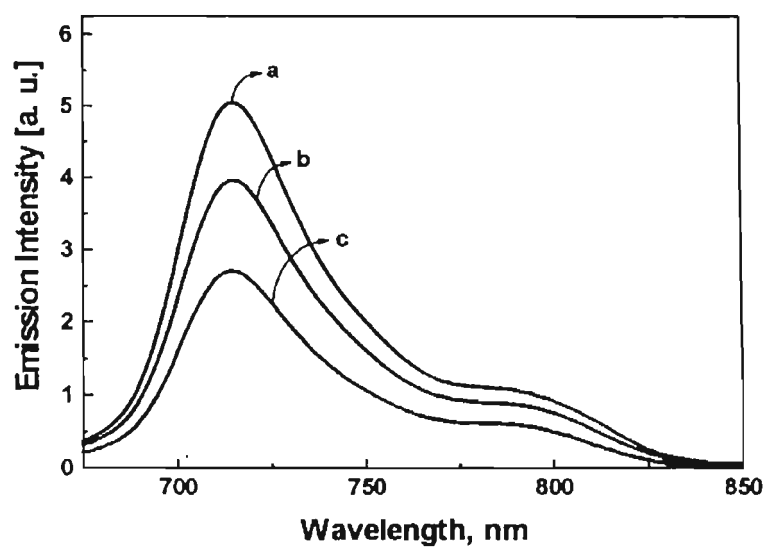


Figure 4.5. Emission spectra of the fullerene-heteroaromatic dyads (2 and 3) and the model compound (4) in toluene: (a) 4, (b) 2, (c) 3 (Absorbance of the solutions were adjusted to 0.1 at the excitation wavelength, 470 nm).

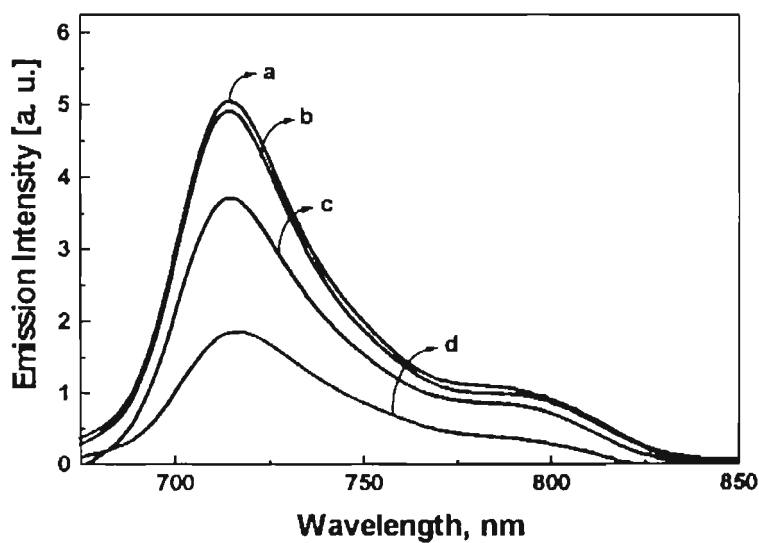


Figure 4.6. Emission spectra of the substituted fullerene-aniline dyads (5-7) and the model compound (4) in toluene: (a) 7, (b) 4, (c) 6, (d) 5 (Absorbance of the solutions were adjusted to 0.1 at the excitation wavelength, 470 nm).

trifluoroacetic acid (TFA) in benzonitrile solution of the dyads. In the case of fullerene-aniline dyads, an enhancement in emission intensity was observed on addition of TFA (trace b in Figure 4.8). As indicated in Section 4.3.3, heteroaromatic compounds such as N-methylphenothiazine and N-methylphenoxazine undergo direct oxidation<sup>51</sup> in presence of acids and this limits us from studying the effect of TFA in the fluorescence of the fullerene-heteroaromatic dyads.

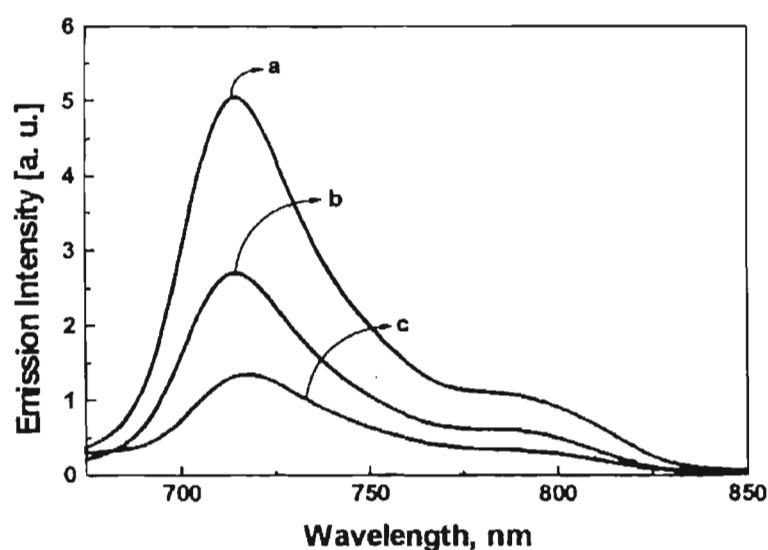


Figure 4.7. Effect of solvent polarity on the fluorescence of the fullerene-heteroaromatic dyad **3** (compared with the model compound **4**): (a) model compound **4** in toluene, (b) **3** in toluene, (c) **3** in benzonitrile (Absorbance of the solutions was adjusted to 0.1 at the excitation wavelength, 470 nm).

The rate constants and quantum yields for charge separation ( $k_{cs}$  and  $\phi_{cs}$ ) via excited singlet states of the dyads, were estimated from the corresponding fluorescence quantum yield of the dyad ( $\phi$ ) and the quantum yield and lifetime of the model compound<sup>22,52</sup> ( $\phi_{ref}$  and  $\tau_{ref}$ , respectively), using Equations 4.1 and 4.2. The rate constants and quantum yields for charge separation for the fullerene-



heteroaromatic dyads and the fullerene-aniline dyads are tabulated in Tables 4.1 and 4.2, respectively.

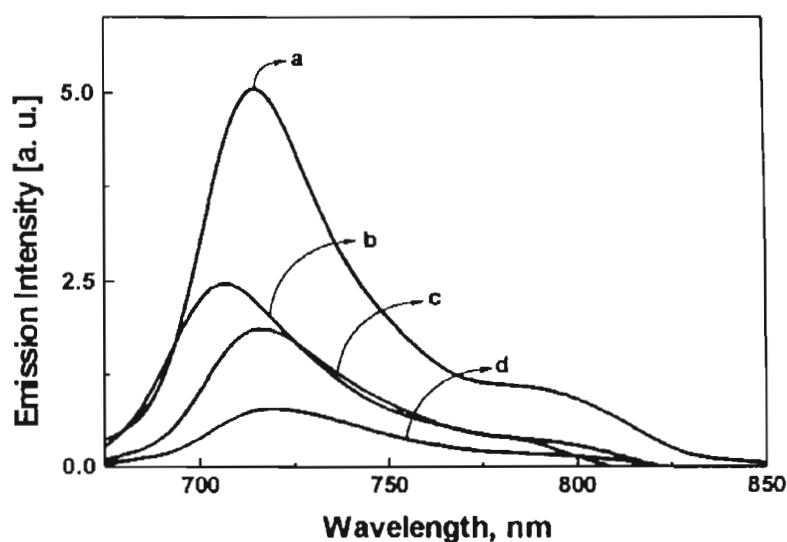


Figure 4.8. Effect of solvent polarity on the fluorescence of fullerene-*p*-anisidine dyad **5** (compared with the model compound **4**): (a) model compound **4** in toluene, (b) **5** in benzonitrile/25 mM TFA, (c) **5** in toluene, (d) **5** in benzonitrile (Absorbance of the solutions were adjusted to 0.1 at the excitation wavelength, 470 nm).

**Table 4.1.** Fluorescence quantum yield ( $\phi_f$ ), rate constant of charge separation ( $k_{cs}$ ) and quantum yield of charge separation ( $\phi_{cs}$ ) for the dyads **1-3**

dyad	toluene		dichloromethane		benzonitrile	
	$\phi_f \times 10^4$	$k_{cs} \times 10^{-9} \text{ s}^{-1}$	$\phi_f \times 10^4$	$k_{cs} \times 10^{-9} \text{ s}^{-1}$	$\phi_f \times 10^4$	$k_{cs} \times 10^{-9} \text{ s}^{-1}$
<b>1</b>	5.3	0.10	2.7	0.95	2.7	0.95
<b>2</b>	4.8	0.20	3.5	0.56	3.2	0.68
<b>3</b>	3.5	0.56	2.0	1.56	1.8	1.80

$$k_{cs} = [(\phi_{ref}/\phi) - 1] / \tau_{ref} \quad \text{-----} \quad \text{(Eq. 4.1)}$$

$$\phi_{cs} = k_{cs} / [(1/\tau_{ref}) - k_{cs}] \quad \text{-----} \quad \text{(Eq. 4.2)}$$

**Table 4.2.** Fluorescence quantum yield ( $\phi_f$ ), rate constant of charge separation ( $k_{cs}$ ) and quantum yield of charge separation ( $\phi_{cs}$ ) for the dyads 5-7

dyad	toluene		dichloromethane		benzonitrile	
	$\phi_f \times 10^4$	$k_{cs} \times 10^{-9} \text{ s}^{-1}$ ( $\phi_{cs}$ )	$\phi_f \times 10^4$	$k_{cs} \times 10^{-9} \text{ s}^{-1}$ ( $\phi_{cs}$ )	$\phi_f \times 10^4$	$k_{cs} \times 10^{-9} \text{ s}^{-1}$ ( $\phi_{cs}$ )
5	2.6	1.09 (47%)	1.3	3.01 (78%)	1.2	3.33 (80%)
6	4.9	0.19 (18%)	2.3	1.34 (62%)	2.3	1.34 (62%)
7	6.8	-	3.3	0.64 (45%)	3.1	0.74 (49%)

#### 4.3.5. Transient absorption studies<sup>53</sup>

We have earlier investigated the dynamics of the photoinduced electron transfer in unsubstituted fullerene-aniline dyads and these results are presented in Section 2.3.6. Based on the steady state fluorescence and transient absorption studies, possibility of an intramolecular electron transfer in these dyads (in toluene) was ruled out. In a polar solvent such as benzonitrile, the existence of charge separated intermediates was observed in dyad systems in which the anilinic donor is linked to the *para*- as well as *ortho*- positions of phenyl group of fullero(1-methyl-2-phenyl)pyrrolidine through three methylene chains. The detailed investigations on the dynamics of charge recombination were not followed in these systems, due to the interference of the triplet excited state and the low yield of the radical pairs.

The light induced electron transfer in fullerene-based systems possessing the heteroaromatic donor groups such phenothiazine (dyad 2) and phenoxazine (dyad 3) were investigated, as representative examples, using nanosecond laser flash photolysis techniques. In the case of the fullerene-heteroaromatic dyads, a decrease in the quantum yield of fluorescence was observed (Table 4.1) even in a nonpolar solvent such as toluene (Section 4.3.4). Forward electron transfer process in these systems is thermodynamically favorable due to the low ionization potential of the heteroaromatic donor group. The time-resolved spectra of the fullerene-heteroaromatic dyads 2 and 3, recorded in toluene, do not indicate the presence of charge-separated intermediates (in the nanosecond time scale). A representative example is displayed in Figure 4.9. The transient absorption spectra of dyads 2 and 3 are similar to that of the model compound 4, which does not possess a donor group, and characterized as the triplet excited state.

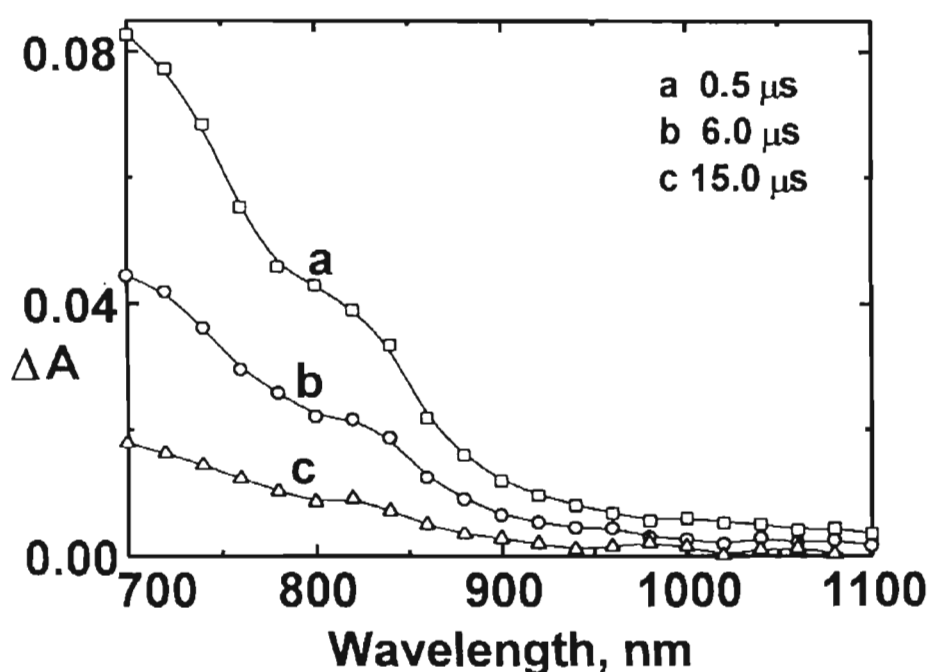


Figure 4.9. Time-resolved difference absorption spectra, recorded following 337 nm laser pulse excitation, of the dyad 2 in toluene at different delay times.

Based on the steady state emission and transient absorption studies, it can be concluded that two processes deactivate the singlet excited state of the dyad in toluene, (i) the intersystem crossing and (ii) the charge separation. Due to the nonpolar nature of toluene, the resulting charge-separated intermediates formed are not stabilized and the rapid charge recombination seems to be the reason for not observing the intermediates, in the nanosecond time domain.

The laser flash photolysis of the fullerene-heteroaromatic dyads was carried out in polar solvents such as benzonitrile. Figures 4.10A and 4.10B show the nanosecond transient absorption spectra of the fullerene-phenothiazine dyad 2 in the visible and near-infrared (NIR) regions, respectively. In contrast to the spectrum in toluene, the dyad 2 possesses two absorption maxima in benzonitrile, in the visible region (450 nm and 520 nm) and in deoxygenated benzonitrile. Based on the previous reports and pulse radiolytic oxidation experiments these bands are characterized as the radical cation of phenothiazine.<sup>54</sup> Figure 4.11A shows the absorption-time profile recorded at 520 nm and exhibits monoexponential decay with a lifetime of 260 ns. The well-resolved intense NIR band with maximum around 1010 nm provides an unambiguous evidence for the formation of C<sub>60</sub> radical anion (Figure 4.10B). The absorption-time decay profile at 1010 nm is displayed in Figure 4.11B. The lifetime of the radical anion ( $\tau = 260$  ns) was estimated by fitting the decay curve to first order kinetics and presented in Table 4.3. Time resolved transient absorption spectra of fullerene-phenoxazine dyad 3, recorded following 337 nm laser pulse excitation, are shown in Figure 4.12. The sharp intense absorption band with maximum around 530 nm is attributed to the radical cation of phenoxazine. The absorption spectrum corresponding to the radical anion of C<sub>60</sub>,

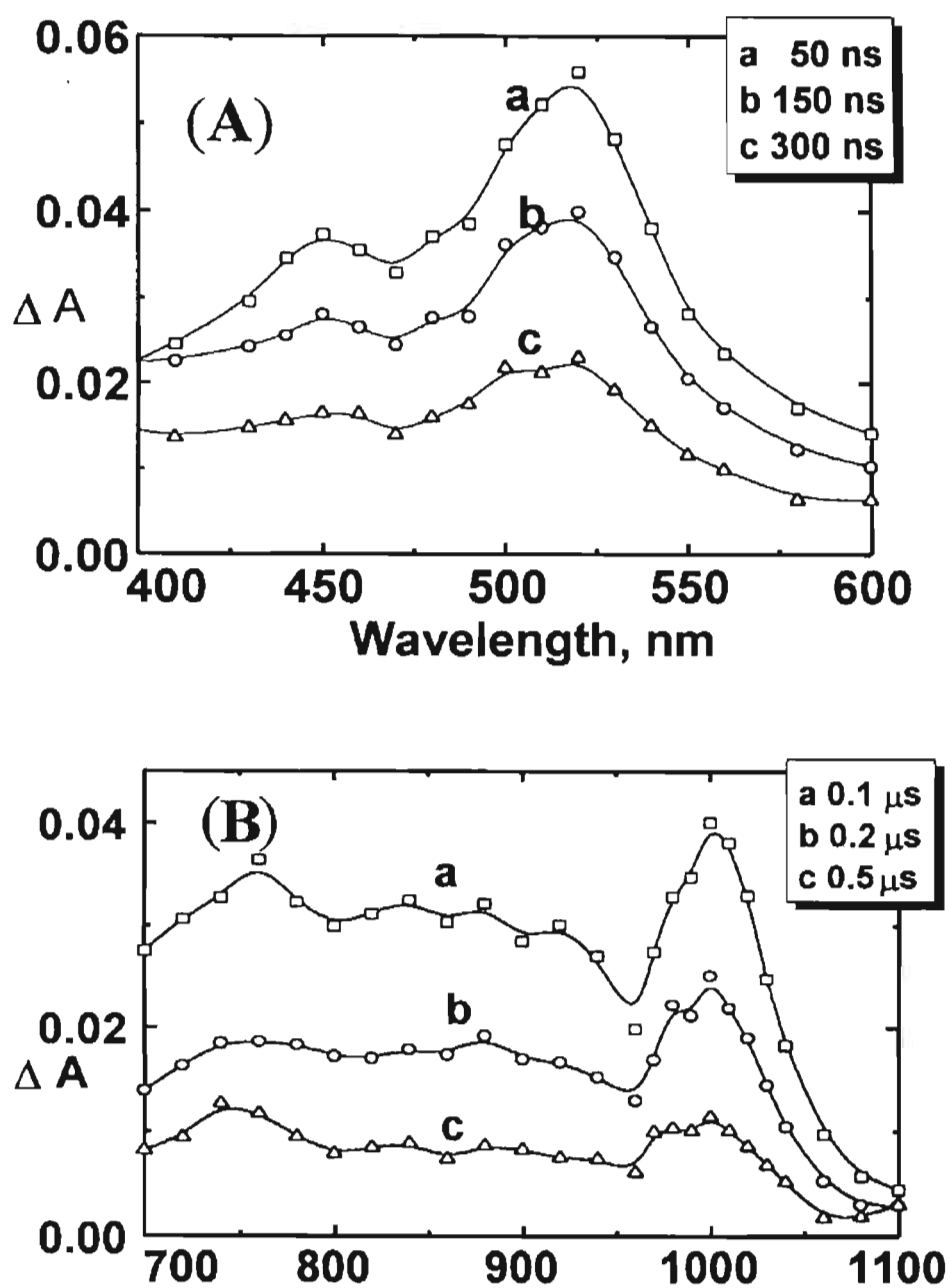


Figure 4.10. Time resolved difference absorption spectra of the of dyad 2, recorded in the visible (A) and NIR (B) regions.

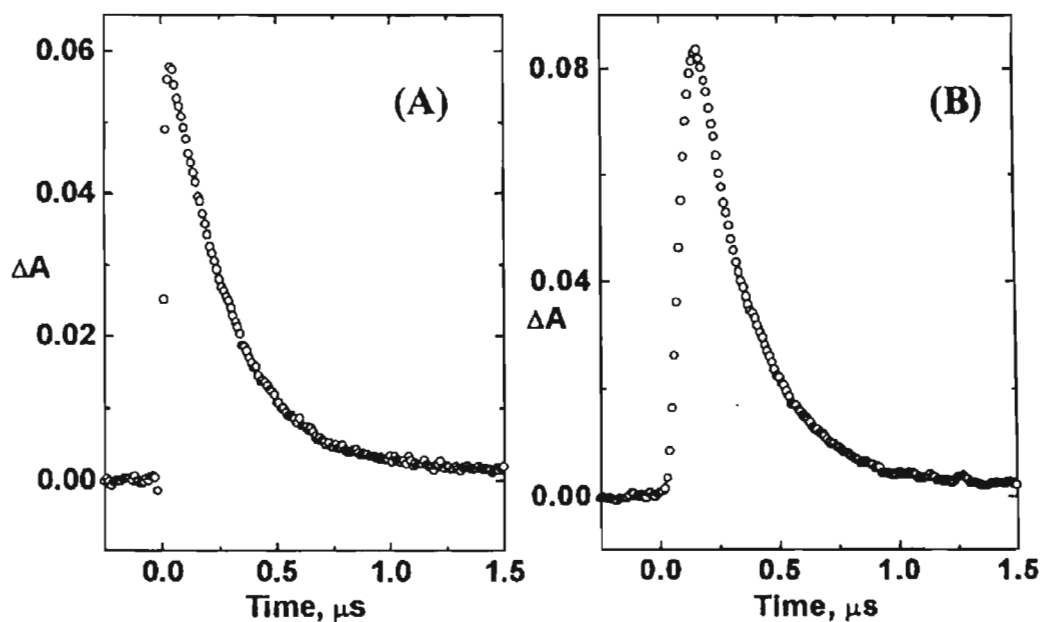


Figure 4.11. Absorption-time decay profile recorded of the dyad 2 in deoxygenated benzonitrile: (A) 520 nm and (B) 1010 nm.

**Table 4.3.** Rate of charge recombination ( $k_{cr}$ ) and the quantum yields of charge separation ( $\phi_{cs}$ ) for dyads 2 and 3 in benzonitrile.

Dyad	$k_{cr}$	$\phi_{cs}$
2	$3.8 \times 10^6$	88%
3	$3.1 \times 10^6$	39%

recorded using the NIR detector is shown in the inset of Figure 4.12. The lifetimes of both the radical anion of  $C_{60}$  and radical cation of phenoxazine exhibit a monoexponential decay profile ( $\tau = 320$  ns).

In contrast to the fullerene-aniline system, the fullerene-heteroaromatic dyads possess several important features. The charge-separated intermediates

formed in fullerene-heteroaromatic dyads are long-lived compared to anilinic systems presented in Chapter 2. The triplet excited state of model compound 4

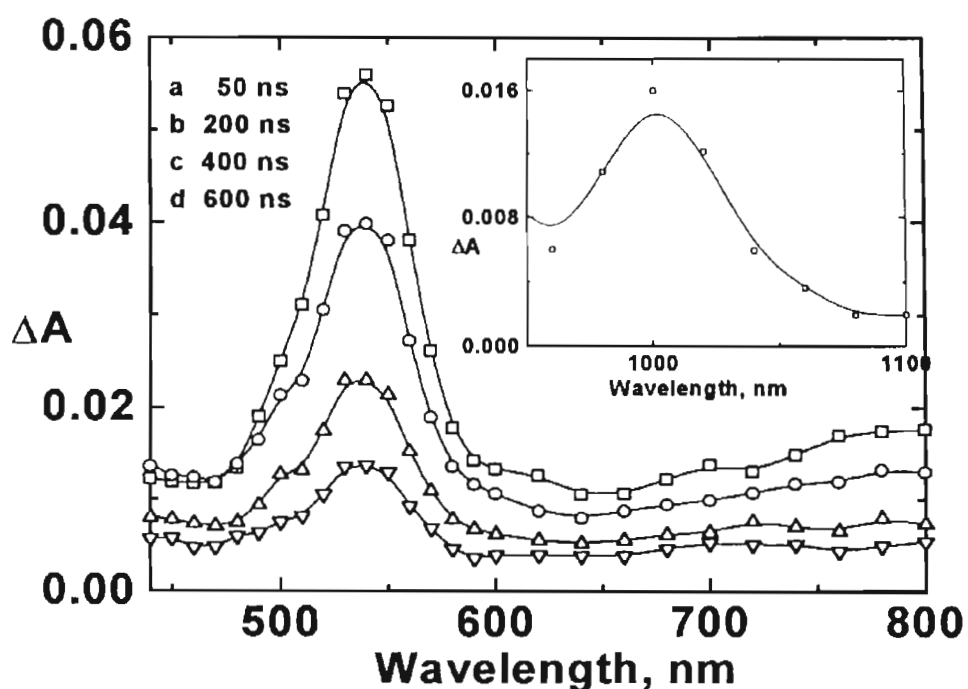


Figure 4.12. Time resolved difference absorption spectra of the dyad **3**, recorded in the visible region, in deoxygenated benzonitrile: Inset shows time resolved difference absorption spectrum of the dyad **3**, recorded in the NIR region.

possesses an intense absorption with maximum around 700 nm ( $\epsilon = 16,000$ ). It is interesting to note that the transient absorption spectrum of fullerene-heteroaromatic dyads possess very little absorption in the 700 nm region, in benzonitrile. It is quite likely that the triplet state is short lived and that it may be involved in the charge separation process. Based on the steady state fluorescence and transient absorption studies it can be concluded that the photoinduced electron transfer in these dyads originates from a singlet excited state. The quantum yields of the charge separation in these systems were estimated by a relative method and the results are summarized in Table 4.3.

#### 4.4. Conclusions

Compared to the unsubstituted fullerene-aniline dyad, an increase in the rate constants and quantum yields of charge separation were observed for the fullerene-heteroaromatic dyads as well as in the case of the fullerene-*p*-anisidine and the fullerene-*p*-toluidine dyads, even in a non-polar solvent such as toluene. The fluorescence quenching is attributed to an electron transfer process to the excited singlet state of fullerene. An increase in the rate constants and quantum yields of charge separation is observed, both in the case of the fullerene-heteroaromatic dyads and the fullerene-aniline dyads, with a decrease in the oxidation potential of the donor group. The semiflexible nature of the bridging unit, used in the present studies, is having an important role in achieving high quantum yields of charge separation. By the suitable tuning of the ionization potential of the donor group, we were able to generate long-lived charge separated states with high yields ( $\phi_{cs}$  is 90% for dyad 2) in fullerene-based D-B-A systems and the existence of charge separated intermediates was confirmed through laser flash photolysis techniques.

#### 4.5. Experimental Section

##### 4.5.1. Synthesis of fullerene-heteroaromatic dyads, fullerene-*p*-anisidine and fullerene-*p*-toluidine dyads

Fullerene-heteroaromatic dyads and fullerene-*p*-anisidine and fullerene-*p*-toluidine dyads were synthesized through the pathways shown in Schemes 4.1 and 4.2, respectively. Purity of all these dyads was confirmed by HLPC.<sup>48</sup> The preparation of N-( $\omega$ -bromoalkyl)heteroaromatic derivatives<sup>55-58</sup> were reported earlier. We have adopted a different procedure by first converting the corresponding heteroaromatic compounds to N-( $\omega$ -hydroxyalkyl)heteroaromatics and subsequently



treating them with phosphorus tribromide. The synthesis of the fullerene-aniline dyad **7**<sup>24</sup> was reported earlier.

#### 4.5.1.1. General method for the preparation 10-( $\omega$ -hydroxyalkyl)heteroaromatics (**9**, **12** and **14**)

A mixture of phenothiazine, **8** (or phenoxazine **11**) (20 mmol), potassium carbonate (20 mmol), potassium iodide (100 mg) and bromo- or chloro- alcohol (20 mmol) was refluxed in *o*-dichlorobenzene (20 mL) for 95 h. On cooling, the solvent was removed under reduced pressure and the crude product was chromatographed over silica gel (100-200 mesh).

**Compound 9.** Elution of the column using chloroform gave 3.4 g (70 %) of **9** as a viscous liquid; IR (neat)  $\nu_{\max}$  3383, 3070, 2956, 2883, 1599, 1577, 1467, 1333, 1290, 1257, 1164, 1134, 1109, 1041, 934, 890, 855, 751, 661, 623, 483  $\text{cm}^{-1}$ ;  $^1\text{H}$  NMR ( $\text{CDCl}_3$ )  $\delta$  3.40-3.58 (2H, m,  $\text{NCH}_2$ ), 3.62-4.00 (3H, t with a broad shoulder,  $\text{OCH}_2$  and OH), 6.60-7.50 (8H, m, aromatic);  $^{13}\text{C}$  NMR ( $\text{CDCl}_3$ )  $\delta$  46.15, 62.48, 114.73, 115.78, 121.80, 126.19, 127.21, 161.00; exact mass calcd. for  $\text{C}_{14}\text{H}_{13}\text{NSO}$  ( $\text{M}^+$ ) 243.0718, found 243.0713 (FAB, high resolution mass spectroscopy).

**Compound 12.** Elution of the column using chloroform gave 3.6 g (70%) of **12** as a viscous liquid; IR (neat)  $\nu_{\max}$  3402, 3071, 2939, 2882, 1599, 1576, 1488, 1464, 1441, 1363, 1306, 1254, 1132, 1061, 1044, 930, 864, 756, 537  $\text{cm}^{-1}$ ;  $^1\text{H}$  NMR ( $\text{CDCl}_3$ )  $\delta$  1.90-2.20 (2H, m,  $\text{CH}_2$ ), 3.65 (2H, t,  $\text{CH}_2$ ), 3.95 (2H, t,  $\text{CH}_2$ ), 6.60-7.50 (8H, m, aromatic);  $^{13}\text{C}$  NMR ( $\text{CDCl}_3$ )  $\delta$  29.45, 44.06, 60.56, 115.60, 122.58, 125.48, 127.50, 145.26, 159.04; exact mass calcd. for  $\text{C}_{15}\text{H}_{15}\text{NSO}$  ( $\text{M}^+$ ) 257.0874, found 257.0892 (FAB, high resolution mass spectroscopy).

**Compound 14.** Elution of the column using chloroform gave 3.86 g (80%) of 14 as a viscous liquid (reported as solid with mp 68 °C);<sup>56</sup> IR (neat)  $\nu_{\max}$  3419, 3076, 2938, 2882, 1598, 1493, 1383, 1274, 1129, 1069, 1047, 921, 843, 742  $\text{cm}^{-1}$ ;  $^1\text{H}$  NMR ( $\text{CDCl}_3$ )  $\delta$  1.6-2.0 (2H, m,  $\text{CH}_2$ ), 2.5 (1H, s, OH), 3.3-3.9 (4H, m,  $\text{OCH}_2$  and  $\text{NCH}_2$ ), 6.5-6.9 (8H, m, aromatic);  $^{13}\text{C}$  NMR ( $\text{CDCl}_3$ )  $\delta$  27.92, 40.57, 69.36, 111.25, 115.16, 120.62, 123.51, 133.18, 144.82; exact mass calcd. for  $\text{C}_{15}\text{H}_{15}\text{NO}_2$  ( $\text{M}^+$ ) 241.1103, found 241.1108 (FAB, high resolution mass spectroscopy).

#### 4.5.1.2. General method for the preparation of 10-( $\omega$ -bromoalkyl)heteroaromatics (10, 13 and 15)

To an ice-cold solution of a N-( $\omega$ -hydroxyalkyl)heteroaromatic compound (5 mmol) in methylene chloride (10 mL) was added  $\text{PBr}_3$  (5 mmol), over a period of 30 min. The reaction mixture was further stirred at room temperature for an additional period of 3 h and quenched with ice-cold water. The pH was adjusted to 7-8 and the organic portion was extracted with dichloromethane. The solvent was removed under reduced pressure and the crude product was chromatographed on silica gel (100-200 mesh).

**Compound 10.** Elution of the column with a mixture (1:4) of chloroform and hexane gave 1.1 g (70 %) of 10, mp 70-71 °C; IR (KBr)  $\nu_{\max}$  3074, 2929, 2859, 1599, 1578, 1490, 1467, 1366, 1333, 1288, 1256, 1217, 1164, 1135, 1110, 1064, 909, 748, 585  $\text{cm}^{-1}$ ;  $^1\text{H}$  NMR ( $\text{CDCl}_3$ )  $\delta$  3.62 (2H, t,  $\text{CH}_2$ ), 4.26 (2H, t,  $\text{CH}_2$ ), 6.80-7.00 (m), 7.10-7.20 (m) (8H, aromatic);  $^{13}\text{C}$  NMR ( $\text{CDCl}_3$ )  $\delta$  27.81, 49.31, 115.14, 123.09, 125.27, 127.46, 127.69, 144.15; exact mass calcd. for  $\text{C}_{14}\text{H}_{12}\text{NSBr}$  ( $\text{M}^+$ ) 304.9874, found 304.9896 (FAB, high resolution mass spectroscopy).

**Compound 13.** Elution of the column using a mixture of (1:4) of chloroform and hexane gave 1.45 g (91%) of **13** as a viscous liquid; IR (neat)  $\nu_{\max}$  3072, 2934, 2861, 1599, 1578, 1338, 1288, 1253, 1194, 1162, 1132, 1108, 1042, 908, 750  $\text{cm}^{-1}$ ;  $^1\text{H}$  NMR ( $\text{CDCl}_3$ )  $\delta$  2.30 (2H, quintet,  $\text{CH}_2$ ), 3.52 (2H, t,  $\text{CH}_2$ ), 4.07 (2H, t,  $\text{CH}_2$ ), 6.88-6.95 and 7.14-7.24 (8H, m, aromatic);  $^{13}\text{C}$  NMR ( $\text{CDCl}_3$ )  $\delta$  29.18, 30.48, 44.54, 115.05, 122.22, 125.17, 126.78, 127.11, 144.51; exact mass calcd. for  $\text{C}_{15}\text{H}_{14}\text{NSBr}$  ( $\text{M}^+$ ) 319.0030, found 319.0010 (FAB, high resolution mass spectroscopy).

**Compound 15.** Elution of the column using a mixture (1:4) of chloroform and hexane gave 0.89 g (59%) of **15**, mp 55 °C; IR (KBr)  $\nu_{\max}$  3074, 2969, 2916, 1598, 1496, 1383, 1275, 1217, 1133, 1046, 915, 814, 740, 562  $\text{cm}^{-1}$ ;  $^1\text{H}$  NMR ( $\text{CDCl}_3$ )  $\delta$  2.0-2.4 (2H, m,  $\text{CH}_2$ ), 3.3-3.9 (4H, m,  $\text{NCH}_2$  and  $\text{BrCH}_2$ ), 6.4-7.0 (8H, m, aromatic);  $^{13}\text{C}$  NMR ( $\text{CDCl}_3$ )  $\delta$  27.65, 30.61, 42.15, 111.13, 115.40, 120.95, 123.54, 132.85, 144.85; exact mass calcd. for  $\text{C}_{15}\text{H}_{14}\text{NOBr}$  ( $\text{M}^+$ ) 303.0259, found 303.0258 (FAB, high resolution mass spectroscopy).

#### 4.5.1.3. General method for the preparation of N-((*p*-formylphenoxy)alkyl)-heteroaromatics (**17**, **19** and **21**)

A mixture of the appropriate bromide (2 mmol), *p*-hydroxybenzaldehyde (4 mmol) and potassium carbonate (2 mmol) was refluxed in dry acetone (10 mL) for 12 h. The reaction mixture was cooled, filtered and concentrated under reduced pressure. The crude product was chromatographed over silica gel (100-200 mesh).

**Compound 17.** Elution of the column using a mixture (1:4) of chloroform and petroleum ether (bp 60-80 °C) gave 0.42 g (60 %) of **17**, mp 124-125 °C; IR (KBr)  $\nu_{\max}$  3043, 2927, 1666, 1609, 1586, 1523, 1463, 1413, 1351, 1252, 1170, 1041, 811,

752, 576  $\text{cm}^{-1}$ ;  $^1\text{H}$  NMR ( $\text{CDCl}_3$ )  $\delta$  4.36 (4H, s,  $\text{OCH}_2$  and  $\text{NCH}_2$ ), 6.90-6.99 (m), 7.10-7.20 (m), 7.80 (d) (12H, aromatic), 9.86 (1H, s, CHO);  $^{13}\text{C}$  NMR ( $\text{CDCl}_3$ )  $\delta$  46.79, 65.50, 115.16, 115.54, 123.27, 125.68, 127.69, 127.95, 130.46, 132.22, 145.00, 163.66, 191.02; exact mass calcd. for  $\text{C}_{21}\text{H}_{17}\text{NSO}_2$  ( $\text{M}^+$ ) 347.0980, found 347.0968 (FAB, high resolution mass spectroscopy).

**Compound 19.** Elution of the column using a mixture (1:4) of chloroform and petroleum ether (bp 60-80  $^\circ\text{C}$ ) gave 0.58 (80 %) of **19**, mp 97-98  $^\circ\text{C}$ ; IR (KBr)  $\nu_{\text{max}}$  3071, 2958, 2878, 2739, 1696, 1604, 1582, 1514, 1465, 1395, 1315, 1262, 1163, 1111, 1058, 963, 833, 752, 650, 614  $\text{cm}^{-1}$ ;  $^1\text{H}$  NMR ( $\text{CDCl}_3$ )  $\delta$  2.25 (2H, quintet,  $\text{CH}_2$ ), 3.90-4.30 (4H, m,  $\text{NCH}_2$  and  $\text{OCH}_2$ ), 6.60-8.10 (12H, m, aromatic), 9.80 (1H, s, CHO);  $^{13}\text{C}$  NMR ( $\text{CDCl}_3$ )  $\delta$  26.55, 43.56, 65.54, 114.80, 115.61, 122.68, 125.69, 127.24, 127.57, 129.93, 131.84, 145.05, 163.82, 190.67; exact mass calcd. for  $\text{C}_{22}\text{H}_{19}\text{NSO}_2$  ( $\text{M}^+$ ) 361.1137, found 361.1132 (FAB, high resolution mass spectroscopy).

**Compound 21.** Elution of the column using a mixture (1:4) of chloroform and petroleum ether (bp 60-80  $^\circ\text{C}$ ) gave 0.59 (85 %) of **21**, mp 75-76  $^\circ\text{C}$ ; IR (KBr)  $\nu_{\text{max}}$  3078, 2987, 2877, 2749, 1700, 1605, 1498, 1383, 1310, 1274, 1221, 1163, 1132, 1114, 1068, 1049, 912, 831, 737, 650, 618  $\text{cm}^{-1}$ ;  $^1\text{H}$  NMR ( $\text{CDCl}_3$ )  $\delta$  2.00-2.30 (2H, m,  $\text{CH}_2$ ), 3.50-3.80 (2H, m,  $\text{CH}_2$ ), 4.00-4.30 (2H, t,  $\text{CH}_2$ ), 6.45-6.70 (m), 6.98 (d) and 7.85 (d) (12H, m, aromatic), 9.85 (1H, s, CHO);  $^{13}\text{C}$  NMR ( $\text{CDCl}_3$ )  $\delta$  25.03, 40.36, 65.42, 111.13, 114.65, 115.34, 120.89, 123.54, 130.05, 131.84, 132.94, 144.76, 163.46, 190.52; exact mass calcd. for  $\text{C}_{22}\text{H}_{19}\text{NO}_3$  ( $\text{M}^+$ ) 345.1365, found 345.1363 (FAB, high resolution mass spectroscopy).

#### 4.5.1.4. General method for the synthesis of fullerene-heteroaromatic dyads (1-3)

A mixture of C<sub>60</sub> (0.1 mmol), the appropriate N-substituted heteroaromatic aldehydes (0.1 mmol) and N-methylglycine (0.1 mmol) in toluene (75 mL) was stirred under reflux for 10 h. The reaction mixture was cooled and removal of the solvent under reduced pressure gave a solid residue, which was chromatographed over silica gel (100-200 mesh) to give the appropriate dyads. The yields of the dyads reported are based on the amount of C<sub>60</sub> consumed.

**Dyad 1.** Elution with a mixture (1:2) of toluene and petroleum ether (bp 60-80 °C) gave 23 mg (32%) of unreacted C<sub>60</sub> followed by 48 mg (65%) of the dyad 1, mp > 400 °C; IR (KBr)  $\nu_{\max}$  2954, 2783, 1567, 1517, 1467, 1292, 1247, 1173, 1129, 1109, 1039, 835, 748, 666, 637, 609, 531 cm<sup>-1</sup>; <sup>1</sup>H NMR (CDCl<sub>3</sub>)  $\delta$  2.76 (3H, s, NCH<sub>3</sub>), 4.22 (1H, d, CH of pyrrolidine ring, J = 9.36 Hz), 4.28 (4H, s, NCH<sub>2</sub> and OCH<sub>2</sub>), 4.86 (1H, s, CH of pyrrolidine ring), 4.95 (1H, d, CH of pyrrolidine ring, J = 9.36 Hz), 6.80-6.93(m), 7.11-7.25 (m), 7.66 (br.s) (12H, aromatic); <sup>13</sup>C NMR (CDCl<sub>3</sub>+CS<sub>2</sub>)  $\delta$  39.93, 46.80, 64.91, 68.88, 69.95, 77.47, 83.05, 114.76, 115.14, 122.84, 125.03, 127.37, 127.53, 128.26, 128.93, 129.42, 130.45, 130.52, 135.23, 136.01, 136.08, 139.13, 139.62, 139.89, 140.85, 140.90, 141.20, 142.04, 142.23, 144.16, 144.70, 145.18, 145.72, 146.05, 146.25, 146.75, 147.23, 153.50, 154.00, 156.48, 158.44; exact mass calcd. for C<sub>83</sub>H<sub>22</sub>N<sub>2</sub>SO (M<sup>+</sup>) 1094.1453, found 1094.1417 (FAB, high resolution mass spectroscopy).

**Dyad 2.** Elution of the column with a mixture (1:2) of toluene and petroleum ether (bp 60-80 °C) gave 25 mg (35%) of unchanged C<sub>60</sub> followed by 43 mg (60%) of the dyad 2, mp > 400 °C; IR (KBr)  $\nu_{\max}$  2958, 2924, 2858, 1616, 1554, 1460, 1249,

1212, 1173, 1104, 1070, 1019, 797, 749, 529  $\text{cm}^{-1}$ ;  $^1\text{H}$  NMR ( $\text{CDCl}_3$ )  $\delta$  2.24-2.29 (2H, m,  $\text{CH}_2$ ), 2.78 (3H, s,  $\text{NCH}_3$ ), 4.02-4.14 (4H, m,  $\text{NCH}_2$  and  $\text{OCH}_2$ ), 4.24 (1H, d, CH of pyrrolidine ring,  $J = 9.34$  Hz) 4.87 (1H, s, CH of pyrrolidine ring), 4.96 (1H, d, CH of pyrrolidine ring,  $J = 9.34$  Hz), 6.89-6.93 (m), 7.11-7.16 (m), 7.66 (br.s) (12 H, aromatic);  $^{13}\text{C}$  NMR ( $\text{CDCl}_3+\text{CS}_2$ )  $\delta$  26.91, 39.94, 43.93, 65.29, 68.94, 69.99, 83.16, 96.23, 114.65, 115.50, 122.58, 125.44, 127.22, 127.51, 128.99, 130.41, 135.76, 136.55, 136.78, 139.57, 139.90, 140.15, 140.16, 141.52, 141.66, 141.80, 142.01, 142.09, 142.26, 142.54, 142.67, 142.97, 143.13, 144.37, 144.61, 145.03, 145.22, 145.45, 145.53, 145.76, 145.91, 146.11, 146.34, 146.77, 147.27, 153.61, 154.07, 156.26, 158.86; exact mass calcd. for  $\text{C}_{84}\text{H}_{24}\text{N}_2\text{SO}$  ( $\text{MH}^+$ ) 1109.1682, found 1109.1724 (FAB, high resolution mass spectroscopy).

**Dyad 3.** Elution of the column with a mixture (1:2) of toluene and petroleum ether (bp 60-80  $^\circ\text{C}$ ) gave 20 mg (28%) of unchanged  $\text{C}_{60}$  followed by 49 mg (62%) of the dyad 3, mp > 400  $^\circ\text{C}$ ; IR (KBr)  $\nu_{\text{max}}$  2971, 2794, 1617, 1498, 1265, 1096, 1027, 805  $\text{cm}^{-1}$ ;  $^1\text{H}$  NMR ( $\text{CDCl}_3$ )  $\delta$  2.12-2.15 (2H, m,  $\text{CH}_2$ ), 2.80 (3H, s,  $\text{NCH}_3$ ), 3.75 (2H, t,  $\text{CH}_2$ ), 4.10 (2H, t,  $\text{CH}_2$ ), 4.26 (1H, d, CH of pyrrolidine ring,  $J = 9.36$  Hz), 4.90 (1H, s, CH of pyrrolidine ring), 4.98 (1H, d, CH of pyrrolidine ring,  $J = 9.36$  Hz), 6.53-6.72 (m), 6.98(d), 7.72 (br.s) (12 H, aromatic);  $^{13}\text{C}$  NMR ( $\text{CDCl}_3+\text{CS}_2$ )  $\delta$  25.53, 39.94, 40.75, 65.06, 68.95, 70.01, 77.45, 83.17, 111.23, 114.61, 115.40, 120.94, 123.64, 129.27, 130.53, 133.10, 135.74, 136.55, 136.84, 139.57, 139.83, 140.16, 141.46, 141.60, 141.81, 142.57, 142.67, 142.96, 143.10, 144.42, 144.67, 144.82, 145.22, 145.43, 145.78, 145.94, 146.13, 146.30, 146.46, 146.72, 147.30, 153.58, 154.04, 156.32, 158.69; exact mass calcd. for  $\text{C}_{84}\text{H}_{24}\text{N}_2\text{O}_2$  ( $\text{MH}^+$ ) 1093.1916, found 1093.1929 (FAB, high resolution mass spectroscopy).

#### 4.5.1.5. Preparation of N-((2-hydroxy)-1-ethyl)-*p*-anisidine (23) and N-((2-hydroxy)-1-ethyl)-*p*-toluidine (27)

A mixture of *p*-anisidine (22) or *p*-toluidine (23) (0.1 mol), ethylene chlorohydrin (0.1 mol), potassium carbonate (0.2 mol), and iodine (100 mg) was heated under reflux in 1-butanol (80 mL) for 30 h. On cooling, the solvent was removed under reduced pressure to give a reddish brown liquid.

**Compound 23.** The residual liquid on column chromatography on silica gel (100-200 mesh) using a mixture (1:4) of petroleum ether (boiling point 60-80 °C) and chloroform gave 14.2 g (85%) of 23, bp 187-189 °C (30 mm); IR (neat)  $\nu_{\max}$  3393, 2944, 2841, 1626, 1534, 1465, 1242, 1183, 1129, 1038, 916, 823, 694, 526  $\text{cm}^{-1}$ ;  $^1\text{H}$  NMR ( $\text{CDCl}_3$ )  $\delta$  2.86 (2H, br.s, NH and OH), 3.21 (2H, t,  $\text{NCH}_2$ ), 3.73 (3H, s,  $\text{OCH}_3$ ), 3.77 (2H, t,  $\text{OCH}_2$ ), 6.60 (d), 6.77 (d) (4H, aromatic);  $^{13}\text{C}$  NMR ( $\text{CDCl}_3$ )  $\delta$  47.21, 55.80, 61.19, 114.84, 114.92, 142.22, 152.53; exact mass calcd. for  $\text{C}_9\text{H}_{13}\text{NO}_2$  ( $\text{M}^+$ ) 167.0946, found 167.0931 (FAB, high resolution mass spectroscopy).

**Compound 27.** The residual liquid on column chromatography on silica gel (100-200 mesh) using a mixture (1:4) of petroleum ether (bp 60-80 °C) and chloroform gave 13.6 g (90 %) of 27, bp 162-164 °C (30 mm); IR (neat)  $\nu_{\max}$  3397, 3031, 2928, 2877, 1623, 1526, 1465, 1324, 1264, 1187, 1132, 1066, 918, 810, 757, 511  $\text{cm}^{-1}$ ;  $^1\text{H}$  NMR ( $\text{CDCl}_3$ )  $\delta$  2.25 (3H, s,  $\text{CH}_3$ ), 2.95 (2H, br.s, NH and OH), 3.24 (2H, t,  $\text{NCH}_2$ ), 3.78 (2H, t,  $\text{OCH}_2$ ), 6.57 (d), 6.99 (d) (4H, aromatic);  $^{13}\text{C}$  NMR ( $\text{CDCl}_3$ )  $\delta$  20.29, 46.46, 61.09, 113.48, 127.17, 129.71, 145.72; exact mass calcd. for  $\text{C}_9\text{H}_{13}\text{NO}$  ( $\text{M}^+$ ) 151.0997 found 151.0986 (FAB, high resolution mass spectroscopy).

**4.5.1.6. Preparation of N-methyl,N-{(2-hydroxy)-1-ethyl}-*p*-anisidine (24) and N-methyl,N-{(2-hydroxy)-1-ethyl}-*p*-toluidine (28)**

A mixture of N-{(2-hydroxy)-1-ethyl}-*p*-anisidine (23) or N-{(2-hydroxy)-1-ethyl}-*p*-toluidine (27) (50 mmol), methyl iodide (50 mmol), potassium carbonate (0.1 mol), and iodine (100 mg) was heated under reflux in acetonitrile (80 mL) for 24 h. On cooling, the solvent was removed under reduced pressure to give a reddish brown liquid, which was chromatographed on silica gel (100-200 mesh).

**Compound 24.** Elution of the column using chloroform gave 7.7 g (85 %) of 24, bp 170-172 °C (30 mm); IR (neat)  $\nu_{\max}$  3407, 2956, 2841, 1623, 1520, 1465, 1362, 1295, 1248, 1185, 1128, 1040, 818, 755, 676  $\text{cm}^{-1}$ ;  $^1\text{H}$  NMR ( $\text{CDCl}_3$ )  $\delta$  2.30-2.54 (1H, s, OH), 2.77 (3H, s,  $\text{NCH}_3$ ), 3.24 (2H, t,  $\text{NCH}_2$ ), 3.65-3.77 (5H, m,  $\text{OCH}_3$  and  $\text{OCH}_2$ ), 6.51-7.36 (4H, m, aromatic);  $^{13}\text{C}$  NMR ( $\text{CDCl}_3$ )  $\delta$  39.48, 55.63, 56.89, 59.59, 114.20, 115.97, 144.97, 152.54; exact mass calcd. for  $\text{C}_{10}\text{H}_{15}\text{NO}_2$  ( $\text{M}^+$ ) 181.1103, found 181.1090 (FAB, high resolution mass spectroscopy).

**Compound 28.** Elution of the column using chloroform gave 7.0 g (85 %) of 28, bp 165-168 °C (30 mm); IR (neat)  $\nu_{\max}$  3399, 3019, 2928, 2877, 2807, 1623, 1571, 1524, 1484, 1366, 1230, 1192, 1129, 1047, 982, 963, 805, 521  $\text{cm}^{-1}$ ;  $^1\text{H}$  NMR ( $\text{CDCl}_3$ )  $\delta$  2.20 (3H, s,  $\text{CH}_3$ ), 2.85 (3H, s,  $\text{NCH}_3$ ), 3.34 (2H, t,  $\text{NCH}_2$ ), 3.70 (2H, t,  $\text{OCH}_2$ ), 6.69 (d), 7.00 (d) (4H, aromatic);  $^{13}\text{C}$  NMR ( $\text{CDCl}_3$ )  $\delta$  20.27, 39.06, 56.02, 59.86, 113.82, 126.93, 129.75, 148.11; exact mass calcd. for  $\text{C}_{10}\text{H}_{15}\text{NO}$  ( $\text{M}^+$ ) 165.1154, found 165.1149 (FAB, high resolution mass spectroscopy).



**4.5.1.7. Preparation of N-methyl,N-{(2-bromo)-1-ethyl}-*p*-anisidine (25) and N-methyl,N-{(2-bromo)-1-ethyl}-*p*-toluidine (29)**

To an ice cold solution N-methyl,N-{(2-hydroxy)-1-ethyl}-*p*-anisidine (24) or N-methyl,N-{(2-hydroxy)-1-ethyl}-*p*-toluidine (28) (15 mmol) in dichloromethane (20 mL), was added PBr<sub>3</sub> (15 mmol), dropwise, in each case, over a period of 30 minutes. The reaction mixture was further stirred at room temperature for a period of 3 h. The reaction was quenched with ice-cold water and the pH was adjusted to 7-8. The organic portion was extracted with dichloromethane and the solvent was removed under vacuum. The crude product was chromatographed on silica gel (100-200 mesh).

**Compound 25.** Elution of the column with a mixture (1:10) of petroleum ether (bp 60-80 °C) and chloroform gave 2.38 g (65%) of 25 as a heavy liquid; IR (neat)  $\nu_{\max}$  3054, 2955, 2912, 2838, 1629, 1519, 1464, 1350, 1276, 1249, 1213, 1181, 1096, 1041, 949, 816, 700, 537 cm<sup>-1</sup>; <sup>1</sup>H NMR (CDCl<sub>3</sub>)  $\delta$  2.85 (3H, s, NCH<sub>3</sub>), 3.35 (2H, t, CH<sub>2</sub>), 3.57 (2H, t, OCH<sub>2</sub>), 3.68 (3H, s, OCH<sub>3</sub>), 6.62 (d), 6.77 (d) (4H, aromatic); <sup>13</sup>C NMR (CDCl<sub>3</sub>)  $\delta$  28.60, 39.18, 55.67, 55.78, 114.28, 114.97, 142.92, 152.19; exact mass calcd. for C<sub>10</sub>H<sub>14</sub>NOBr (M<sup>+</sup>) 244.0259, found 244.0246 (FAB, high resolution mass spectroscopy).

**Compound 29.** Elution of the column with a mixture (1:10) of petroleum ether (bp 60-80 °C) and chloroform gave 2.38 g (70%) of 29 as a heavy liquid; IR (neat)  $\nu_{\max}$  3076, 3020, 2968, 2933, 2871, 2826, 1622, 1523, 1466, 1370, 1349, 1276, 1212, 1171, 1122, 1095, 1076, 950, 804, 705, 649, 519 cm<sup>-1</sup>; <sup>1</sup>H NMR (CDCl<sub>3</sub>)  $\delta$  2.17 (3H, s, CH<sub>3</sub>), 2.89 (3H, s, NCH<sub>3</sub>), 3.36 (2H, t, CH<sub>2</sub>), 3.61 (2H, t, CH<sub>2</sub>), 6.55 (d), 6.96 (d) (4H, aromatic); <sup>13</sup>C NMR (CDCl<sub>3</sub>)  $\delta$  20.21, 28.50, 38.74, 54.87, 112.41,

126.41, 129.91, 146.07; exact mass calcd. for  $C_{10}H_{14}NBr$  ( $M^+$ ) 227.0310, found 227.0305 (FAB, high resolution mass spectroscopy).

**4.5.1.8. Preparation of N-methyl,N-{2(-*p*-formylphenoxy)-1-ethyl}-*p*-anisidine (30) and N-methyl,N-{2(-*p*-formylphenoxy)-1-ethyl}-*p*-toluidine (31)**

A mixture of the appropriate bromide (5 mmol), *p*-hydroxybenzaldehyde (10 mmol) and potassium carbonate (10 mmol) was refluxed in dry acetone (15 mL) for 12 h. The reaction mixture was cooled, filtered and concentrated under reduced pressure. The crude product was chromatographed over silica gel (100-200 mesh).

**Compound 30.** Elution of the column with a mixture (1:4) of chloroform and hexane gave 1.21 g (85%) of **30**, mp 55-56 °C; IR (KBr)  $\nu_{\max}$  3051, 2942, 2838, 2750, 1701, 1606, 1582, 1519, 1473, 1432, 1365, 1313, 1249, 1164, 1139, 1116, 1040, 818, 678, 649, 616, 518  $cm^{-1}$ ;  $^1H$  NMR ( $CDCl_3$ )  $\delta$  2.97 (3H, s,  $NCH_3$ ), 3.69 (2H, t,  $NCH_2$ ), 3.75 (3H, s,  $OCH_3$ ), 4.18 (2H, t,  $OCH_2$ ), 6.74 (d), 6.83 (d), 6.96 (d), 7.79 (d) (8H, aromatic), 9.85 (1H, s, CHO);  $^{13}C$  NMR ( $CDCl_3$ )  $\delta$  39.73, 52.88, 55.72, 65.81, 114.43, 114.73, 114.82, 129.89, 131.90, 143.68, 151.95, 163.72, 190.70; exact mass calcd. for  $C_{17}H_{19}NO_3$  ( $M^+$ ) 285.1365, found 285.1360 (FAB, high resolution mass spectroscopy).

**Compound 31.** Elution of the column with a mixture (1:4) of chloroform and hexane gave 1.21 g (90%) of **31**, mp 48-49 °C; IR (KBr)  $\nu_{\max}$  3080, 3015, 2929, 2877, 2830, 2744, 1696, 1606, 1583, 1523, 1480, 1458, 1431, 1367, 1313, 1259, 1221, 1163, 1139, 1115, 1047, 834, 806, 651, 616, 519  $cm^{-1}$ ;  $^1H$  NMR ( $CDCl_3$ )  $\delta$  2.25 (3H, s,  $CH_3$ ), 3.01 (3H, s,  $NCH_3$ ), 3.74 (2H, t  $NCH_2$ ), 4.19 (2H, t,  $OCH_2$ ), 6.68 (d), 6.95 (d), 7.05 (d), 7.79 (d) (8H, aromatic), 9.85 (1H, s, CHO);  $^{13}C$  NMR ( $CDCl_3$ )  $\delta$  20.17, 39.36, 52.11, 65.73, 112.64, 114.77, 126.21, 129.83, 130.06,

131.94, 146.73, 163.76, 190.73; exact mass calcd. for  $C_{17}H_{19}NO_2$  ( $M^+$ ) 269.1412, found 269.1416 (FAB, high resolution mass spectroscopy).

#### 4.5.1.9. Synthesis of fullerene-*p*-anisidine and fullerene-*p*-toluidine dyads 5 and 6

A mixture of  $C_{60}$  (0.2 mmol), N-methyl-N{2(*p*-formylphenoxy)-1-ethyl}-*p*-anisidine (**30**) or N-methyl-N{2(-*p*-formylphenoxy)-1-ethyl}-*p*-toluidine (**31**) (0.2 mmol) and N-methylglycine (0.2 mmol) in toluene (145 mL) was stirred under reflux for 10 h. The reaction mixture was cooled and removal of the solvent under reduced pressure gave a solid residue, which was chromatographed over silica gel (100-200 mesh) to give the appropriate dyads.

**Dyad 5.** Elution with a mixture (1:3) of toluene and petroleum ether (bp 60-80 °C) gave 40 mg (28%) of unchanged  $C_{60}$ . Further elution with a mixture (1:1) of toluene and petroleum ether gave 72 mg (48%) of the fullerene-*p*-anisidine dyad, **5**, mp > 400 °C; IR (KBr)  $\nu_{max}$  3009, 2935, 2855, 2792, 1616, 1578, 1501, 1474, 1450, 1412, 1333, 1296, 1241, 1175, 1131, 1062, 1034, 830, 805, 779, 609, 526  $cm^{-1}$ ;  $^1H$  NMR ( $CDCl_3$ )  $\delta$  2.78 (3H, s,  $NCH_3$ ), 2.95 (3H, s,  $NCH_3$ ), 3.65 (2H, t,  $NCH_2$ ), 3.75 (3H, s,  $OCH_3$ ), 4.12 (2H, t,  $OCH_2$ ), 4.23 (1H, d, CH of pyrrolidine ring,  $J = 9.45$  Hz), 4.87 (1H, s, CH of pyrrolidine ring), 4.97 (1H, d, CH of pyrrolidine ring,  $J = 9.45$  Hz), 6.73 (d), 6.82 (d), 6.92 (d), 7.68 (br.s) (8H, aromatic);  $^{13}C$  NMR ( $CDCl_3+CS_2$ )  $\delta$  29.74, 39.64, 39.89, 53.05, 55.66, 65.33, 68.89, 69.95, 83.09, 114.23, 114.55, 114.81, 129.05, 130.38, 135.68, 136.70, 139.64, 139.93, 140.22, 141.69, 142.00, 142.04, 142.50, 143.76, 143.93, 144.22, 144.52, 145.16, 145.40, 145.75, 146.04, 146.87, 147.30, 151.74, 153.55, 154.10, 156.45, 158.73; exact mass calcd. for  $C_{79}H_{24}N_2O_2$  ( $M^+$ ) 1033.1916, found 1033.1877 (FAB, high resolution mass spectroscopy).

**Dyad 6.** Elution with a mixture (1:3) of toluene and petroleum ether (bp 60-80 °C) gave 36 mg (25%) of unchanged C<sub>60</sub> followed by 79 mg (52%) of 6, mp > 400 °C; IR (KBr)  $\nu_{\max}$  2924, 2868, 2852, 2781, 1613, 1565, 1514, 1466, 1426, 1358, 1333, 1298, 1247, 1172, 1037, 800, 766, 527 cm<sup>-1</sup>; <sup>1</sup>H NMR (CDCl<sub>3</sub>)  $\delta$  2.21 (3H, s, CH<sub>3</sub>), 2.75 (3H, s, NCH<sub>3</sub>), 2.97 (3H, s, NCH<sub>3</sub>), 3.68 (2H, t, NCH<sub>2</sub>), 4.10 (2H, t, OCH<sub>2</sub>), 4.21 (1H, d, CH of pyrrolidine ring, J = 9.57 Hz), 4.85 (1H, s, CH of pyrrolidine ring), 4.95 (1H, d, CH of pyrrolidine ring, J = 9.57 Hz), 6.64 (d), 6.89 (d), 6.95 (d), 7.65 (br.s) (8H, aromatic); <sup>13</sup>C NMR (CDCl<sub>3</sub>+CS<sub>2</sub>)  $\delta$  20.21, 29.73, 39.40, 39.91, 52.35, 65.10, 68.88, 69.93, 83.08, 112.58, 114.52, 129.03, 129.76, 130.38, 135.70, 136.50, 136.73, 139.06, 139.86, 140.71, 141.43, 141.55, 141.74, 142.03, 142.20, 142.49, 142.55, 142.86, 143.01, 144.32, 144.57, 144.62, 145.05, 145.17, 145.40, 145.46, 145.71, 145.86, 146.06, 146.25, 146.45, 146.70, 147.20, 153.53, 154.00, 156.26, 158.68; exact mass calcd. for C<sub>79</sub>H<sub>24</sub>N<sub>2</sub>O (M<sup>+</sup>) 1017.1967, found 1017.1953 (FAB, high resolution mass spectroscopy).

#### 4.5.2. Instrumental techniques

All melting points are uncorrected and were determined on a Aldrich melting point apparatus. IR spectra were recorded on a Perkin Elmer Model 882 IR spectrometer and the UV-visible spectra on a Shimadzu 2100 or GBC 918 spectrophotometer. <sup>1</sup>H NMR and <sup>13</sup>C NMR spectra were recorded on a JEOL EX-90 or Bruker DPX-300 MHz spectrometer. Mass spectra were recorded on a JEOL JMAX 505 HA mass spectrometer. The emission spectra were recorded on a Spex-Fluorolog, F112-X equipped with a 450 W Xe lamp and a Hamamatsu R928 photomultiplier tube. The excitation and emission slits were 1 and 4, respectively. A 570 nm long pass filter was placed before the emission monochromator in order to

eliminate the interference from the solvent and solvent spectra were recorded in each case and subtracted. Quantum yields of fluorescence ( $\phi_f$ ) were measured by a relative method. The absorbance of the solution was adjusted to 0.1 at 470 nm and the emission intensity was monitored at 720 nm. N-Methylfulleropyrrolidine dissolved in toluene ( $\phi_f = 6.0 \times 10^{-4}$ ) was used as reference.<sup>37,39</sup>

#### 4.6. References

1. Connolly, J. S.; Bolton, J. R. In *Photoinduced Electron Transfer, Part D*, Fox, M. A.; Channon, M. (Eds.), Elsevier: Amsterdam, 1988, pp 303-393.
2. Wasielewski, M. R. In *Photoinduced Electron Transfer, Part A*, Fox, M. A.; Channon, M. (Eds.), Elsevier: Amsterdam, 1988, pp 161-206.
3. Fox, M. A. In *Photoinduced Electron Transfer III, Topics in Current Chemistry-159*, Matty, J. (Ed.), Springer-Verlag, Berlin, 1991, pp 67-101.
4. Gust, D.; Moore, T. A. In *Photoinduced Electron Transfer III, Topics in Current Chemistry-159*, Matty, J. (Ed.), Springer-Verlag, Berlin, 1991, pp 103-151.
5. Kurreck, H.; Huber, M. *Angew. Chem. Int. Ed. Engl.*, 1995, 34, 849.
6. Lehn, J.-M. *Supramolecular Chemistry: Concepts and perspectives*, VCH, Weinheim, 1995.
7. Carter, F. L. *Molecular Electronic Devices*, Marcel Dekker, New York, 1982.
8. Feringa, B. L.; Jager, W. F.; de Lange, B. *Tetrahedron*, 1993, 49, 8267.
9. Balzani, V.; Maggi, L.; Scandola, F. *Supramolecular Photochemistry*, Balzani, V. (Ed.), Reidel, Holland, 1987, pp. 1-28.
10. Wasielewski, M. R.; Niemczyk, M. P. *J. Am. Chem. Soc.*, 1984, 106, 5043.
11. Wasielewski, M. R.; Niemczyk, M. P.; Svec, W. A.; Pewitt, E. B. *J. Am. Chem. Soc.*, 1985, 107, 1080.
12. Wasielewski, M. R.; Niemczyk, M. P.; Svec, W. A.; Pewitt, E. B. *J. Am. Chem. Soc.*, 1985, 107, 5562.
13. Wasielewski, M. R.; Niemczyk, M. P.; Svec, W. A.; Pewitt, E. B. In *Antennas and Reaction Centers of Photosynthetic Bacteria*, Michel-Beyerle (Ed.) Springer-Verlag, Berlin, 1985, 242.
14. Closs, G. L.; Calcaterra, L. T.; Green, N. J.; Penfield, K. W.; Millar, J. R. *J. Phys. Chem.*, 1986, 90, 3673.

15. Sun, Y.-P. In *Molecular and Supramolecular Photochemistry*, Vol. 1, *Organic Photochemistry*, Ramamurthy, V.; Schanze, K. S. (Eds.), Marcel Dekker, New York 1997, pp 325-390.
16. Foote, C. S. *Top. Curr. Chem.*, 1994, 169, 347.
17. Kamat, P. V.; Asmus, K.-D. *Interface*, 1996, 5, 22.
18. Zhou, F.; Jehoulet, C.; Bard, A. J. *J. Am. Chem. Soc.*, 1992, 114, 11004.
19. Dubois, D.; Kadish, K. M.; Flanagan, S.; Haufler, R. E.; Chibante, L. P. E.; Wilson, L. J. *J. Am. Chem. Soc.*, 1991, 113, 4364.
20. Arbogast, J. W.; Foote, C. S.; Kao, M. *J. Am. Chem. Soc.*, 1992, 114, 2277.
21. Luo, C.; Fujitsuka, M.; Huang, C. -H.; Ito, O. *J. Phys. Chem.*, 1998, 102, 8716.
22. Williams, R. M.; Koeberg, M.; Lawson, J. M.; An, Y. -Z. Rubin, Y.; Paddon-Row, M. N.; Verhoeven, J. W. *J. Org. Chem.*, 1996, 61, 5055.
23. Williams, R. M.; Zwier, J. M.; Verhoeven, J. W. *J. Am. Chem. Soc.*, 1995, 117, 4093.
24. Thomas, K. G.; Biju, V.; George, M. V.; Guldi, D. M.; Kamat, P. V. *J. Phys. Chem.*, 1998, 102, 5341.
25. Thomas, K. G.; Biju, V.; George, M. V.; Guldi, D. M.; Kamat, P. V. *J. Phys. Chem.*, 1998, 102, 0000.
26. Guldi, D. M.; Maggini, M. Scorrano, G.; Prato, M. *J. Am. Chem. Soc.*, 1997, 119, 974.
27. Liddell, P. A.; Kuciauskas, D.; Sumida, J. P.; Nash, B.; Nguyen, D.; Moore, A. L.; Moore, T. A.; Gust, D. *J. Am. Chem. Soc.*, 1997, 119, 1400.
28. Kuciauskas, D.; Lin, S.; Seely, G. R.; Moore, A. L.; Moore, T. A.; Gust, D.; Drovetskaya, T.; Reed, C. A.; Boyd, P. D. W. *J. Phys. Chem.*, 1996, 100, 15926.
29. Liddell, P. A.; Sumida, J. P.; Macpherson, A. N.; Noss, L.; Seely, G. R.; Clark, K. N.; Moore, A. L.; Moore, T. A.; Gust, D. *Photochem. Photobiol.*, 1994, 60, 537.
30. Imahori, H.; Hagiwara, K.; Asoki, M.; Akiyama, T.; Taniguchi, S.; Okada, T.; Shirakawa, M.; Sakata, Y. *J. Am. Chem. Soc.*, 1996, 118, 11771.

31. Imahori, H.; Yamada, K.; Hasegawa, M.; Taniguchi, S.; Okada, T.; Sakata, Y. *Angew. Chem. Int. Ed. Engl.*, **1997**, *36*, 2626.
32. Baran, P. S.; Monaco, R. R.; Khan, A. U.; Schuster, D. I.; Wilson, S. R. *J. Am. Chem. Soc.*, **1997**, *119*, 8363.
33. Imahori, H.; Cardoso, S.; Tatman, D.; Lin, S.; Noss, L.; Seely, G. R.; Sereno, L.; Silber, J. C. D.; Moore, T. A.; Moore, A. L.; Gust, D. *Photochem. Photobiol.*, **1995**, *62*, 1009.
34. Sariciftci, N. S.; Wudl, F.; Heeger, A. J.; Maggini, M.; Scarrano, G.; Prato, M.; Bourassa, J.; Ford, F. C. *Chem. Phys. Lett.*, **1995**, *247*, 510.
35. Maggini, M.; Guldi, D. M.; Mondini, S.; Scorrano, G.; Paolucci, F.; Ceroni, P.; Roffia, S. *Chem. Eur. J.*, **1998**, *4*, 1992.
36. Spreitzer, H.; Daub, J. *Chem. Eur. J.*, **1996**, *2*, 1150.
37. Nocera, D. G. Gray, H. B. *J. Am. Chem. Soc.*, **1981**, *103*, 7349.
38. Infelta, P. P.; Grätzel, M.; Fendler, J. H. *J. Am. Chem. Soc.*, **1980**, *102*, 1479.
39. Domelsmith, L. N.; Munchausen, L. L.; Houk, K. N. *J. Am. Chem. Soc.*, **1977**, *99*, 6506.
40. Manoj, N.; Gopidas, K. R. (private communication)
41. Moroi, Y.; Braun, A. M.; Grätzel, M.; *J. Am. Chem. Soc.*, **1979**, *101*, 567.
42. Sakaguchi, M.; Ittu, M.; Kevan, L. *J. Phys. Chem.*, **1990**, *94*, 870.
43. Younathan, J. N.; Jones, W. E. Jr.; Meyer, T. J. *J. Phys. Chem.*, **1991**, *95*, 488.
44. Guo, Q. -X.; Liang, Z. -X.; Lui, B.; Yao, S. -D. Lui, Y. -C. *J. Photochem. Photobiol. A: Chem.*, **1996**, *93*, 27.
45. Kavarnos, J. G. *Fundamentals of Photoinduced Electron Transfer*, VCH publishers, Inc. New York, **1993**, p 35.
46. Seo, E. T.; Nelson, R. F.; Fritsch, J. M.; Marcus, L. S.; Leedy, O. W.; Adams, R. N. *J. Am. Chem. Soc.*, **1966**, *88*, 3498.



47. Hoke-II, S. H.; Molstad, J.; Dilettato, D.; Jay, M. J.; Carlson, D.; Kahr, B.; Cooks, R. G. *J. Org. Chem.*, **1992**, *57*, 5069.
48. Confirmed on a Cosmosil Buckprep HLPC column.
49. Evaluated using the Sybyl force field method of PC SPARTAN software obtained from Wavefunction, Inc.; 18401, Von Karman, Suite 370, Irvine, CA 92612, USA.
50. Benasson, R. V.; Bienvenue, E.; Fabre, C. Janot, J. -M.; Land, E. J.; Leach, S.; Leboulaire, V.; Rassat, A.; Roux, S. Sata, P. *Chem. Eur. J.*, **1998**, *4*, 270.
51. Biehl, E. R.; Chiou, H.; Keepers, J.; Kennard, S.; Reeves, P. C. *J. Heterocycl. Chem.*, **1975**, *12*, 397.
52. Guldi, D. M.; Maggini, M.; Scarrano, G.; Prato, M. *J. Am. Chem. Soc.*, **1997**, *119*, 974.
53. Transient absorption studies were done in collaboration with Dr. Prashant V. Kamat, Dr. D. M. Guldi and Dr. K. George Thomas at the Radiation Laboratory, University of Notre Dame, Indiana, USA.
54. The identity of this band was further confirmed by the pulse radiolytic oxidation of 10-methylphenothiazine. Radical induced oxidation gave a transient absorption spectrum with maxima at 450 and 520 nm.
55. Mehta, G.; Sambaiah, T.; Maiya, B. G.; Sirish, M.; Dattagupta, A. *J. Chem. Soc. Perkin Trans I.*, **1995**, 295.
56. Bodea, C; Silberg, I In *Advances in Heterocyclic Chemistry, Vol. 9*, Katritzky, A. R.; Boulton, A. J. (Eds.) Academic press, New York, **1968**, pp 321- 460.
57. Ionescu, M.; Mantsch, H. In *Advances in Heterocyclic Chemistry, Vol. 8*, Katritzky, A. R.; Boulton, A. J. (Eds.) Academic press, New York, **1968**, pp 83-113.
58. Frangatos, G.; Kohan, G.; Chubb, F. L. *Can. J. Chem.*, **1960**, *38*, 1021.